Charles University, Faculty of Science
Univerzita Karlova, Přírodovědecká fakulta

Ph.D. study program: Animal Physiology

Doktorský studijní program: Fyziologie živočichů

Mgr. Daniel Benák

Epitranscriptomics and cardioprotective interventions
Epitranskriptomika a kardioprotektivní intervence

Doctoral thesis

Supervisor: RNDr. Markéta Hlaváčková, Ph.D.

Prague, 2024

Declaration of the author

I declare that I prepared this Ph.D. thesis on my original work and that all literary sources were properly cited. Neither this work nor a substantial part of it has been used to reach the same or any other academic degree. I have clearly stated the extent of my contribution to the research presented in the thesis. AI tools were used to improve the grammatical quality of the text.

Prague, 10. 4. 2024

…….

Daniel Benák

Acknowledgments

Firstly, I extend my heartfelt gratitude to my supervisor, RNDr. Markéta Hlaváčková, Ph.D., for her invaluable guidance and unwavering patience throughout my research journey. Her support was instrumental in making this work possible.

I am also grateful to my colleagues for their professional assistance and valuable insights which significantly contributed to the experiments, culminating in the writing of this thesis. Special thanks to Prof. RNDr. František Kolář, CSc.; RNDr. Kristýna Holzerová, Ph.D.; Mgr. Jaroslav Hrdlička, Ph.D.; Mgr. Dita Sotáková, Ph.D.; RNDr. Petra Alánová, Ph.D.; Prof. MUDr. Bohuslav Ošťádal, DrSc.; Ing. František Papoušek, CSc.; and RNDr. Jan Neckář, Ph.D.

I would also like to extend my appreciation to Associate Prof. Mark Olsen and Prof. Mati Karelson for providing inhibitors of FTO and ALKBH5, which were crucial to our investigations.

Acknowledgment is due to the Proteomics Core Facility at the Institute of Physiology of the Czech Academy of Sciences and RNDr. Marek Vrbacký, Ph.D. for the proteomic analysis, as well as the Metabolomics Core Facility at the same institute and Doc. Ing. Tomáš Čajka, Ph.D. for the metabolomic and lipidomic profiling.

I am thankful also to all others who have provided support, advice, or recommendations throughout this endeavor.

Last but not least, I would like to thank the laboratory animals that paid the ultimate price.

This study was supported by the Grant Agency of Charles University (grant numbers 200317 and 668220).

List of publications related to this thesis

Statement about the extent of participation

Original articles

1. **Benak D**, Sotakova-Kasparova D, Neckar J, Kolar F, Hlavackova M (2019). Selection of optimal reference genes for gene expression studies in chronically hypoxic rat heart. Mol Cell Biochem. 461(1-2):15-22. *IF = 2.795*

   My contribution: I was involved in RNA isolation, reverse transcription of RNA into DNA, DNase treatment, and RT-qPCR runs (together with Dita Sotáková-Kašparová). I analyzed the stability of candidate reference genes using the GenEx software, employing NormFinder, geNorm, and BestKeeper algorithms for this analysis. Additionally, I drafted the manuscript, contributing to the interpretation of results and the creation of figures.

2. Semenovykh D, **Benak D**, Holzerova K, Cerna B, Telensky P, Vavrikova T, Kolar F, Neckar J, Hlavackova M (2022). Myocardial m6A regulators in postnatal development: effect of sex. Physiol Res. 71(6):877-882. *IF = 2.1*

   My contribution: I was involved in sample collection, protein concentration assessment, RT-qPCR experiments, and revision of the manuscript.

3. **Benak D**, Holzerova K, Hrdlicka J, Kolar F, Olsen M, Karelson M, Hlavackova M (2024). Epitranscriptomic regulation in fasting hearts: implications for cardiac health. RNA Biol. 21(1):1-14. *IF = 4.1*

   My contribution: I participated in the conceptualization of the study (together with Markéta Hlaváčková). I was responsible for animal handling, executing the fasting regimen, and sample preparation. I determined the glycemia and hematocrit levels after the fasting. I also performed the following molecular and cellular methods: RNA isolation, reverse transcription, RT-qPCR experiments, m^6A/m quantification, SDS-PAGE and Western blot, cardiomyocyte isolation and culture, and SYTOX green nucleic acid staining. I was also involved in m^6A RNA immunoprecipitation (together with Kristýna Holzerová and Markéta Hlaváčková).

Review articles

1. **Benak D**, Kolar F, Zhang L, Devaux Y, Hlavackova M (2023). RNA modification m^6Am: the role in cardiac biology. Epigenetics. 18(1):2218771. *IF = 3.7*

2. **Benak D**, Benakova S, Plecita-Hlavata L, Hlavackova M (2023). The role of m^6A and m^6Am RNA modifications in the pathogenesis of diabetes mellitus. Front Endocrinol (Lausanne). 14:1223583. *IF = 5.2*

3. **Benak D**, Kolar F, Hlavackova M (2024). Epitranscriptomic regulations in the heart. Physiol Res. (online) *IF = 2.1*

My contribution: Drafting the articles and creation of figures.

On behalf of all co-authors, I confirm that the information stated above regarding Daniel Benák's contributions to the mentioned articles is accurate.

RNDr. Markéta Hlaváčková, Ph.D.

Abstract

Ischemic heart disease stands as the foremost global cause of mortality. Myocardial ischemia results in damage to cardiomyocytes which can further lead to impaired heart function. However, the extent of ischemic injury hinges not only on the intensity and duration of the ischemic stimulus but also on cardiac tolerance to ischemia. Therefore, it is extremely important to unravel the molecular basis of cardioprotective interventions such as adaptation to chronic hypoxia or fasting. We focused on the novel epitranscriptomic mechanisms around RNA modifications – N^6-methyladenosine (m^6A) and N^6,2'-O-dimethyladenosine (m^6Am). Our findings revealed that while most epitranscriptomic modifiers displayed differential regulation in the heart following hypoxic adaptation and fasting, demethylases (ALKBH5 and FTO) were consistently upregulated after these cardioprotective interventions. Furthermore, we detected a discernible reduction in cardiac total RNA methylation levels after fasting. On the contrary, transcripts *Nox4* and *Hdac1*, both of which play a role in the cytoprotective action of ketone bodies, exhibited increased methylation in hearts of fasting rats. Finally, inhibition of epitranscriptomic demethylases ALKBH5 and FTO decreased the hypoxic tolerance of adult rat primary cardiomyocytes isolated from fasting rats. Collectively, our findings underscore the intricate regulation of the epitranscriptomic machinery surrounding m^6A and m^6Am modifications in cardioprotective interventions like adaptation to chronic hypoxia and fasting. Therefore, this complex regulation may play an important role in the induction of the cardioprotective phenotype.

Abstrakt

Ischemická choroba srdeční je celosvětově nejčastější příčinou úmrtí. Ischemie myokardu vede k poškození kardiomyocytů, což může vést k poruše srdeční funkce. Rozsah ischemického poškození však závisí nejen na intenzitě a délce trvání ischemického podnětu, ale také na toleranci srdce vůči ischemii. Objasnění molekulárního pozadí kardioprotektivních intervencí, jako je adaptace na chronickou hypoxii nebo hladovění, tak nabývá zásadního významu. Proto jsme se zaměřili na nové epitranskriptomické regulace dvou rozšířených modifikací RNA – N^6-methyladenosinu (m^6A) a N^6,2'-O-dimethyladenosinu (m^6Am). Zjistili jsme, že většina epitranskriptomických regulátorů v srdci reaguje na hypoxickou adaptaci a na hladovění odlišným způsobem, demetylázy (ALKBH5 a FTO) byly ale v obou případech zvýšeny. Po hladovění bylo navíc v srdci patrné znatelné snížení hladin celkové metylace RNA. Hladina metylace v transkriptech *Nox4* a *Hdac1*, které se účastní cytoprotektivních drah spouštěných ketolátkami, ale byla naopak zvýšena. V neposlední řadě, inhibice epitranskriptomických demetyláz ALKBH5 a FTO vedla ke snížení hypoxické tolerance kardiomyocytů izolovaných z hladovějících potkanů. Celkově naše zjištění ukazují na regulaci epitranskriptomických modifikací m^6A a m^6Am při kardioprotektivních intervencích, jako je adaptace na chronickou hypoxii a hladovění. Epitranskriptomické regulace tedy mohou hrát podstatnou úlohu při indukci kardioprotekce.

Table of contents

1. INTRODUCTION

According to the World Health Organization, ischemic heart disease (IHD) ranks as the leading cause of death worldwide, highlighting a critical area of concern in public health [1]. Myocardial ischemia causes damage to cardiomyocytes, potentially resulting in compromised heart function. The extent of this ischemic injury is influenced not only by the severity and duration of the ischemic event but also by the intrinsic resilience of the heart to such ischemic stress [2]. Given this context, investigating the molecular basis of unconventional cardioprotective interventions, such as adaptation to chronic hypoxia or fasting, becomes increasingly relevant.

Recently, RNA modifications (= epitranscriptomic modifications) emerged as a novel layer of gene expression regulation in molecular biology. Alterations in the cardiac epitranscriptome have been observed across a spectrum of physiological conditions and disease states, illustrating its significance in cardiac health and disease. Several experimental studies indicated that the protection of cardiomyocytes from adverse effects like hypoxia-reoxygenation (H/R) injury can be achieved by influencing protein levels of various epitranscriptomic regulators [3-12]. However, whether cardioprotective methods such as adaptation to chronic hypoxia or fasting are associated with altered epitranscriptomic machinery has been unknown.

To bridge this knowledge gap, we analyzed the effect of a 3-week adaptation to chronic hypoxia or 3-day fasting (both cardioprotective regimes) on epitranscriptomic regulations in left ventricles (LV) of the heart. Our research on the LVs from hypoxic and fasting rats was guided by three principal objectives: 1) whether the levels of epitranscriptomic regulators are affected; 2) whether the overall methylation level is regulated in total RNA; and 3) whether specific transcripts of cardioprotective genes are differentially methylated? Building upon these findings, we investigated whether the inhibition of demethylases influences the hypoxic tolerance of cardiomyocytes isolated from fasting animals, thereby providing new insights into the intricate molecular mechanisms that underlie cardiac resilience and protection.

2. LITERATURE REVIEW

2.1. Cardioprotective interventions

IHD manifests clinically as myocardial infarction (MI) and ischemic cardiomyopathy [13]. So far, the only effective treatment of MI is limited to the rapid coronary reperfusion. Typically, this is accomplished through coronary artery bypass grafting (CABG) or primary percutaneous coronary intervention (PCI) [14, 15]. PCI was introduced into medical practice in the 1970s and has since become the gold standard for treating IHD as it avoids the morbidity associated with surgical revascularization as in CABG [15, 16]. Other clinical strategies include pharmacotherapy (e.g., thrombolytic agents [17], statins [18], beta-blockers [19], and ACE inhibitors [20]). Pharmacological treatment can be categorized into three levels of prevention: primary prevention, which aims to prevent an injury before it occurs; secondary prevention, which seeks to minimize the impact of an injury at its initial stages; and tertiary prevention, which focuses on managing long-term health issues resulting from the injury [21].

Cardioprotective interventions aim to reduce the risk of heart disease or mitigate the negative outcomes associated with heart-related illnesses. Among cardioprotective interventions used mainly in the experimental setting, ischemic conditioning is notable for its ability to reduce infarct size and limit heart failure (HF). Ischemic preconditioning involves brief episodes of ischemia interspersed with short reperfusion periods before a prolonged ischemic event [22], while ischemic postconditioning applies a similar approach following prolonged ischemia [23]. Interestingly, ischemic conditioning is not necessarily confined to the heart; inducing ischemia in a distant organ may also have cardioprotective effects [24]. Within clinical settings, the cardioprotective remote ischemic conditioning stimulus can be achieved through sequential inflation and deflation of a pneumatic cuff placed on the upper arm or thigh, creating short periods of ischemia followed by reperfusion. In numerous clinical trials involving patients with MI, this method has been shown to enhance myocardial salvage and decrease the infarct size when applied before or during

reperfusion [25-28]. However, other studies did not report any beneficial effects of remote ischemic conditioning on clinical outcomes [29, 30], leaving the effectiveness of this approach in clinical practice controversial.

Other interventions including adaptation to chronic hypoxia, fasting, acclimation to moderate cold, whole-body hyperthermia, or vagus nerve stimulation are also associated with cardioprotective effects [2, 31-34]. This study focused on two cardioprotective interventions studied in our lab – adaptation to chronic hypoxia and fasting (Fig. 1). Gaining a deeper insight into the molecular mechanisms underlying these different cardioprotective phenomena could pave the way for novel therapeutic approaches in clinical medicine.

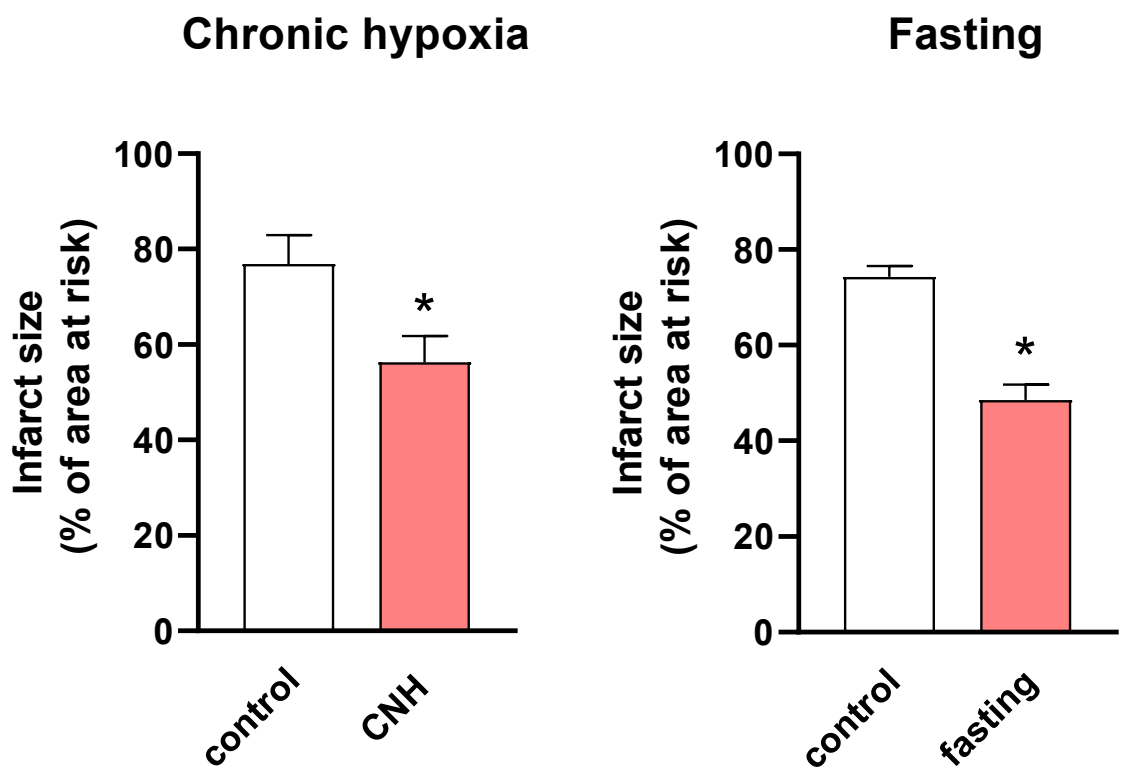

Fig. 1: Infarct-size limiting effect of adaptation to chronic hypoxia and fasting. Both experimental cardioprotective methods were used in this study. CNH – continuous normobaric hypoxia. Modified from Alanova et al. [2] and Snorek et al. [31].

2.1.1. Adaptation to chronic hypoxia

Chronic hypoxia is characterized by a consistent state of low oxygen availability. Different mechanisms can induce chronic myocardial hypoxia: ischemic hypoxia is the result of reduced or interrupted blood flow through the coronary arteries; systemic hypoxia is caused by a drop in the partial pressure of oxygen (pO_2) in the arterial blood; and anemic hypoxia is characterized by a reduced oxygen transport capacity of the blood [35].

In experimental *in vivo* settings, exogenous methods of chronic hypoxia can be broadly categorized into hypobaric hypoxia and normobaric hypoxia, which are typically simulated in hypoxic chambers (Fig. 2). Hypobaric hypoxia is induced by reducing the barometric pressure in the environment (hypobaric chamber), leading to a decrease in pO_2 [36]. This method simulates hypoxic conditions at high altitudes where barometric pressure is naturally low. In contrast, normobaric hypoxia is associated with a decrease in the percentage of oxygen in the inspired air, achieved by altering the gas composition while maintaining normal barometric pressure [37, 38]. Additionally, hypoxic stimuli can be either continuous or intermittent, and the strength and duration of exposure can vary [36, 37, 39].

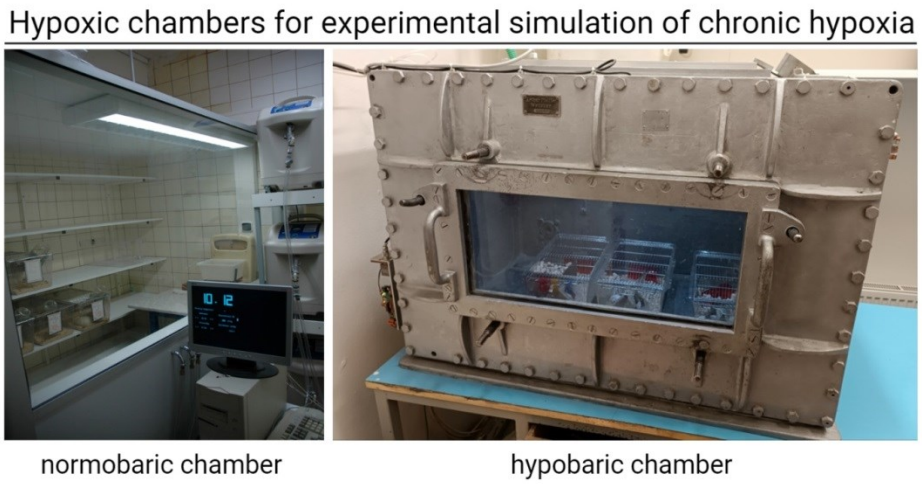

Fig. 2: Adaptation of animals to chronic hypoxia in hypoxic chambers.

In the middle of the previous century, observations first indicated that residents of high-altitude areas exhibited a lower incidence of MI [40]. This early observation laid the groundwork

for further research, which subsequently confirmed the cardioprotective effects of systemic hypoxia through experimental studies [2]. Interestingly, it has been demonstrated that the cardiac protection conferred by chronic hypoxia against acute ischemia-reperfusion (I/R) injury is significantly more durable than that provided by any form of ischemic conditioning [41]. However, the protective benefits of chronic hypoxia and ischemic conditioning do not combine to provide additive benefits, implying that they may share a common underlying cardioprotective pathway or mechanism [42].

The body's adaptation to chronic hypoxia involves various molecular, cellular, and physiological changes that can have cardioprotective effects. Exposure to low oxygen levels can lead to the up-regulation of certain transcription factors, such as HIF-1 (hypoxia-inducible factor 1) [43]. HIF-dependent expression of EPO (erythropoietin) leads to increased erythropoiesis and VEGFA (vascular endothelial growth factor A) results in enhanced angiogenesis [39, 44-48]. Cells also adapt to decreased oxygen availability through a HIF-dependent switch from oxidative to glycolytic metabolism [49]. However, adaptation to chronic hypoxia is very complex and many other genes and proteins are affected by low oxygen levels [50, 51]. Altogether, these adaptations can enhance myocardial resistance to ischemia (acute hypoxia) and reduce I/R injury. While chronic hypoxia may offer cardioprotective effects, it also has potential negative effects, such as pulmonary hypertension [52].

2.1.2. Fasting

Fasting involves voluntary abstinence from food for a specified period. There are several forms of fasting, even though the terminology is not entirely well-defined [53]. Intermittent fasting (IF) involves alternating between fasting periods and regular eating intervals. Time-restricted eating/feeding (TRE/F) is a popular form of IF that typically involves consuming food within a daily window of 12 h or less, often narrowed to 8 h [54]. The 5:2 diet, another popular variation of IF, incorporates 2 fasting days (consecutive or not) within a week [55]. However, probably the most frequently experimentally studied IF method is alternate-day fasting (AFD) [56, 57]. Short-term

fasting (STF) and long-term fasting (LTF, also known as prolonged fasting) describe single fasting periods lasting from several hours to multiple days, respectively [31, 58, 59]. It is important to note that time runs on vastly different timescales in laboratory animals compared to humans. For instance, the basal metabolic rate in rats is 6.4 times higher than in humans. When considering protein turnover, the disparity is even more pronounced, with a 9.6-fold difference. In terms of relative life expectancy, rats age roughly 27 times faster than humans [60]. Therefore, when selecting a fasting model for experimental protocols, it's essential to take these factors into account.

Fasting is associated with a metabolic switch towards lipids and also the production of ketone bodies in the liver. Ketone bodies, mainly acetoacetate and β-hydroxybutyrate, serve not only as fuel for extrahepatic tissues but also promote resistance to oxidative and inflammatory stress. They initiate the activation of important cell-protective regulators, such as NRF2 (nuclear factor erythroid 2-related factor 2), sirtuins, or AMPK (AMP-activated kinase), as reviewed by Kolb et al. [61] (Fig. 3). Thus, it is generally accepted that fasting effectively protects the heart against major endpoints of acute I/R injury [31]. Yet, some studies reported that the heart is better protected against MI in the fed state compared to the fasted state (18-h fasting) [62]. Another study showed that treatment of hypoxic cardiomyocytes with β-hydroxybutyrate decreased the viability of these cells [63]. These conflicting data clearly show that understanding the molecular processes in the fasting heart is inadequate and needs more attention.

Despite its benefits, fasting should be approached with caution. Excessive fasting or fasting without proper guidance may lead to adverse effects such as ketoacidosis and other health issues, particularly in individuals with underlying health conditions [64].

Current research continues to explore the optimal forms, durations, and frequencies of fasting for various health outcomes, including cardioprotection. Ongoing studies aim to unravel the complex interplay between fasting-induced metabolic shifts and their impact on cardiovascular health, aiming to optimize fasting strategies for clinical and preventive healthcare.

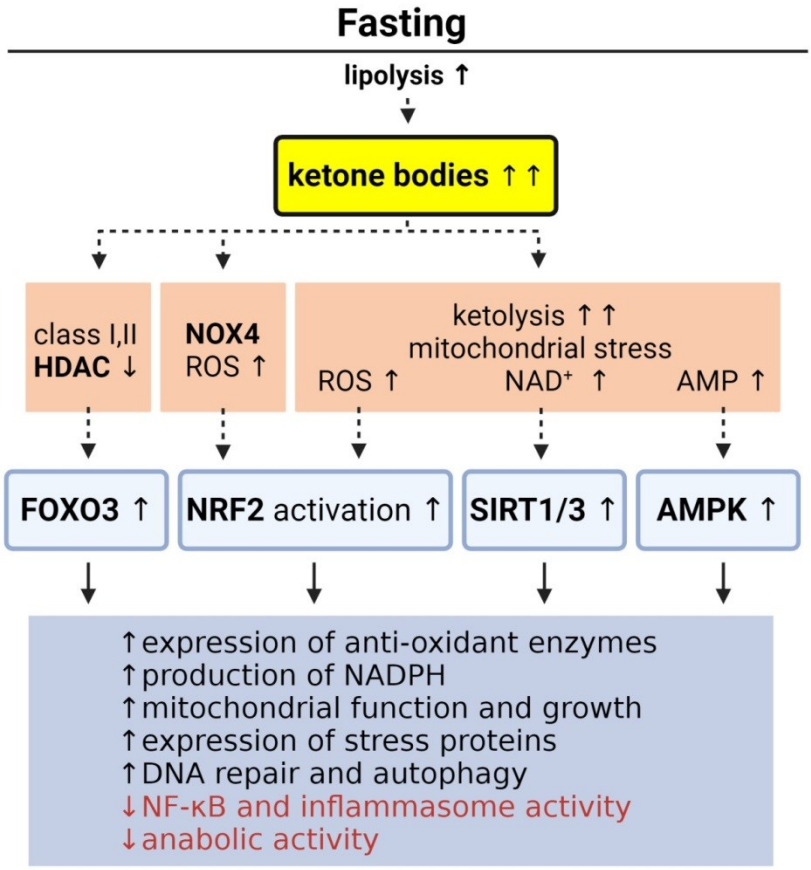

Fig. 3: Scheme of cell-protective functions of ketone bodies. AMP – adenosine monophosphate; AMPK – AMP-activated kinase; FOXO3 – forkhead box O3; HDAC – histone deacetylase; NAD^+ – nicotinamide adenine dinucleotide; NADPH – nicotinamide adenine dinucleotide phosphate hydrogen; NF-κB – nuclear factor kappa-light-chain-enhancer of activated B cells; NOX4 – NADPH oxidase 4; NRF2 – nuclear factor erythroid 2-related factor 2; ROS – reactive oxygen species; SIRT1/3 – sirtuins 1/3. Modified from Kolb et al. [61]. Created with BioRender.

2.2. Epitranscriptomics

The central dogma of molecular biology, introduced by Francis Crick in 1957, states that DNA carrying genetic information is transcribed into RNA, which is subsequently translated into proteins [65]. This whole process is under the control of epigenetic mechanisms involving chemical modifications to the DNA, to the proteins that package DNA into chromatin (histones), or to the RNA molecules transcribed from the DNA (Fig. 4). Importantly, the epigenome (which encompasses DNA modifications and histone modifications) and the epitranscriptome (RNA modifications) are responsive to various environmental factors such as diet, stress, and exposure to toxins. Thus, it is reasonable to expect that adaptation to chronic hypoxia and fasting could influence the

epitranscriptome as well. Epigenetic modifications can lead to heritable phenotypic changes without altering the underlying DNA or RNA sequence [66-68].

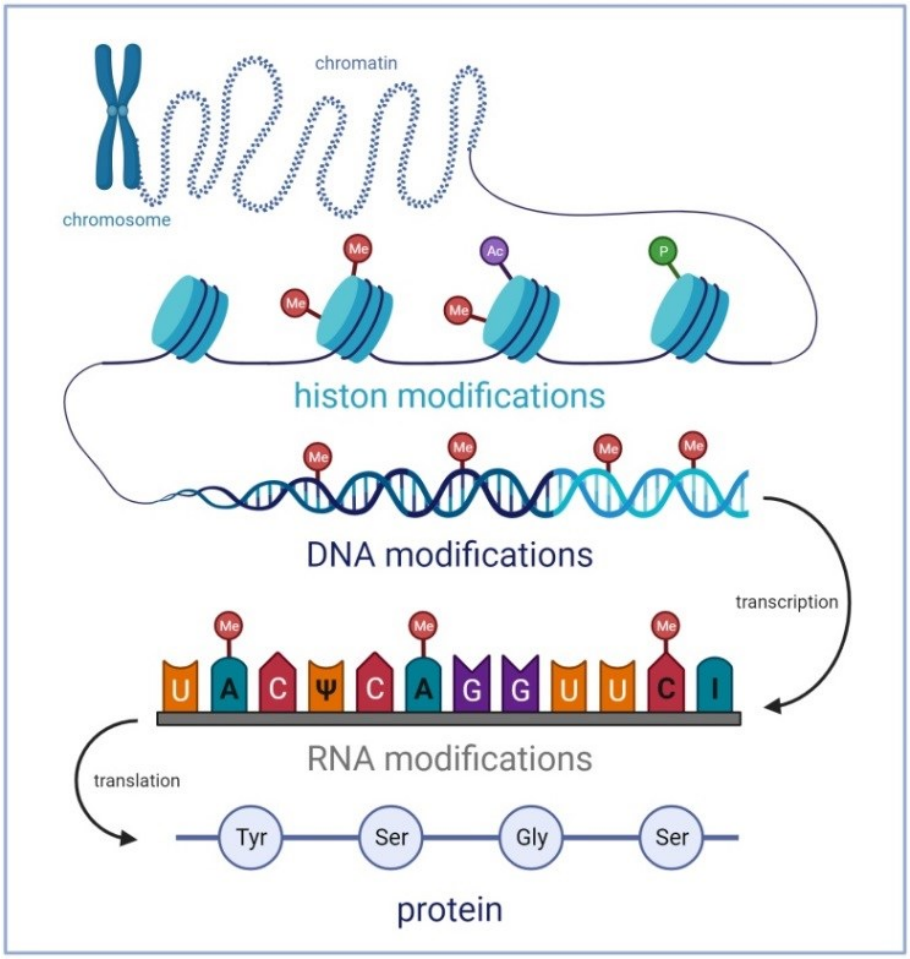

Fig. 4: Basic overview of epigenetic modifications. Created with BioRender. Taken from Benak et al. [69] (Attachment VII).

The rapidly developing research field of epitranscriptomics has introduced a novel layer of gene expression regulation into molecular biology. To date, over 170 chemical modifications have been described in RNA so far (common RNA modifications shown in Fig. 5) [70]. The largest number and widest diversity of modifications occur in tRNA (transfer RNA) [71]. However, while tRNA and rRNA (ribosomal RNA) modifications have been known and studied for decades, mRNA (messenger RNA) modifications have been poorly characterized for a long time [68]. N^6-methyladenosine (m^6A) is one of the most prevalent and well-studied modifications in mRNA. If the adenosine is already methylated at the 2'-O position (Am), methylation of such nucleoside makes

220 N^6,2'-O-dimethyladenosine (m^6Am). The effects of RNA modifications are mediated by proteins
221 called writers (methylation deposition), readers (binding of modified RNA), and erasers
222 (methylation removal). Moreover, some RNA-binding proteins prefer unmodified transcripts over
223 modified transcripts (m^6A-repelled proteins) [72]. Dynamic regulation of epitranscriptomic
224 modifications can affect key stages of the RNA life cycle, including splicing, export, decay, and
225 translation [73, 74].

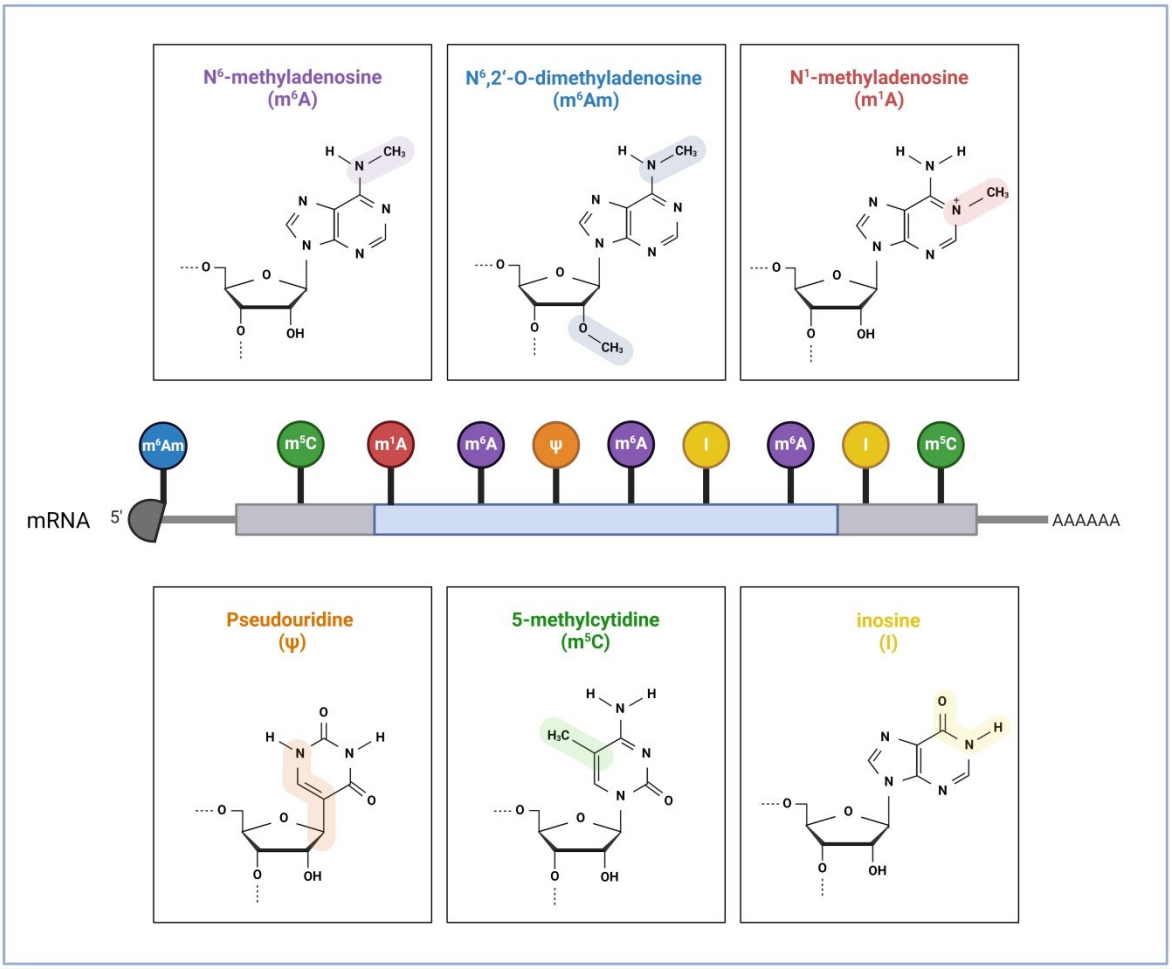

226

227 **Fig. 5:** Common mRNA modifications. Created with BioRender. Taken from Benak et al. [69]
228 (Attachment VII).

229 ### 2.2.1. N^6-methyladenosine (m^6A)

230 The m^6A was identified in 1974 [75]. It is a methylation that occurs in the N^6-position of
231 adenosine (Fig. 6).

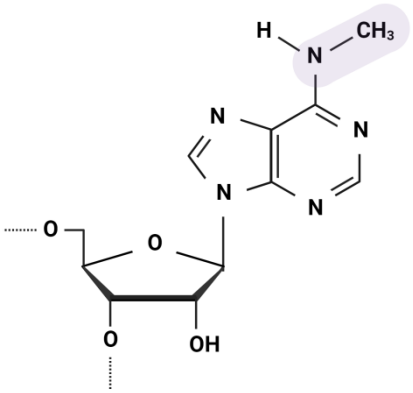

Fig. 6: Chemical structure of N^6-methyladenosine (m^6A). Created with BioRender.

However, it was the discovery of the m^6A eraser in 2011 that provided the first evidence of reversible posttranscriptional modifications in mRNAs and got the mRNA modifications into the spotlight of researchers [76]. Now we know that there is a variety of proteins regulating this dynamic epitranscriptomic modification (Fig. 7).

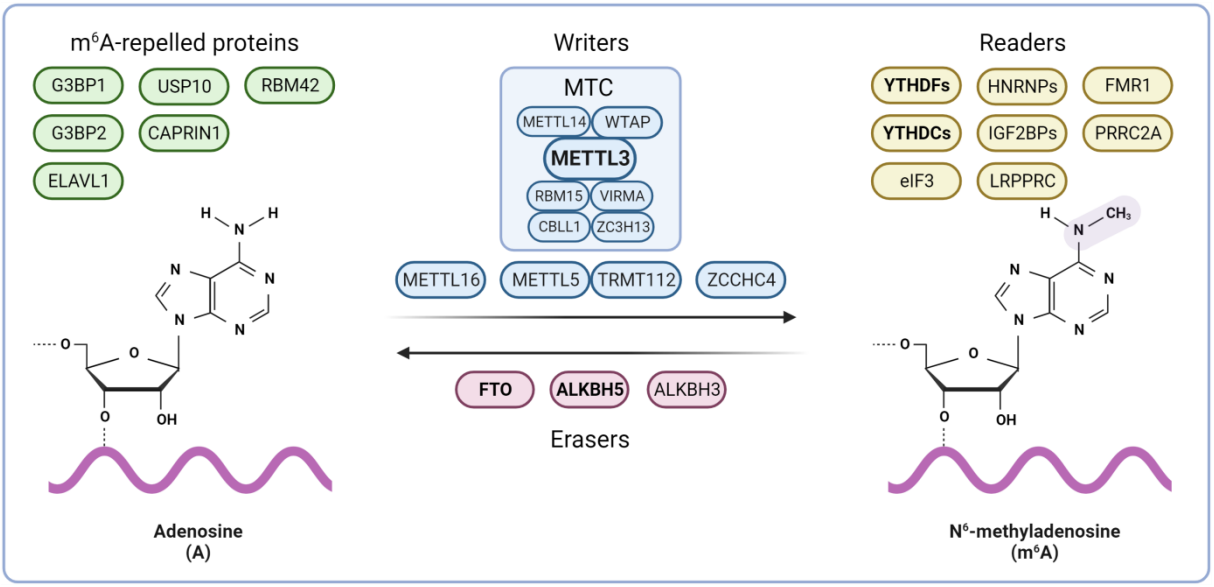

Fig. 7: Overview of m^6A regulators. ALKBH3/5 – alkB family member 3/5; CAPRIN1 – cell cycle associated protein 1; CBLL1 – cbl proto-oncogene like 1; eIF3 – eukaryotic initiation factor 3; ELAVL1 – ELAV-like protein 1; FMR1 – fragile X messenger ribonucleoprotein 1; FTO – fat mass and obesity-associated protein; G3BP1/2 – G3BP stress granule assembly factor 1/2; HNRNPs – heterogeneous nuclear ribonucleoproteins; IGF2BPs – insulin-like growth factor 2 mRNA binding proteins; LRPPRC – leucine rich pentatricopeptide repeat containing; METTL3/5/14/16 – methyltransferase-like 3/5/14/16; MTC – multicomponent methyltransferase complex; PRRC2A – proline rich-coil 2A; RBM15/42 – RNA binding motif protein 15/42; TRMT112 – tRNA methyltransferase activator subunit 11-2; USP10 – ubiquitin specific peptidase 10; VIRMA – vir-like m6A methyltransferase associated; WTAP – Willms' tumor 1-associating protein; YTHDCs – YTH

domain-containing proteins; YTHDFs – YTH domain-containing family proteins; ZC3H13 – zinc finger CCCH-type containing 13; ZCCHC4 – zinc finger CCHC-type containing 4. Created with BioRender.

The m^6A is one of the most prevalent modifications in mRNA. It generally occurs in the consensus motif DRACH (D= G, A or U; R = G or A; H = A, C or U), however, only 1-5% of these sites are methylated *in vivo* [77-79]. On average, the mRNA contains 3 m^6A methylation sites [80]. However, a comprehensive analysis of mRNA methylation revealed that most mRNAs exhibit 1 m^6A peak (single methylation site or a cluster of adjacent m^6A residues), while some surpass more than 20 m^6A peaks [81]. In the heart, approximately one-quarter of the transcripts exhibit m^6A RNA methylation [82]. The m^6A modification is highly abundant near stop codons and in the 3‘ untranslated region (3‘UTR) and less common in 5’UTR of mRNAs [81]. Co-transcriptional deposition of m^6A to mRNAs is affected by histone modifications, and in turn, m^6A affects gene expression via the regulation of histone modifications [83, 84]. The m^6A modification alters the RNA structure by forcing the rotation of the methylamino group to an anti-conformation position, destabilizing the thermodynamics of the RNA duplex, which enables the binding of RNA binding proteins [79]. The presence or absence of m^6A in mRNA influences its stability, regulates gene expression, and therefore significantly affects cellular physiology [85]. Besides mRNA, m^6A has been observed in rRNA, tRNA, lncRNA (long non-coding RNA), snRNA (small nuclear RNA), circ-RNA (circular RNA), and miRNA (microRNA) [86].

2.2.1.1. m^6A writers

Multicomponent methyltransferase complex (MTC) is responsible for the deposition of the methyl group to adenosine, forming m^6A. The core component of MTC is comprised of methyltransferase-like 3 (METTL3), which acts as the catalytic subunit of the MTC, and methyltransferase-like 14 (METTL14), which facilitates RNA binding [87, 88]. Willms’ tumor 1-associating protein (WTAP) is another primary regulatory subunit of the MTC; it interacts with the METTL3/METTL14 heterodimer and localizes the MTC to nuclear speckles [89]. Additional components of the MTC include RNA-binding motif protein 15 (RBM15) which recruits

the MTC to U-rich regions adjacent to the m^{6}A residues [90]; vir-like m^{6}A methyltransferase associated (VIRMA) which mediates preferential methylation in the 3'UTR and near the stop codon [91]; cbl proto-oncogene like 1 (CBLL1, also known as HAKAI) which is essential for m^{6}A methylation in *Arabidopsis* (however its principal ubiquitin ligase activity is independent of m^{6}A-function) [92]; and zinc finger CCCH-type containing 13 (ZC3H13) which regulates the nuclear retention of the MTC [93].

Apart from the MTC, methyltransferase-like 16 (METTL16) also promotes the methylation of mRNAs, U6 snRNAs, and various non-coding RNAs [94-96]. Methyltransferase-like 5 (METTL5) in complex with tRNA methyltransferase activator subunit 11-2 (TRMT112) methylates human 18S rRNA and zinc finger CCHC-type containing 4 (ZCCHC4) mediates methylation of 28S rRNA [96-98].

2.2.1.2. m^{6}A erasers

The removal of the methyl group is mediated by three known demethylases. AlkB homolog 5 (ALKBH5) is the primary m^{6}A eraser responsible for the demethylation of m^{6}A in mRNA and snRNA [99, 100]. Fat mass and obesity-associated protein (FTO) is not an m^{6}A-specific demethylase, however, m^{6}A is the preferable target of FTO in the nucleus, where it binds to multiple RNA species (e.g. mRNA, snRNA, tRNA) [76, 101, 102]. ALKBH3 was described to promote the demethylation of mammalian tRNA [103]. Interestingly, the eraser responsible for rRNA demethylation has not been identified [104].

2.2.1.3. m^{6}A readers

The biological functions of m^{6}A are mediated by many m^{6}A readers which recognize and selectively bind to m^{6}A-modified RNAs. The key readers include YTH domain-containing family proteins 1-3 (YTHDF1-3) and YTH domain-containing proteins 1-2 (YTHDC1-2). While readers YTHDF1-3 mediate especially mRNA degradation, YTHDC1 regulates mRNA splicing and YTHDC2 promotes translation [105-111].

In addition to YTH proteins (the most prominent m^{6}A readers), eIF3 (eukaryotic initiation factor 3) binds to m^{6}A in 5‘ UTR and promotes cap-independent translation [112]. Reader HNRNPA2B1 (heterogeneous nuclear ribonucleoprotein A2/B1) binds to m^{6}A-modified mRNAs, modulating alternative splicing [113]. Other HNRPs were also identified as m^{6}A readers, such as HNRNPC (mRNA splicing) [114], HNRNPD (mRNA degradation) [115], and HNRNPG (mRNA splicing) [116]. IGF2BP1-3 proteins (insulin-like growth factor 2 mRNA-binding proteins 1-3) also bind to m^{6}A and promote the stability and storage of their target mRNAs and therefore affect gene expression output [117]. Other m^{6}A reader proteins – FMR1 (fragile X messenger ribonucleoprotein 1) [72, 118, 119] or PRRC2A (proline-rich coiled-coil 2A) [120] have been also shown to stabilize m^{6}A-containing mRNAs. LRPPRC (leucine rich pentatricopeptide repeat containing) has been also described as an m^{6}A reader [72]. METTL16 serves as both m^{6}A writer and reader of U6 snRNA and promotes splicing [94].

2.2.1.4. m^{6}A-repelled proteins

Unlike m^{6}A readers, many RNA binding proteins have a preference for unmodified mRNAs versus m^{6}A-containing mRNAs. One such m^{6}A-repelled protein is G3BP1 (Ras-GTPase-activating protein SH3 domain-binding protein), a known stress granule protein. G3BP1 binding to target mRNAs results in their stabilization [72, 119]. The m^{6}A was also reported to disrupt the binding of stress granule proteins G3BP2 (G3BP stress granule assembly factor 2), USP10 (ubiquitin specific peptidase 10), CAPRIN1 (cell cycle associated protein 1), and RBM42 (RNA binding motif protein 42) [72]. Similarly, loss of m^{6}A methylation enhances the binding of ELAVL1 (ELAV-like protein 1), which is also known as HuR (human antigen R), a well-established RNA stabilizer [121].

2.2.1.5. Roles of the m^{6}A modification in cardiac physiology

The m^{6}A modification plays a key role in cardiac physiology (Fig. 8), affecting the heart from ontogenetic development through various regulatory mechanisms. The m^{6}A machinery controls key aspects of cardiomyocyte growth, proliferation, and differentiation [122-125]. Children born with a

loss-of-function mutation in the *FTO* gene exhibited heart defects (ventricular septal defect, atrioventricular defect, patent ductus arteriosus) and hypertrophic cardiomyopathy and died before 3 years of age [126]. Furthermore, various genetic variants of m^{6}A regulators are associated with cardiovascular diseases (CVDs) such as MI, acute coronary syndrome, increased rejection risk in heart transplant patients, and sudden cardiac death [127-133].

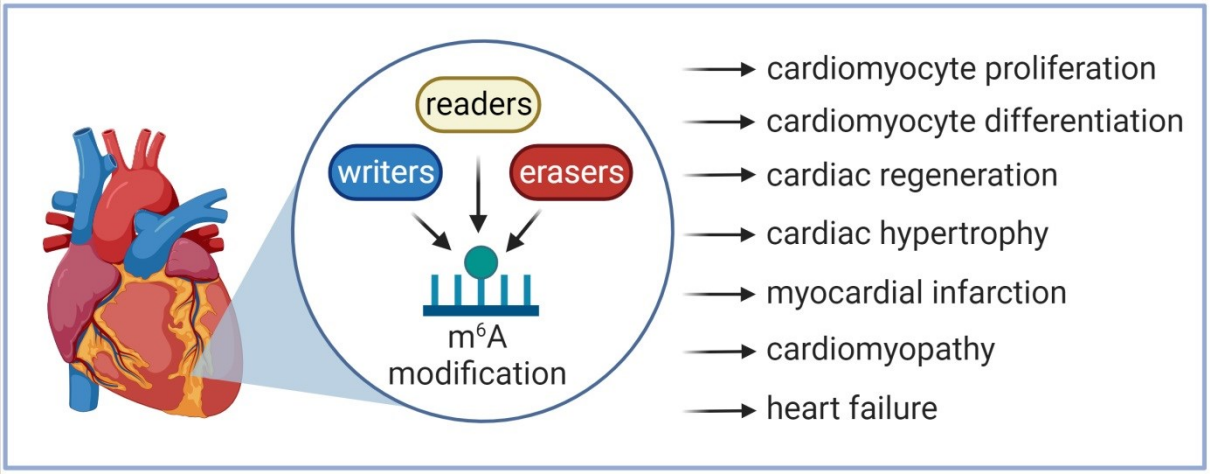

Fig. 8: Role of m^{6}A modification in the heart. m^{6}A – N^6-methyladenosine. Created with BioRender. Taken from Benak et al. [69] (Attachment VII).

The m^{6}A modification also exerts control over cardiac hypertrophy, with studies suggesting that enhanced m^{6}A RNA methylation leads to compensated cardiac hypertrophy, while diminished m^{6}A is associated with eccentric cardiomyocyte remodeling and dysfunction [134-137]. It has been demonstrated that m^{6}A regulators likely affect the immune-inflammatory response and fibrosis in the heart tissue during MI [138]. For example, MTC subunits (METTL3, WTAP) exert profibrotic effects while FTO displays antifibrotic effects in cardiac fibroblasts [139-141]. Dysregulation of m^{6}A machinery and alterations in m^{6}A methylation patterns also contribute to the progression of HF [7, 82, 142-146]. Altered cardiac m^{6}A patterns were evident also in diabetic cardiomyopathy, exhibiting distinct dysregulation in type 1 diabetes mellitus (T1DM) and type 2 diabetes mellitus (T2DM) [147-149] (Attachment VI). The heterogeneous role of m^{6}A modification in CVDs has been extensively reviewed [86, 150-158].

Altered m^6A levels have potential utility as biomarkers, as seen in patients with coronary artery disease (CAD) who exhibit significantly lower urine m^6A levels compared to healthy individuals [159].

Given the dysregulation of cardiac m^6A machinery under various pathophysiological conditions, targeting m^6A modifiers emerges as a potential avenue for cardioprotection. Studies indicate that demethylases FTO and ALKBH5 can protect cardiomyocytes from detrimental effects [3-10], while loss of METTL3 or METTL14 may alleviate myocardial injury and promote heart regeneration [11, 12]. Consequently, understanding the intricacies of m^6A regulations in the heart could pave the way for innovative cardioprotective strategies involving specific pharmacological activators or inhibitors targeting m^6A modifiers.

2.2.2. N^6,2'-O-dimethyladenosine (m^6Am)

The m^6Am modification is distinct from the similar m^6A due to its methylation at the 2'-O position (Fig. 9). It has been described in two RNA classes so far: mRNA and snRNA. In mRNA, m^6Am is commonly found as part of the mRNA cap and is situated at the transcription start, adjacent to the well-known 5'-terminal modification – 7-methylguanosine [160, 161]. This modification appears in at least 30-40% of all vertebrate mRNA transcripts [160]. In certain cell lines, the prevalence of m^6Am is even higher. For example, in HEK293T cells, 92% of capped mRNAs feature m^6Am, while only 8% contain the singly methylated Am [162]. The incorporation of m^6Am into mRNA notably enhances its stability [163]. In snRNA, m^6Am is also found at internal sites and plays a role in pre-mRNA splicing [164].

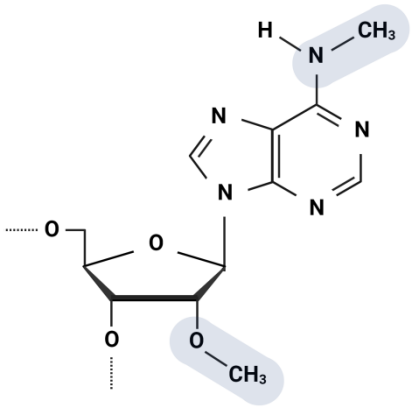

Fig. 9: Chemical structure of N^6,2'-O-dimethyladenosine (m^6Am). Created with BioRender.

2.2.2.1. m^6Am writers

N^6-methylation of Am to m^6Am is catalyzed by two known enzymes (Fig. 10): phosphorylated CTD interacting factor 1 (PCIF1) and methyltransferase-like 4 (METTL4).

In 2019, PCIF1 was characterized as a cap-specific adenosine-N^6-methyltransferase (also called CAPAM which primarily methylates the cap and not the adenosine residues within the RNA body) [162, 165]. Nonetheless, more recent findings suggest that PCIF1 can also carry out methylation activities on internal adenosines (both A and Am), albeit with lower affinities [166]. This writer has direct and indirect impacts on RNA stability and transcription [163, 167-169].

The second m^6Am writer, METTL4, was described in 2020. It catalyzes the formation of internal m^6Am formation within U2 snRNA and affects pre-mRNA splicing [170, 171]. Additionally, METTL4 is involved in the methylation of N^6-methyldeoxyadenosine (6mA), a modification found in mitochondrial DNA (mtDNA), especially under stress conditions [172].

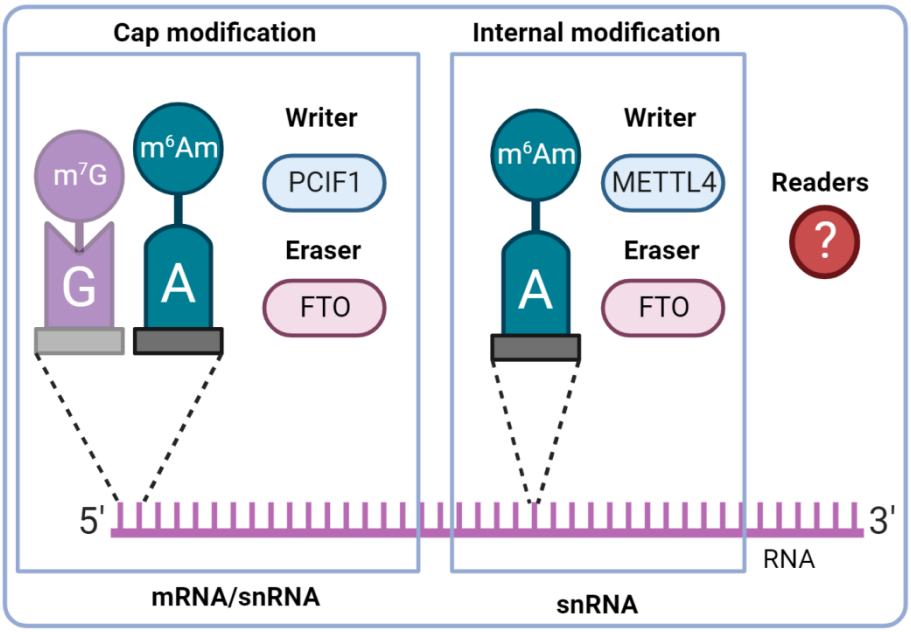

Fig. 10: Basic overview of m^{6}Am modification. A – adenosine; G – guanosine; FTO – fat mass and obesity-associated; m^{6}Am – N^6,2′-O-dimethyladenosine; m^{7}G − 7-methylguanosine; METTL4 – methyltransferase-like 4; PCIF1 – phosphorylated CTD interacting factor 1. Created with BioRender. Taken from Benak et al. [173] (Attachment V).

2.2.2.2. m^{6}Am erasers

To date, FTO is the only known eraser for m^{6}Am. Initially, FTO was characterized as an m^{6}A demethylase [76]. However, a 2017 study reported that FTO exhibits a higher preference for demethylating m^{6}Am over m^{6}A [163, 174]. Recent findings suggest that FTO's substrate preference could be influenced by its cellular localization, which can vary among cell types. Specifically, in the nucleus, FTO primarily targets m^{6}A, while cytosolic FTO predominantly demethylates m^{6}Am [101]. This cytosolic demethylation activity for m^{6}Am by FTO was later corroborated by other researchers [102]. In cardiomyocytes, FTO is present in both the cytosol and the nucleus [175]. FTO demethylates m^{6}Am in both mRNA and snRNA [101]. Beyond m^{6}A and m^{6}Am, FTO can also target N^1-methyladenosine (m^{1}A) in transfer RNA (tRNA) [101, 163].

2.2.2.3. m^{6}Am readers

As of now, no readers that mediate the biological functions of m^{6}Am have been identified. However, several readers are known to bind the more extensively studied m^{6}A modification. This raises the question of whether these RNA-binding proteins can also recognize and bind the similar

396 m^6Am modification. Notably, YTHDF3, a key m^6A reader, has been found not to bind m^6Am-
397 containing transcripts [176]. Therefore, there is a pressing need to identify specific m^6Am readers.

398 *2.2.2.4. Roles of m^6Am modification in cardiac physiology*

399 While much attention has been focused on m^6A, the role of m^6Am modification in cardiac
400 physiology is largely unexplored. Several challenges hinder m^6Am research: 1) numerous m^6A
401 detection methods fail to distinguish between similar m^6A and m^6Am modifications; 2) FTO is not a
402 specific demethylase as it has affinities to m^6Am, m^6A, and m^1A; 3) METTL4 can catalase 6mA
403 methylation besides m^6Am methylation. Consequently, the potential impact of m^6Am on cardiac
404 function may be erroneously attributed to m^6A in various studies [173].

405 Beyond the non-specific demethylase FTO (included in chapter 2.2.1.5.), limited knowledge
406 exists regarding the involvement of m^6Am and its regulators in cardiac processes. Analysis of
407 publicly available RNA-seq datasets from human LVs of failing and non-failing hearts revealed some
408 regulatory changes in *METTL4* (down-regulation) and *PCIF1* (up-regulation) [173] (Attachment V).
409 Besides that, the role of m^6Am in the heart seems to be an uncharted territory.

3. HYPOTHESIS AND AIMS OF THE THESIS

We hypothesize that regulation of epitranscriptomic machinery, particularly demethylases ALKBH5 and FTO, and the subsequent changes in RNA methylation levels, play a crucial role in enhancing cardiac tolerance to ischemia through mechanisms initiated by chronic hypoxia and fasting, thereby contributing to the cardioprotective phenotype.

1) The primary objective was to analyse changes in epitranscriptomic regulation associated with chronic hypoxia and fasting by:
    a. assessing the levels of m^6A and m^6Am regulators in the LV
    b. measuring the levels of total m^6A+m^6Am (m^6A/m) methylation in the total RNA isolated from LVs
    c. evaluating the levels of m^6A/m methylation in specific transcripts of cardioprotective genes
2) The secondary objective was to examine effect of specific inhibitors of ALKBH5 and FTO on the hypoxic tolerance of primary cardiomyocytes isolated from fasting rats.

4. MATERIALS AND METHODS

4.1. Animals and experimental protocol

Adult (12-week-old) male rats (Wistar) were used in our experimental protocols. All animals were housed in a controlled environment with a stable temperature (23 °C) and a 12 h light-dark cycle (light from 6:00 AM).

***Adaptation to chronic hypoxia*:** Rats were subjected to moderate continuous normobaric hypoxia (CNH; 10% O_2) for 3 weeks inside a normobaric chamber equipped with hypoxic generators (Everest Summit, Hypoxico, USA). No reoxygenation occurred during this period. The control rats were kept in room air for an equivalent period.

Fasting: Rats in the experimental group were deprived of food for 3 days but had unrestricted access to water [31]. The control group was fed *ad libitum*. There was a gradual decrease in blood glucose levels (Tab. 5) from an initial 6.2 mmol/l to 3.5 mmol/l by the first day, 3.7 mmol/l by the second day, and 3.9 mmol/l by the third day of fasting (glycemia from the tail blood was measured using a glucometer). On average, after 3 days of fasting, the rats lost 17% of body weight (BW) while control rats gained 3% of BW by the same period (Tab. 5). The hearts of fasting rats were smaller by 16% compared to control rats after normalization to tibia length (Tab. 5). The hematocrit (assessed by the capillary micromethod; Tab. 5) in fasting rats (45.6) was significantly higher than in controls (40.3).

Our experiments adhered to the guidelines outlined in the Guide for the Care and Use of Laboratory Animals (published by the National Academy of Science, National Academy Press, Washington, USA). Experimental protocols were approved by the Animal Care and Use Committee of the Institute of Physiology CAS.

4.1.1. In-depth characteristics of the fasting model

Considering that a 3-day fast represents a significantly prolonged fasting period for rats, characterized by their high basal metabolic rates, and has been observed to cause a reduction in

heart size among other effects, a series of more in-depth analyses were conducted. These analyses aimed to thoroughly investigate the consequences of such fasting. They encompassed the evaluation of the metabolic profile in the plasma samples, a detailed analysis of the cardiac proteomic profile, and a comprehensive assessment of heart function to better understand the full range of physiological changes induced by extended fasting in these animals.

4.1.1.1. Untargeted lipidomics and metabolomics in plasma samples

The lipidomic and metabolomic analysis was performed by the Metabolomics service laboratory. Global lipidomic and metabolomic profiling of plasma samples was conducted using a combined untargeted and targeted workflow for the lipidome, metabolome, and exposome analysis (LIMeX) with some modifications [177-179]. Briefly, the process included a biphasic solvent system extraction using cold methanol and methyl *tert*-butyl ether for sample preparation. Four distinct liquid chromatography-mass spectrometry (LC-MS) platforms were employed for comprehensive profiling, addressing both lipidomics (using reversed-phase LC-MS in both positive and negative ion modes) and metabolomics (utilizing hydrophilic interaction chromatography for polar metabolites and reversed-phase liquid chromatography in negative ion mode). Quality control was assured through randomization of samples, regular injection of quality control samples, and analysis of procedure blanks, among other measures. Data processing involved the MS-DIAL software, with metabolite and lipid annotation achieved through a combination of in-house and external libraries. This extensive procedure ensured detailed and accurate profiling of the lipidome and metabolome in plasma samples.

4.1.1.2. Proteomic analysis

The proteomic analysis was performed by the Proteomics service laboratory. Briefly, heart samples were pulverized in liquid nitrogen, solubilized in 1% SDS, and processed according to the SP4 no-glass bead protocol [180]. About 500 ng of tryptic peptides were separated on a 50 cm C18 column using a 2.5 h elution gradient and were analyzed in data-independent acquisition (DIA)

mode on an Orbitrap Exploris 480 (Thermo Fisher Scientific, USA) mass spectrometer equipped with a FAIMS unit. Raw files were processed in Spectronaut 14 (Biognosys, Switzerland) using the library created from data-dependent acquisition runs of all samples and pooled sample fractionated to 8 fractions by Pierce High pH Reversed-Phase Peptide Fractionation Kit (Thermo Fisher Scientific, USA). UniProt UP000002494_10116.fasta release 2021_01 proteome file was used.

4.1.1.3. Echocardiography and heart catheterization

GE Vivid 7 Dimension (GE Vingmed Ultrasound, Norway) with a 12 MHz linear matrix probe M12L was used to assess the geometry and function of the LVs of animals after 3 days of fasting [181]. Animals underwent anesthesia using a 2% isoflurane (Forane, Abbott Laboratories, United Kingdom) solution mixed with room air and were positioned on a heating pad. Their rectal temperature was maintained at 36.5 °C ± 1 °C. Basic 2-D and M-modes were recorded both on the long axis and short axis. Heart rate (HR) and the following parameters of LV geometry were evaluated: end-diastolic and end-systolic LV cavity diameter (LVDd, LVDs), anterior wall thickness (AWTd, AWTs), and posterior wall thickness (PWTd, PWTs). Fractional shortening (FS), relative wall thickness (RWT), and cardiac index (CI) were derived as follows: $FS = 100*[(LVDd-LVDs)/LVDd]$; $RWT = 100*[(AWTd+PWTd)/LVDd]$; $CI = [(\pi/3)*LVDd^3]-[(\pi/3)*LVDs^3]*HR/BW$.

Following the echocardiographic examination, LV catheterization through the right carotid artery using the SPR-407 microtip pressure catheter was performed as described previously [182]. Data were acquired using MPVS 300 (Millar, Houston, USA) and PowerLab 8/30 (ADInstruments, UK). End-diastolic pressure (Ped), end-systolic pressure (Pes), developed pressure (Pdev), and peak rate of pressure development and decline ($+(dP/dt)_{max}$, $-(dP/dt)_{max}$, respectively) were assessed from 5 consecutive pressure cycles using LabChart Pro (ADInstruments, UK).

4.2. Tissue sampling

Immediately after the end of the adaptation to chronic hypoxia or fasting period, the rats were killed by cervical spine dislocation. The hearts were quickly excised, washed in cold (0°C)

saline, and divided into the right ventricle (RV), LV, and septum [25]. All harvested tissue segments were weighed, frozen, and stored in liquid nitrogen until use. The heart weight of fasting animals was normalized to tibial length.

4.3. RNA isolation, cDNA synthesis, and RT-qPCR

Total RNA was isolated from each LV sample utilizing RNAzol® RT, following the manufacturer's recommendations. RNA concentration was quantified using NanoDrop 1000 (Thermo Fisher Scientific, USA). For cDNA synthesis, 1 µg of total RNA was employed with the RevertAid H Minus First Strand cDNA Synthesis Kit (Thermo Fisher Scientific, USA) and random primers, adhering to the provided protocol.

RT-qPCR (reverse transcription-quantitative polymerase chain reaction) was carried out on a LightCycler® 480 (Roche Diagnostics, Switzerland) in a 20 µl reaction volume using TaqMan Gene Expression Assays (Tab. 1; Thermo Fisher Scientific, USA) and 5x HOT FIREPol Probe qPCR Mix Plus (NO ROX) (Solis Biodyne, Estonia). The thermal cycling conditions comprised an initial enzyme activation at 95 °C for 15 min, followed by 45 amplification cycles (15 s at 95 °C and 1 min at 60 °C) [26]. Data interpretation followed guidelines from qPCR courses provided by TATAA Biocenter (http://www.tataa.com/courses/).

Table 1. TaqMan Gene Expression Assays

Gene	Catalog nr.	Assay ID	Specification
Alkbh5	4351372	Rn01750503_m1	FAM-MGB
Fto	4331182	Rn01538186_m1	FAM-MGB
Mettl3	4331182	Rn01414796_m1	FAM-MGB
Mettl4	4351372	Rn04244733_m1	FAM-MGB
Pcif1	4351372	Rn01423448_m1	FAM-MGB
Ythdc1	4331182	Rn00591592_m1	FAM-MGB
Ythdc2	4351372	Rn01256278_m1	FAM-MGB
Ythdf1	4331182	Rn00620538_m1	FAM-MGB
Ythdf2	4351372	Rn01180761_m1	FAM-MGB
Ythdf3	4351372	Rn01289124_m1	FAM-MGB

Alkbh5 – alkB family member 5; *Fto* – fat mass and obesity-associated; *Hprt* – hypoxanthine phosphoribosyltransferase 1; *Mettl3/4* – methyltransferase-like 3/4; *Nupl2* – nucleoporin-like 2*; Pcif1* – phosphorylated CTD interacting factor 1; *Sdha* – succinate dehydrogenase complex flavoprotein subunit A; *Tomm22* – translocase of outer mitochondrial membrane 22; *Top1* – DNA topoisomerase I; *Ythdf1-3* – YTH domain-containing family protein 1-3; *Ythdc1-2* – YTH domain-containing protein 1-2; *Ywhaz* – tyrosin-3-monooxygenase/tryptophan 5 monooxygenase activation protein zeta.

4.3.1. Selection of optimal reference genes and RT-qPCR data normalization

For reliable data normalization [27], the following genes commonly used as reference genes were preselected for a stability analysis (TaqMan Gene Expression Assays in Tab. 2): actin beta (*Actb*); beta-2-microglobulin (*B2m*); glyceraldehyde-3-phosphate dehydrogenase (*Gapdh*); hypoxanthine phosphoribosyltransferase 1 (*Hprt1*); nucleoporin like 2 (*Nupl2*); ribosomal protein, large, P1 (*Rplp1*); succinate dehydrogenase complex flavoprotein subunit A (*Sdha*); translocase of outer mitochondrial membrane 22 (*Tomm22*); DNA topoisomerase I (*Top1*); ubiquitin C (*Ubc*); tyrosin-3-monooxygenase/tryptophan 5 monooxygenase activation protein zeta (*Ywhaz*). Genes with bias in their intragroup or intergroup variations were excluded from the analysis. The remaining candidate genes were evaluated by NormFinder and geNorm algorithms using GenEx software and standard deviations of candidate Cq values were obtained by the BestKeeper software tool. The final consensus was achieved by the calculation of the geometric mean of the three ranking values for each candidate gene resulting in an overall stability score.

In hypoxic experiments, *Top1* and *Nupl2* were selected as the most stable reference genes and were used for normalization [37] (Attachment II). In fasting experiments, normalization was carried out using *Top1* and *Ywhaz* [183] (Attachment IV).

Table 2. TaqMan Gene Expression Assays for selection of reference genes

Gene	Catalog nr.	Assay ID	Specification
Actb	4331182	Rn00667869_m1	VIC-MGB_PL
B2m	4331182	Rn00560865_m1	VIC-MGB_PL
Gapdh	4331182	Rn01775763_g1	VIC-MGB_PL
Hprt1	4331182	Rn01527840_m1	VIC-MGB_PL
Nupl2	4331182	Rn01442493_m1	VIC-MGB_PL
Rplp1	4331182	Rn03467157_gH	VIC-MGB_PL
Sdha	4331182	Rn00590475_m1	VIC-MGB_PL
Tomm22	4331182	Rn01502295_g1	VIC-MGB_PL
Top1	4331182	Rn00575128_m1	VIC-MGB_PL
Ubc	4331182	Rn01789812_g1	VIC-MGB_PL
Ywhaz	4448484	Rn00755072_m1	VIC-MGB_PL

Actb – actin beta; *B2m* – beta-2-microglobulin; *Gapdh* – glyceraldehyde-3-phosphate dehydrogenase; *Hprt1* – hypoxanthine phosphoribosyltransferase 1; *Nupl2* – nucleoporin like 2 ; *Rplp1* – ribosomal protein, large, P1; *Sdha* – succinate dehydrogenase complex flavoprotein subunit A; *Tomm22* – translocase of outer mitochondrial membrane 22; *Top1* – DNA topoisomerase I; *Ubc* – ubiquitin C; *Ywhaz* – tyrosin-3-monooxygenase/tryptophan 5 monooxygenase activation protein zeta.

4.4. SDS-PAGE and Western blot analysis

LV samples were first pulverized to a fine powder in liquid nitrogen, then subjected to Potter-Elvehjem homogenization using 8 volumes of the homogenization buffer (pH 7.4) containing 12.5 mM TRIS, 2.5 mM EGTA, 250 mM sucrose, 6 mM 2-mercaptoethanol, protease inhibitor cocktail (Roche, Switzerland) and a phosphatase inhibitor cocktail (Roche, Switzerland). Following homogenization, the protein concentration within the homogenates was determined using the Bradford method (Bio-Rad, USA). The LV homogenates were then processed through SDS electrophoresis on 10% polyacrylamide gels (Mini-PROTEAN TetraCell system, Bio-Rad, USA) and the separated proteins were electrotransferred onto PVDF membranes with a pore size of 0.2 µm (Bio-Rad). Afterward, the membranes were blocked using a 5% blotting-grade blocker (Bio-Rad, USA) in TBS mixed with 1% Tween 20, for a duration of 1 h, before being incubated with the selected primary and secondary antibodies (Tab. 3) diluted in a solution containing 1% blotting-grade blocker and 1% Tween 20 in TBS.

559 **Table 3.** Antibody specification

Antibody	Host animal	Clonality	Dilution factor	Incubation	Company	Catalog nr.
anti-ALKBH5	rabbit	monoclonal	1:1400	overnight	Abcam	ab195377
anti-FTO	mouse	monoclonal	1:1000	overnight	Abcam	ab92821
anti-METTL3	rabbit	monoclonal	1:1000	overnight	Abcam	ab195352
anti-METTL4	rabbit	polyclonal	1:1400	overnight	Invitrogen	PA5-97202
anti-PCIF1	rabbit	polyclonal	1:1400	overnight	Invitrogen	PA5-110081
anti-YTHDC1	rabbit	monoclonal	1:1400	overnight	Abcam	ab220159
anti-YTHDC2	rabbit	monoclonal	1:1400	overnight	Abcam	ab220160
anti-YTHDF1	rabbit	polyclonal	1:1400	overnight	Abcam	ab157542
anti-YTHDF2	rabbit	polyclonal	1:1400	overnight	Invitrogen	PA5-70853
anti-YTHDF3	rabbit	polyclonal	1:1400	overnight	Sigma-Aldrich	SAB21022736
anti-mouse	goat	polyclonal	1:10,000	1 h	ThermoFisher	31432
anti-rabbit	goat	polyclonal	1:10,000	1 h	Bio-Rad	170-6515

560 ALKBH5 – alkB family member 5; FTO – fat mass and obesity-associated; METTL3/4 – methyltransferase-like 3/4; PCIF1 – phosphorylated CTD
561 interacting factor 1; YTHDF1-3 – YTH domain-containing family protein 1-3; YTHDC1/2 – YTH domain-containing protein 1/2.

562 To analyze samples from multiple membranes, the same sample was applied to each
563 membrane to serve as an internal control for recalculation. The same amount of protein was loaded
564 on the gels for all samples. The results were recalculated to the total protein amount gained by
565 Ponceau S staining [184]. The visualization of membranes was performed by enhanced
566 chemiluminescence substrates (SuperSignal™ West Dura Extended Duration Substrate or
567 SuperSignal™ West Femto Maximum Sensitivity Substrate, Thermo Scientific, USA) using a
568 ChemiDoc™ system (Bio-Rad, USA).

569 4.5. Targeted proteomic analysis

570 Samples were initially dissolved in 25 µl of loading buffer (containing 0.05% trifluoroacetic
571 acid and 2% acetonitrile) and analyzed using DIA. For targeted analysis, they were spiked with a
572 mixture of 72 isotopically labeled peptides, which contained C-terminal 15N and 13C-labeled
573 arginine and lysine residues (JPT Peptide Technologies GmbH, Germany), to achieve a
574 concentration of 1 fmol/peptide on a column. Before the internal standard (IS) spiking, samples
575 were diluted to approximate a total peptide amount of 1 µg on a column. Since some ISs had
576 detection limits above 1 fmol/peptide on a column, samples were re-spiked to 40 fmol IS peptides
577 on a column for a second injection.

578 For LC-MS analysis, an Ultimate 3000 liquid chromatograph paired with an Exploris 480
579 mass spectrometer equipped with FAIMS was utilized. Peptides were loaded onto a PepMap Neo
580 0.5 cm x 300 µm i.D., 5 µm C18, 100 A trap column (Thermo Fisher Scientific, USA) for 2 min at a
581 flow rate of 17.5 µl/min. Following this, separation and ion spray ionization was carried out on a 50
582 cm x 75 µm i.D. Easy-Spray column with 2 µm C18 particles and 100 A pore size. A solvent gradient
583 transition from 97% mobile phase A (0.1% FA in H_2O) to 35% mobile phase B (0.1% formic acid in
584 80% acetonitrile) was used over 60 min for targeted acquisition and extended to 120 min for DIA
585 analysis. The spray voltage was maintained at 2,000 V throughout all runs. FAIMS was operated in
586 standard resolution mode for Parallel Reaction Monitoring (PRM) analysis, and in low-resolution

mode (inner electrode temp.: 100 °C, outer electrode temp.: 80 °C) for DIA runs. For DIA runs, a fixed compensation voltage of -45 V was used, while for PRM analysis, it was individually optimized for each of the 72 peptides (CVs used: -35, -40, -45, -50, -60, -70). Data-independent mode analysis was performed with the following settings: MS1 resolution of 60,000 within a scan range of 350 to 1,500; injection time of 100 ms and an AGC of 300% (3x10^6). Peptide spectrum generation involved 2x38 staggered MS2 scans with an isolation width of 16 m/z, encompassing precursors from 400 to 1,000 m/z, without overlap. The corresponding instrument settings were: 27% HCD collision energy, 30,000 resolution, 55 ms ion injection time, and an AGC target of 1,000% (1x106). Targeted analysis included PRM scans for light and heavy precursors with isolation widths of 1.6 m/z, a resolution of 60,000; 118 ms ion injection time, an AGC target of 1x10^5, and HCD collision energy set at 27%.

Raw data from DIA runs were processed in the Spectronaut software, while PRM data were analyzed in Skyline-daily. For relative quantification, transition areas were integrated and normalized to isotopically labeled heavy IS peptides. The normalized ratios, both at peptide and protein levels, were exported to Excel for computation of relative changes between groups.

4.6. m^6A/m quantification

The levels of m^6A/m (m^6A + m^6Am) in the total RNA samples extracted from the LVs from fasting rats were quantified using the EpiQuik m6A RNA Methylation Quantification Kit (Epigentek, USA) following the manufacturer's instructions. For each analysis, 300 ng of RNA was used. Absorbance measurements were taken at 450 nm using a Synergy™ HT Multi-Detection Microplate Reader (BioTek, USA) at 450 nm. The m^6A/m percentage in RNA was calculated using the formula: m^6A/m (%) = [(sample OD-negative control OD)/Slope]*100%. The results of this assay were described as m^6A/m levels since this technique does not distinguish between m^6A and m^6Am modifications [173].

4.7. m^{6}A RNA immunoprecipitation (MeRIP)

The immunoprecipitation of m^{6}A/m-modified RNA isolated either from LVs of control, hypoxic, or fasting rats was carried out using Magna MeRIP™ m^{6}A Kit (Merck Millipore, USA) in accordance with the manufacturer's guidelines. In brief, 80 µg of total RNA isolated from LVs was fragmented at 94 °C for 5 min following immunoprecipitation with magnetic beads at 4 °C for 2 h. Subsequently, samples were eluted with an elution buffer containing N^6-Methyladenosine, 5'-monophosphate sodium salt. The eluted RNA was purified using PureLink™ RNA Mini Kit (Thermo Fisher Scientific, USA). Genes potentially involved in hypoxia-induced cardioprotection were selected for analysis of MeRIPed RNA: *Akt1* (AKT serine/threonine kinase 1), *Foxo3* (forkhead box O3), *Hif1a* (hypoxia-inducible factor 1 subunit alpha), *Hk2* (hexokinase 2), *Nfe2l2* (NFE2 like BZIP transcription factor 2), *Pdk4* (pyruvate dehydrogenase kinase 4), *Ppara* (peroxisome proliferator activated receptor alpha), *Ppargc1a* (PPARG coactivator 1 alpha), and *Rela* (RELA proto-oncogene, NF-KB Subunit). Similarly, genes potentially involved in fasting-induced cardioprotection were selected [61]: *Foxo3*, *Hdac1* (histone deacetylase 1), *Hif1a*, *Nfe2l2*, *Nox4* (NADPH oxidase 4), *Prkaa2* (protein kinase AMP-activated catalytic subunit alpha 2), *Rela*, *Sirt1* (sirtuin 1), and *Sirt3* (sirtuin 3). The analysis was conducted through RT-qPCR as previously detailed using TaqMan Gene Expression Assays (Tab. 4; Thermo Fisher Scientific, USA).

Table 4. TaqMan Gene Expression Assays for MeRIP analysis

Gene	Catalog nr.	Assay ID	Specification
Akt1	4331182	Rn00583646_m1	FAM-MGB
Foxo3	4331182	Rn01441087_m1	FAM-MGB
Hdac1	4331182	Rn01519308_g1	FAM-MGB
Hif1a	4331182	Rn01472831_m1	FAM-MGB
Hk2	4331182	Rn00562457_m1	FAM-MGB
Nfe2l2	4331182	Rn00582415_m1	FAM-MGB
Nox4	4331182	Rn00585380_m1	FAM-MGB
Pdk4	4331182	Rn00585577_m1	FAM-MGB
Ppara	4331182	Rn00566193_m1	FAM-MGB
Ppargc1a	4331182	Rn00580241_m1	FAM-MGB
Prkaa2	4331182	Rn00576935_m1	FAM-MGB
Rela	4331182	Rn01502266_m1	FAM-MGB
Sirt1	4331182	Rn01428096_m1	FAM-MGB
Sirt3	4331182	Rn01501410_m1	FAM-MGB

Akt1 – AKT serine/threonine kinase 1; *Foxo3* – forkhead box O3; *Hdac1* – histone deacetylase 1; *Hif1a* – hypoxia inducible factor 1 subunit alpha; *Hk2* – hexokinase 2; *Nfe2l2* – NFE2 like BZIP transcription factor 2; *Nox4* – NADPH oxidase 4; *Pdk4* – pyruvate dehydrogenase kinase 4; *Ppara* – peroxisome proliferator activated receptor alpha; *Ppargc1a* – PPARG coactivator 1 alpha; *Prkaa2* – protein kinase AMP-activated catalytic subunit alpha 2; *Rela* – RELA proto-oncogene, NF-KB Subunit; *Sirt1/3* – sirtuin 1/3.

4.8. AVCM isolation and culture

The rats were administered heparin (5,000 U/kg, i.p.), anesthetized with pentobarbital (60 mg/kg, i.p.), and euthanized by cervical dislocation. The hearts were quickly removed and then perfused for 10 min with a Ca^{2+}-free buffer (10 mM KCl, 1.2 mM K_2HPO_4, 90 mM NaCl, 5 mM $MgSO_4$, 15 mM $NaHCO_3$, 20 mM glucose, and 30 mM taurine, pH 7.4). The medium was then switched to Ca^{2+}-free buffer containing collagenase Type 2 (8,000 U; Worthington, USA), bovine serum albumin (0.2%), and Ca^{2+} (50 µM). All solutions were gassed with a mix of 95% O_2 and 5% CO_2 30 min before their use. After a 60-min digestion period, the LVs were minced, and cardiomyocytes were separated using a sedimentation process in a buffer with gradually increasing Ca^{2+} concentration, reaching a final concentration of 1.2 mM. The isolated cardiomyocytes from the LVs were then carefully suspended in an M199 cell culture medium containing 5% fetal bovine serum, penicillin (100 U/ml), and streptomycin (100 µg/ml). These cells were placed in culture 96-well plates coated

with laminin (at 8,000 cells per well) and incubated (95% air and 5% CO_2 at 37 °C) for 2 h to allow attachment.

4.9. Inhibitors of ALKBH5 and FTO

Pharmacological inhibitors of ALKBH5 (ALKBH5i; [185]) and FTO (FTOi; MO-I-500; [186]) were dissolved in DMSO (dimethyl sulfoxide) as 50 mM and 1 mM stocks, respectively (chemical structure of inhibitors depicted in Fig. 11). Small aliquots were stored at 5 °C (ALKBH5i) and -20 °C (FTOi). DMSO (0.1% concentration) was used as vehicle control.

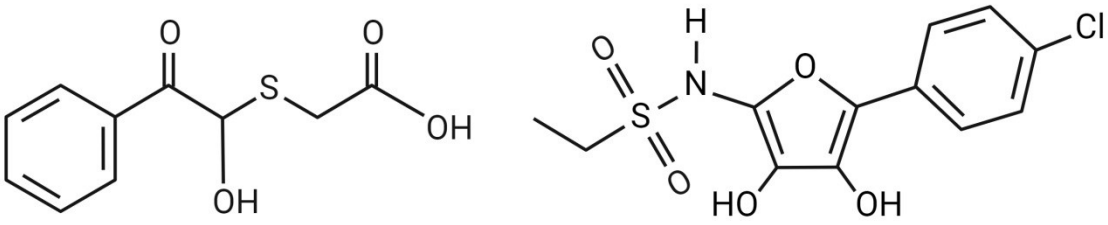

Fig. 11: Chemical structure of ALKBH5i (left) and FTOi (right). Created with BioRender.

The dose-response of the viability of AVCMs (adult ventricular cardiomyocytes) to ALKBH5i and FTOi was tested to select the suitable concentrations for *in vitro* experiments (Fig. 12). The viability of AVCMs was determined after 24 h incubation with ALKBH5i (10, 50, 75, 100, 150 μM) or FTOi (0.5, 1, 2.5, 5, 10, 50 μM) using SYTOX Green nucleic acid stain (S7020) (Invitrogen-Molecular Probes, USA). Based on these results, the 50 μM (ALKBH5i) and 1 μM (FTOi) concentrations, which did not significantly affect the viability of cells during 24 h incubation, have been chosen for the following experiments.

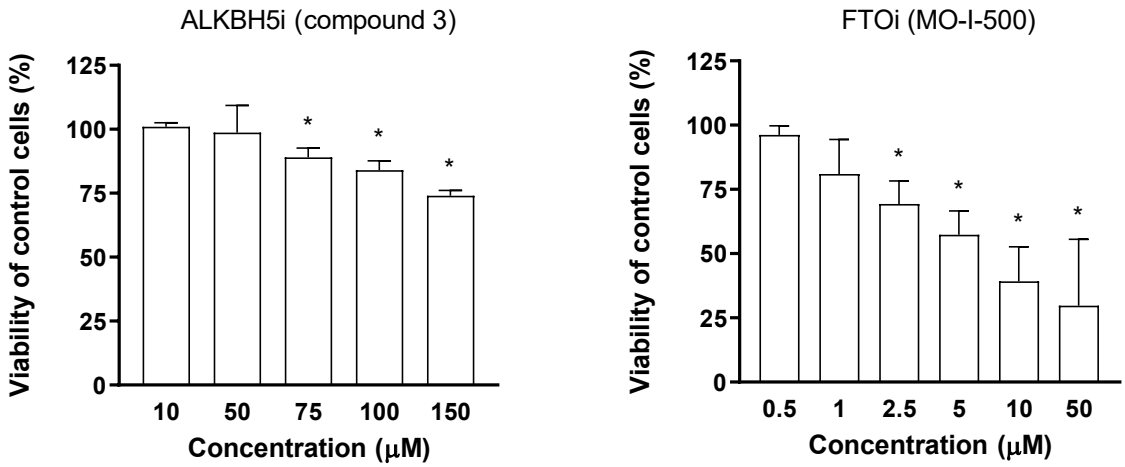

664
665 **Fig. 12:** Effect of different inhibitor concentrations (ALKBH5i and FTOi) on the viability of
666 AVCMs. Values are means ± S.D.; n = 3 – 10; * $p < 0.05$ vs. control group.

667 ## 4.10. Cardiomyocyte tolerance to hypoxia

668 AVCMs from both control and fasting rats were placed in the Xvivo System X3 hypoxic
669 chamber (BioSpherix, USA) and exposed to low oxygen conditions (1% O_2; 5% CO_2; 37 °C) for 24 h.
670 They were cultured in an M199 medium containing either 50 μM ALKBH5i, 1 μM FTOi, or 0.01%
671 DMSO. Control AVCMs were incubated under normoxic conditions (95% air, 5% CO_2, 37 °C) with or
672 without the inhibitors. The survival rate of AVCMS was compared to the untreated normoxic cells.
673 This was assessed using the SYTOX Green nucleic acid stain (S7020) (Invitrogen-Molecular Probes,
674 USA) at the start (after stabilization), after 24 h of treatment, and finally after exposure to 8% Triton
675 X-100 [187]. The survival rate was inferred from the cell membrane integrity, indicated by the
676 inverse relationship of the cells' overall fluorescence. The fluorescence of SYTOX Green was
677 measured at an excitation wavelength of 490 nm and an emission wavelength of 520 nm. This was
678 done in 96-well laminin-coated plates (at 8,000 cells per well) using the Synergy™ HT Multi-
679 Detection Microplate Reader (BioTek, USA).

4.11. Statistical analyses

Each experiment encompassed 6-10 biological replicates per group, with the exception of the MeRIP analysis which had only 3 replicates (due to high demands on the quantity of input material and need to pool samples – each replicate is from 3-4 samples). Statistical evaluations were conducted using GraphPad Prism 8 (GraphPad Software, USA). Data were represented as means ± SD. For the comparison of two groups, an unpaired two-sided Student's t-test was utilized. For comparisons among three or more groups, a one-way ANOVA followed by Tukey's multiple comparisons test was used. A p-value of ≤ 0.05 was considered to indicate statistical significance.

5. RESULTS

5.1. Effect of adaptation to chronic hypoxia on m^{6}A and m^{6}Am regulators in the left ventricles

The transcript levels (assessed by RT-qPCR) of m^{6}A and m^{6}Am regulators were mostly not affected by adaptation to CNH (Fig. 13). The only significantly up-regulated transcript was *Ythdc1* (14% increase), whereas *Ythdf3* was increased (by 22%) at the edge of significance (p = 0.06).

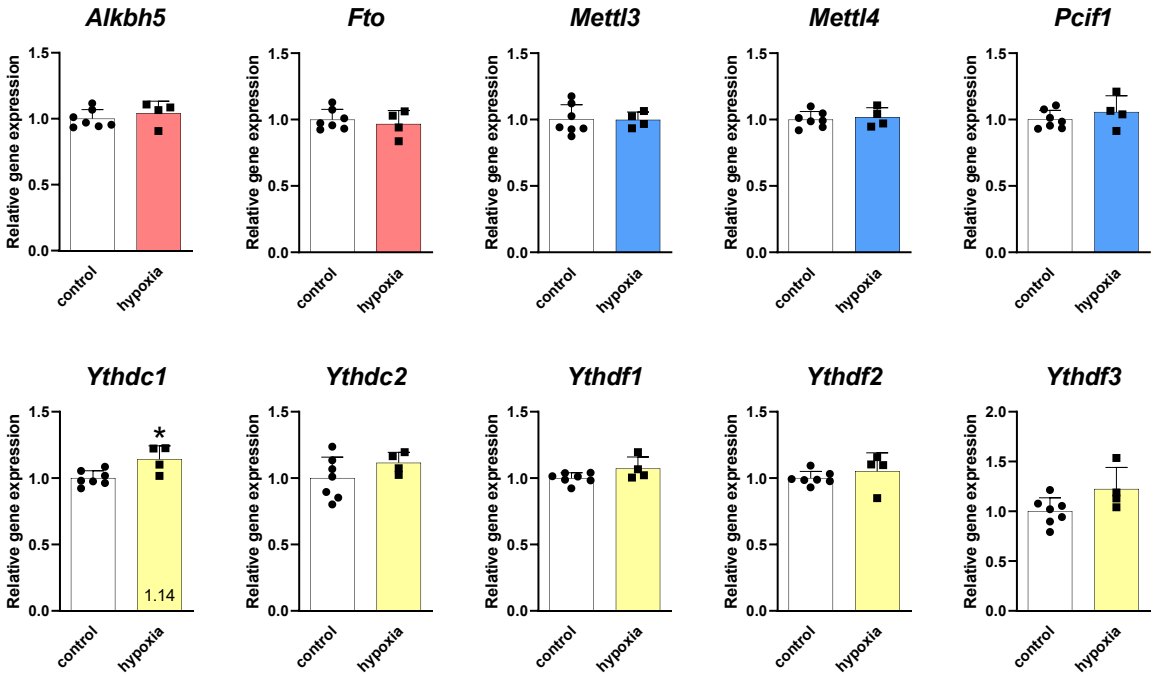

Fig. 13: Effect of adaptation to chronic hypoxia on gene expressions of m^{6}A and m^{6}Am regulators in the left ventricle assessed by RT-qPCR. Erasers are displayed in red, writers in blue, and readers in yellow. The average of the control values is set to 1. Values are means ± SD; n = 4-7; * p < 0.05 (t-test). *Alkbh5* – alkB family member 5; *Fto* – fat mass and obesity-associated; *Mettl3/4* – methyltransferase-like 3/4; *Pcif1* – phosphorylated CTD interacting factor 1; *Ythdf1-3* – YTH domain-containing family protein 1-3; *Ythdc1/2* – YTH domain-containing protein 1/2.

The protein levels (assessed by WB) of m^{6}A and m^{6}Am modifiers were regulated in rat LVs under hypoxic conditions (Fig. 14). Both demethylases increased their levels – ALKBH5 by 106% and FTO by 77%. Out of the methyltransferases, only METTL4 was affected (21% decrease). Readers YTHDC1, YTHDF1, YTHDF2, and YTHDF3 were up-regulated by 58%, 99%, 110%, and 82%,

respectively. Other proteins (METTL3, PCIF1, YTHDC2) remained stable under experimental conditions.

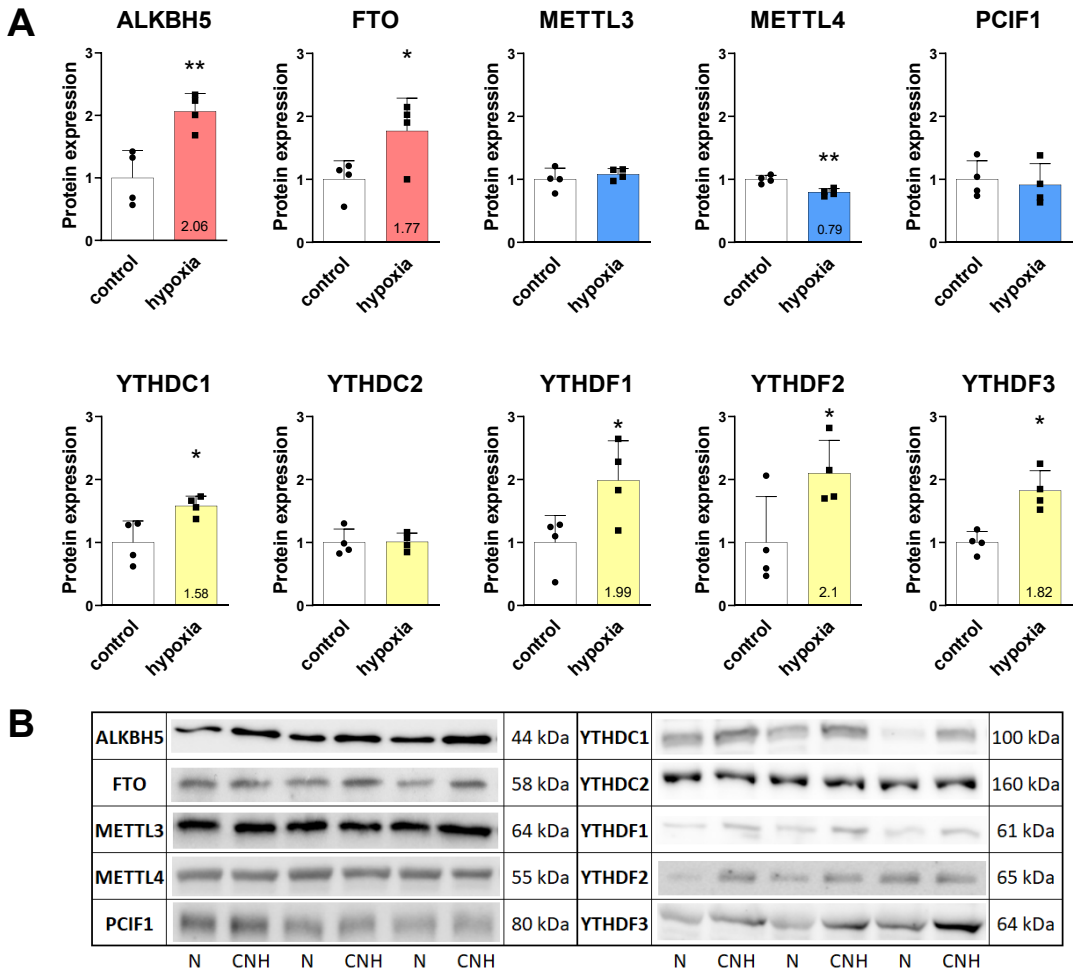

Fig. 14: Effect of adaptation to chronic hypoxia on protein levels of m^6A and m^6Am regulators in the left ventricles assessed by Western blot (A). Erasers are displayed in red, writers in blue, and readers in yellow. The average of the control values is set to 1. Representative Western blot membranes (B). Protein loadings were 40 µg (YTHDF1, YTHDF3), 30 µg (YTHDC1), 20 µg (FTO, ALKBH5, YTHDC2), 15 µg (METTL3, YTHDF2), and 10 µg (METTL4, PCIF1). Values are means ± SD; n = 4; * $p < 0.05$; ** $p < 0.01$ (t-test). ALKBH5 – alkB family member 5; C – control; F – fasting; FTO – fat mass and obesity-associated protein; METTL3/4 – methyltransferase-like 3/4; PCIF1 – phosphorylated CTD interacting factor 1; YTHDF1-3 – YTH domain-containing family protein 1-3; YTHDC1/2 – YTH domain-containing protein 1/2.

Our study, though observing some variations in the data derived from the two different methodologies, indicates that the epitranscriptomic mechanisms in LVs of rats are influenced by adaptation to chronic hypoxia (Fig. 15). The discrepancies observed between the levels of transcripts and proteins may be attributed to distinct regulatory mechanisms at the transcriptional

and translational stages. Moreover, since adaptation to chronic hypoxia is a prolonged protocol, transcript levels could be already normalized.

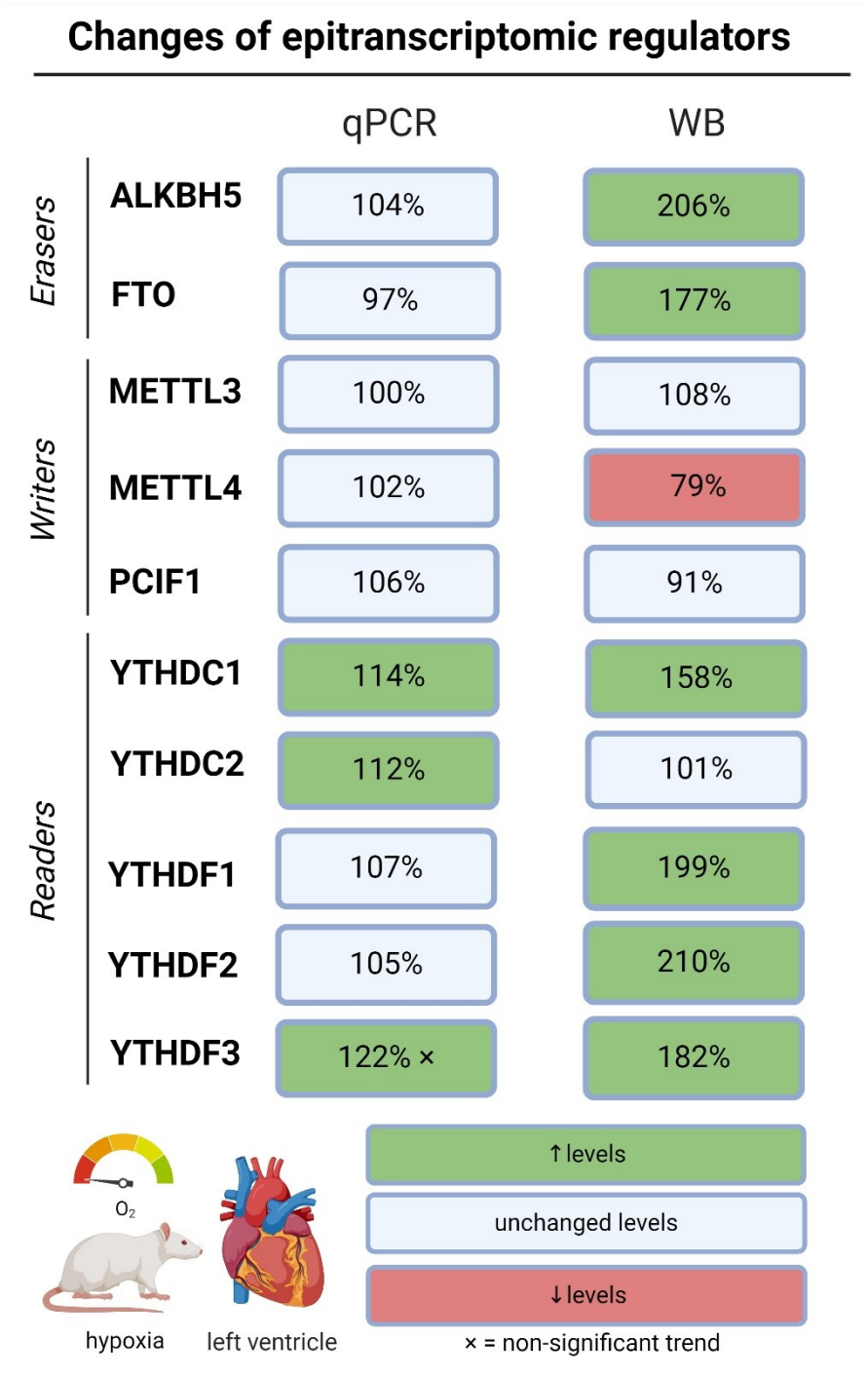

Fig. 15: Levels of m^{6}A and m^{6}Am regulators in the left ventricles of rats adapted to chronic hypoxia assessed by RT-qPCR (qPCR) and Western blot (WB). ALKBH5 – alkB family member 5; FTO – fat mass and obesity-associated protein; METTL3/4 – methyltransferase-like 3/4; PCIF1 – phosphorylated CTD interacting factor 1; YTHDF1-3 – YTH domain-containing family protein 1-3; YTHDC1/2 – YTH domain-containing protein 1/2. Created with BioRender.

5.2. Effect of chronic hypoxia on global m^{6}A/m methylation levels in the left ventricles

The impact of adaptation to chronic hypoxia and fasting on m^{6}A/m methylation of total RNA was assessed in LV samples obtained from both experimental and control rats. Under our conditions, adaptation to chronic hypoxia did not alter the global methylation levels (Fig. 16).

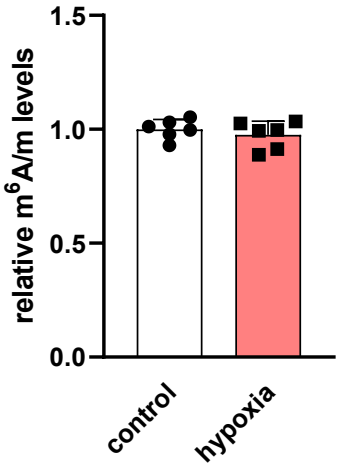

Fig. 16: Global m^{6}A/m levels in the left ventricles of rats adapted to chronic hypoxia. Total RNA was used for this analysis. Values are means ± SD; n = 6.

5.3. Methylation status of transcripts associated with cytoprotective effects of chronic hypoxia

Neither of the selected transcripts (*Akt1*, *Foxo3*, *Hif1a*, *Hk2*, *Nfe2l2*, *Pdk4*, *Ppara*, *Ppargc1a*, *Rela*) was differentially methylated in hypoxic samples (Fig. 17).

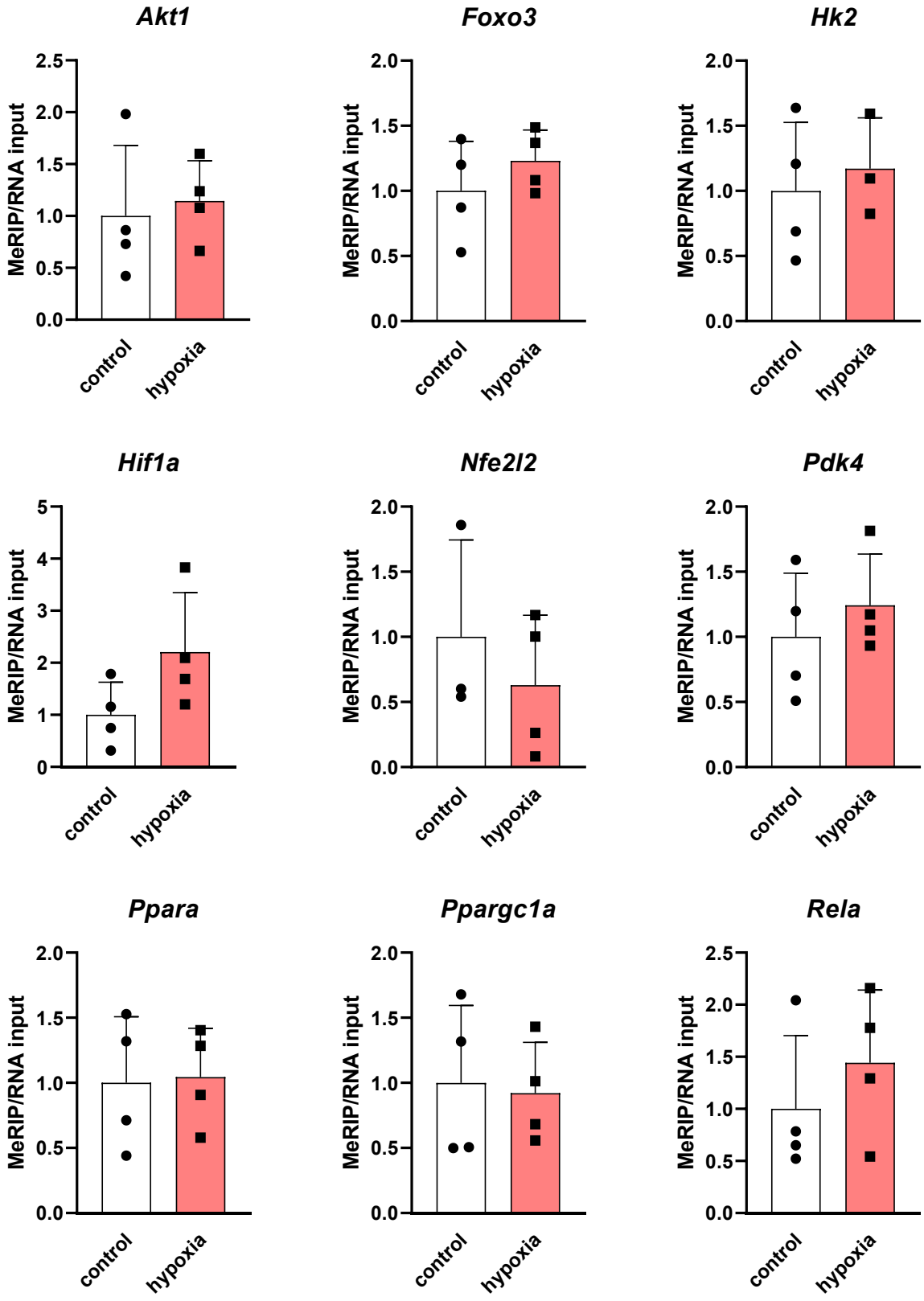

741

742 **Fig. 17**: The m^{6}A/m levels in specific mRNAs isolated from the left ventricles of control and
743 hypoxic rats. The average of the control values is set to 1. Values are means ± SD; n = 3-4; ** p <
744 0.01 (t-test). *Akt1* – AKT serine/threonine kinase 1; *Foxo3* – forkhead box O3; *Hif1a* – hypoxia

inducible factor 1 subunit alpha; *Hk2* – hexokinase 2; *Nfe2l2* – NFE2 like BZIP transcription factor 2; *Pdk4* – pyruvate dehydrogenase kinase 4; *Ppara* – peroxisome proliferator activated receptor alpha; *Ppargc1a* – PPARG coactivator 1 alpha; *Rela* – RELA proto-oncogene, NF-KB Subunit.

5.4. Summary of the chronic hypoxia model results

We showed that the adaptation to 3-week chronic hypoxia affected mostly the protein levels of epitranscriptomic regulators. However, neither total m^6A/m levels nor methylation levels of specific selected transcripts differed.

5.5. Characteristics of the 3-day fasting model

Information in this subsection of Results primarily serves to define the parameters of the experimental model and does not relate to the epitranscriptomic regulations, the main topic of this thesis. Therefore, while these data are briefly elaborated here for contextual understanding, they are not further discussed in the Discussion section. This approach is taken to maintain clarity and focus, ensuring that the discussion remains closely aligned with the central theme of epitranscriptomic regulations, without delving into the detailed intricacies of the experimental model unless directly relevant.

5.5.1. The lipidomic and metabolomic profiling of plasma samples from fasting rats

The lipidomic and metabolomic analysis identified a total of 677 distinct metabolites. Among these, 171 metabolites were down-regulated and 79 up-regulated (Fig. 18). The down-regulated metabolites included mostly triacylglycerols, proline, hippuric acid, phosphatidylinositols, phosphatidylcholines, and lysophosphatidylcholines. These components are typically associated with various metabolic processes, including energy storage and membrane structure. The up-regulated metabolites included free fatty acids, acylcarnitines, and 3-hydroxybutyric acid. This increase in free fatty acids and acylcarnitines suggests an enhanced breakdown of lipids for energy, which is a common response in states of nutrient deprivation. Furthermore, the elevation in 3-hydroxybutyric acid levels is indicative of ketogenesis – a metabolic pathway that becomes prominent during fasting. Ketone bodies like 3-hydroxybutyric acid are produced in the liver from

fatty acids and serve as an alternative energy source during periods when glucose availability is low. These data therefore confirmed a metabolic shift towards lipid utilization and also the production of ketone bodies, which is a characteristic of a fasting state [31, 188].

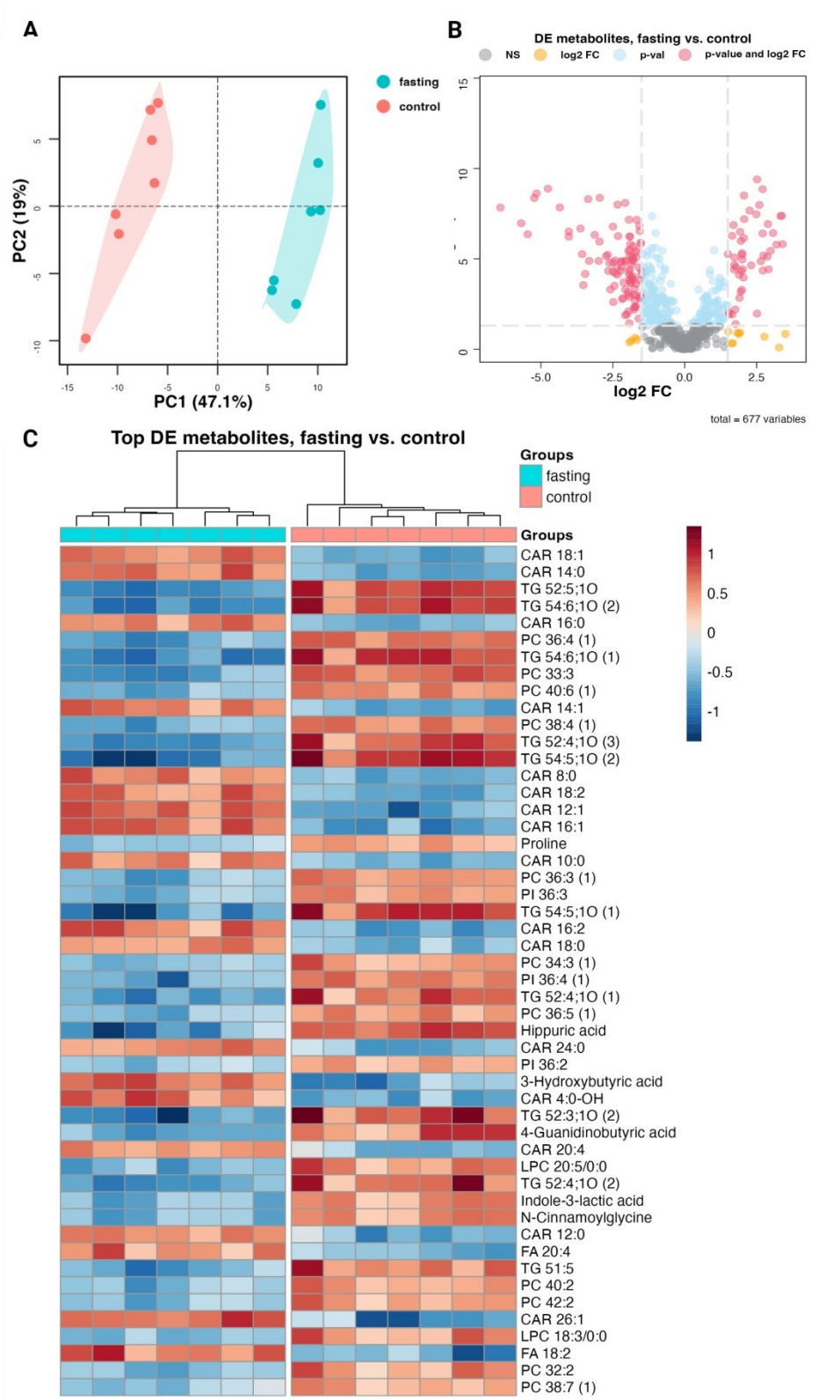

Fig. 18: Effect of fasting on plasma metabolites measured by a multiplatform LC-MS-based approach A) PCA (principal component analysis) showing a clear separation between fasting and control rat plasma samples, suggesting distinct metabolomic profiles associated with the fasting state B) Volcano plot of all (677) metabolites indicating differential levels of metabolites in plasma samples of fasting and control rats C) Heat map of the 50 top significantly changed metabolites; n = 7. Taken from Benak et al. [183] (Attachment IV).

5.5.2. The proteomic analysis of left ventricles from fasting rats

The proteomic analysis captured 4,652 proteins in total, 127 of which were down-regulated and 118 up-regulated (Fig. 19). This analysis primarily highlights significant adaptations in metabolic pathways typical for fasting. According to the KEGG database (Fig. 20), key findings include the activation of the peroxisome pathway (17 affected proteins), indicating enhanced fatty acid oxidation, a critical metabolic shift during fasting when the body relies more on fatty acids instead of glucose for energy. Additionally, the biosynthesis of unsaturated fatty acids was also affected (6 affected proteins), reflecting the heart's metabolic flexibility in utilizing different lipid species for energy. There was also notable involvement of the complement and coagulation cascades (11 affected proteins), suggesting changes in the cardiac immune response and blood clotting mechanisms, which may be adaptive responses to protect the heart under nutrient-deprived conditions. These insights point to a complex interplay of metabolic and immune processes in the heart during fasting. Interestingly, the HIF-1 signaling pathway was also affected in LVs from fasting rats (5 affected proteins) which suggests a complex adaptive response to maintain cardiac function and integrity. It indicates a switch to more hypoxia-tolerant metabolic pathways, possibly as a way to conserve energy and protect heart tissue during the nutritional stress of fasting. Furthermore, this overlap in the HIF-1 signaling pathway during fasting underscores a potential shared mechanism in promoting increased hypoxic tolerance, as observed in both chronic hypoxia and fasting conditions.

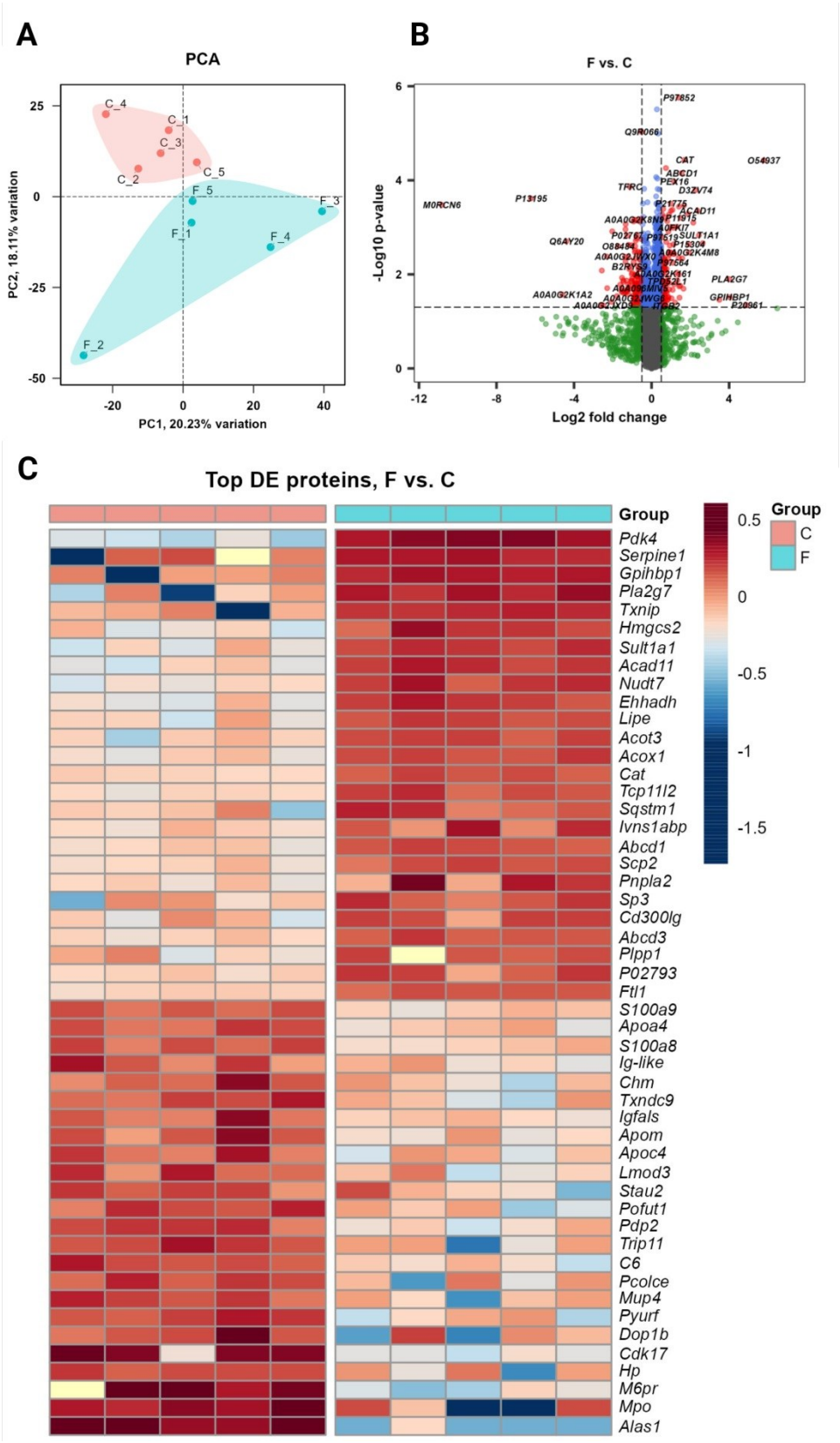

Fig. 19: Effect of fasting on cardiac proteomic profile A) PCA (principal component analysis) showing a clear separation between fasting and control proteomic profiles, suggesting distinct proteomic profiles associated with the fasting state B) Volcano plot of all (4652) metabolites indicating differential levels of proteins in cardiac samples of fasting and control rats C) Heat map of the 50 top significantly changed proteins; n = 5.

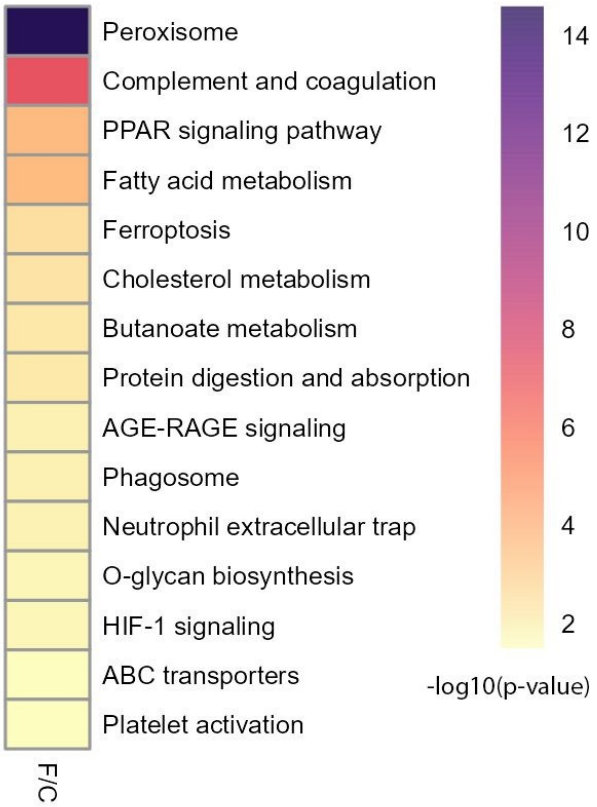

Fig. 20: KEGG Annotation heat map of the main pathways affected by fasting.

5.5.3. Geometry and function of hearts of fasting rats

The echocardiographic evaluation of the heart geometry and function (Tab. 5) revealed no significant differences in wall thickness between control and fasting rats. LVDd was decreased in fasting rats, while LVDs remained similar in both groups. Fasting rats exhibited lower FS and HR. However, CI, which measures cardiac output relative to BW, did not show a notable difference between the two groups. LV catheterization indicated no significant differences in Pes or Ped between the experimental groups. Fasting did not significantly alter the developed pressure in the heart. Although $+(dP/dt)_{max}$ was reduced in fasting rats, $-(dP/dt)_{max}$ was not impacted by fasting.

Overall, while fasting led to some changes like decreased heart size, key parameters related to heart functionality, such as wall thickness, CI, and developed pressure, were not significantly affected by the 3-day fasting period. This suggests that 3-day fasting might not have a drastic impact on the overall functionality of the heart in rats.

820 **Table 5.** Characteristics of the fasting model

	Control rats	Fasting rats		
BW change (%)	3 ± 2.16	-17 ± 2.22*		
HW/Tibia (%)	25.5 ± 1.50	22 ± 1.47***		
Hematocrit (%)	40.3 ± 4.49	45.6 ± 2.97*		
Glycemia (mmol/l)	6.2 ± 0.43	D1 3.5 ****	D2 3.7****	D3 3.9****
AWTd (mm)	1.96 ± 0.13	1.85 ± 0.15		
AWTs (mm)	2.81 ± 0.09	2.66 ± 0.23		
PWTd (mm)	1.83 ± 0.13	1.90 ± 0.19		
PWTs (mm)	2.71 ± 0.14	2.67 ± 0.24		
RWT (%)	49.88 ± 5.59	51.41 ± 3.67		
LVDd (mm)	7.63 ± 0.42	7.23 ± 0.17*		
LVDs (mm)	4.64 ± 0.27	4.72 ± 0.22		
FS (%)	39.9 ± 1.8	35.1 ± 3.4*		
HR (bpm)	350 ± 19.9	327 ± 22*		
CI (ml/min/kg)	306 ± 62	276 ± 33		
Pes (mmHg)	86.63 ± 5.69	89.38 ± 4.34		
Ped (mmHg)	4.00 ± 1.38	4.28 ± 2.25		
Pdev (mmHg)	82.63 ± 4.88	85.10 ± 4.47		
+(dP/dt)$_{max}$ (mmHg/s)	7,008 ± 529	5,453 ± 417*		
-(dP/dt)$_{max}$ (mmHg/s)	-7,080 ± 529	-6,592 ± 616		

821

822 Values are means ± SD; n = 8-10; * $p < 0.01$; *** $p < 0.001$, **** $p < 0.0001$. AWTd – end-
823 diastolic anterior wall thickness; AWTs – end-systolic anterior wall thickness; bpm – beats per

minute; BW – body weight; CI – cardiac index; FS – fractional shortening; HR – heart rate; HW – heart weight; LVDd – end-diastolic LV diameter; LVDs – end-systolic LV diameter; Ped – end-diastolic pressure; Pes – end-systolic pressure; Pdev – developed pressure; PWTd – end-diastolic posterior wall thickness; PWTs – end-systolic posterior wall thickness; RWT – relative wall thickness; +(dP/dt)max – peak rate of pressure development; -(dP/dt)max – peak rate of pressure decline. Taken from Benak et al. [183] (Attachment IV).

5.6. Effect of fasting on m^{6}A and m^{6}Am regulators in the left ventricles

After fasting, the changes were more pronounced compared to CNH adaptation (Fig. 21). Transcript levels of both demethylases were increased – *Alkbh5* by 23% and *Fto* by 17%. Among the writers, *Mettl3* increased by 26%, and *Pcif1* by 22%. Regarding readers, *Ythdc1* levels increased by 23% and *Ythdf3* levels decreased by 15%. Other transcripts (*Mettl4*, *Ythdc2, Ythdf1*, *Ythdf2*) remained stable in the LVs of fasting rats.

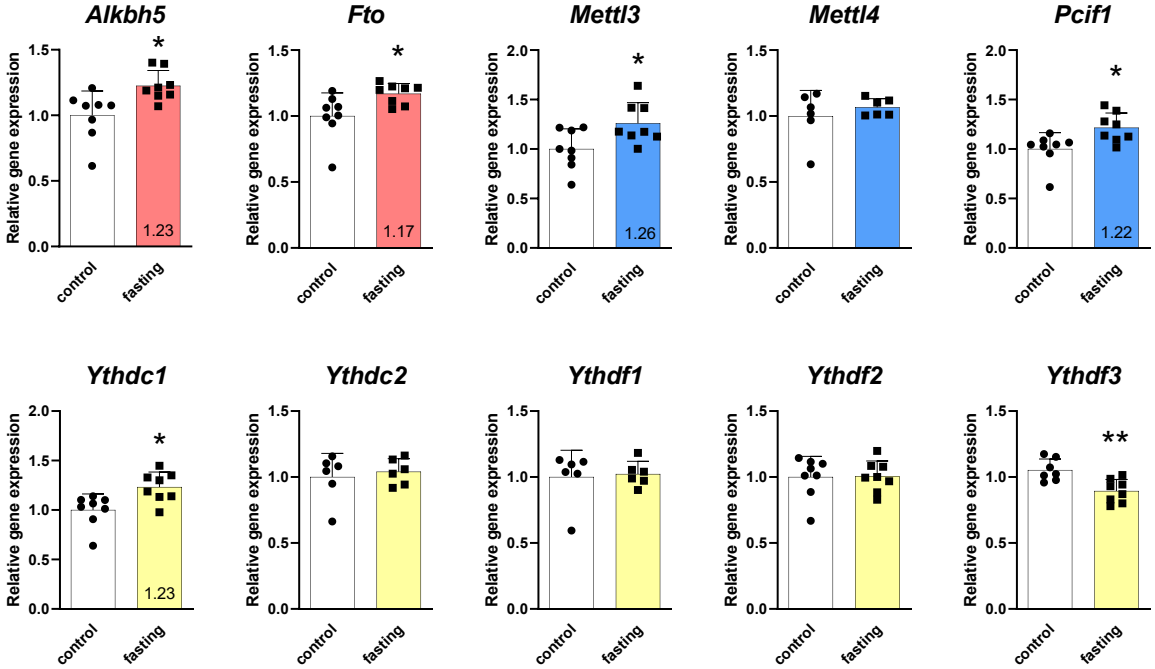

Fig. 21: Effect of fasting on gene expressions of m^{6}A and m^{6}Am regulators in the left ventricle assessed by RT-qPCR. Erasers are displayed in red, writers in blue, and readers in yellow. The average of the control values is set to 1. Values are means ± SD; n = 6-8; * $p < 0.05$; ** $p < 0.01$ (t-test). *Alkbh5* – alkB family member 5; *Fto* – fat mass and obesity-associated; *Mettl3/4* – methyltransferase-like 3/4; *Pcif1* – phosphorylated CTD interacting factor 1; *Ythdf1-3* – YTH domain-containing family protein 1-3; *Ythdc1/2* – YTH domain-containing protein 1/2. Taken from Benak et al. [183] (Attachment IV).

Protein levels of cardiac m^{6}A and m^{6}Am modifiers were also vastly affected by fasting (Fig. 22). Both demethylases were up-regulated – ALKBH5 by 65% and FTO by 22%. Regarding

methyltransferases, only PCIF1 was regulated (23% decrease). Readers YTHDF1, YTHDF2, YTHDF3, and YTHDC2 were increased by 67%, 74%, 74%, and 71%, respectively. Other proteins (METTL3, METTL4, YTHDC1) remained stable after fasting.

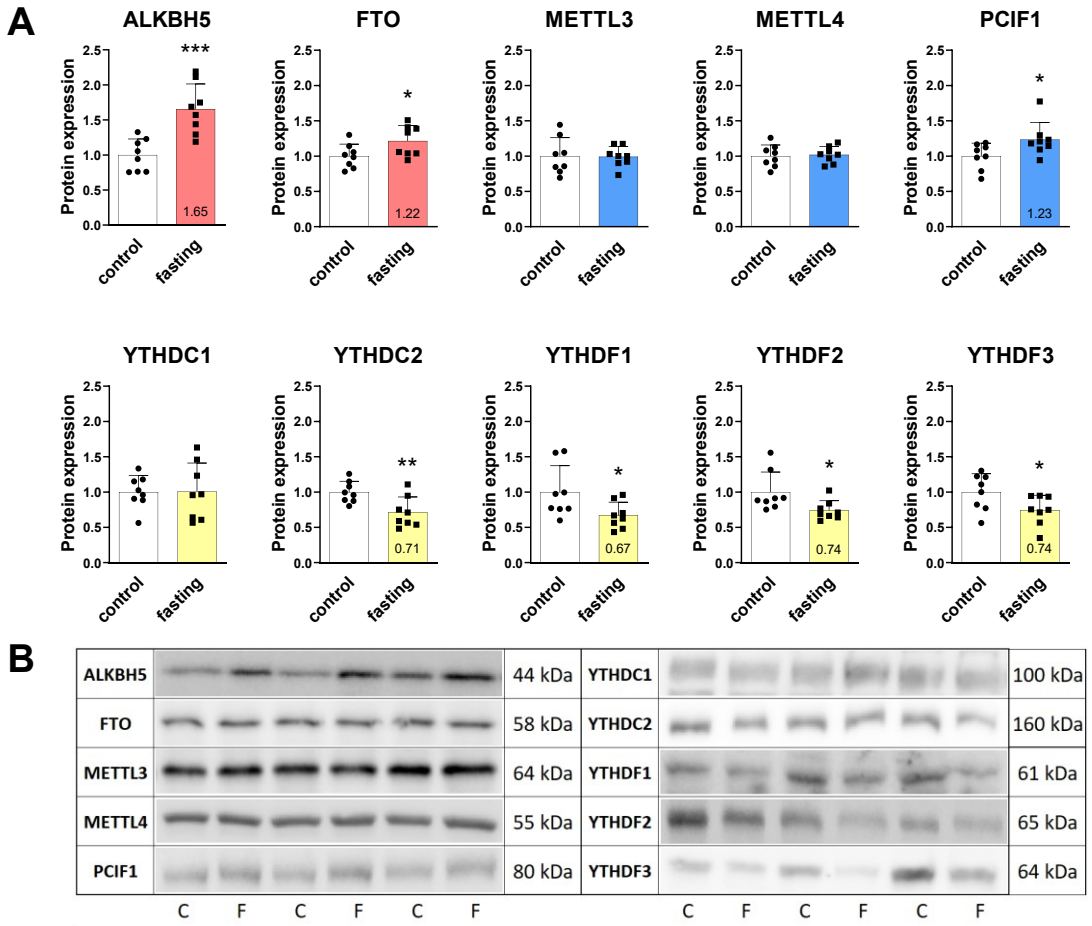

Fig. 22: Effect of fasting on protein levels of m^6A and m^6Am regulators in the left ventricles assessed by Western blot (A). Erasers are displayed in red, writers in blue, and readers in yellow. The average of the control values is set to 1. Representative Western blot membranes (B). Protein loadings were 40 µg (YTHDF1, YTHDF3), 30 µg (YTHDC1), 20 µg (FTO, ALKBH5, YTHDC2), 15 µg (METTL3, YTHDF2), and 10 µg (METTL4, PCIF1). Values are means ± SD; n = 8; * $p < 0.05$; ** $p < 0.01$; *** $p < 0.001$ (t-test). ALKBH5 – alkB family member 5; C – control; F – fasting; FTO – fat mass and obesity-associated protein; METTL3/4 – methyltransferase-like 3/4; PCIF1 – phosphorylated CTD interacting factor 1; YTHDF1-3 – YTH domain-containing family protein 1-3; YTHDC1/2 – YTH domain-containing protein 1/2. Taken from Benak et al. [183] (Attachment IV).

Regarding the proteomic analysis, a total of 49 peptides were detected in fasting samples and 18 of these peptides were significantly affected by fasting, while 3 peptides levels were altered at the edge of significance (Fig. 23). Out of the 2 peptides measured for each protein, the peptide with more major changes was mentioned further in the text.

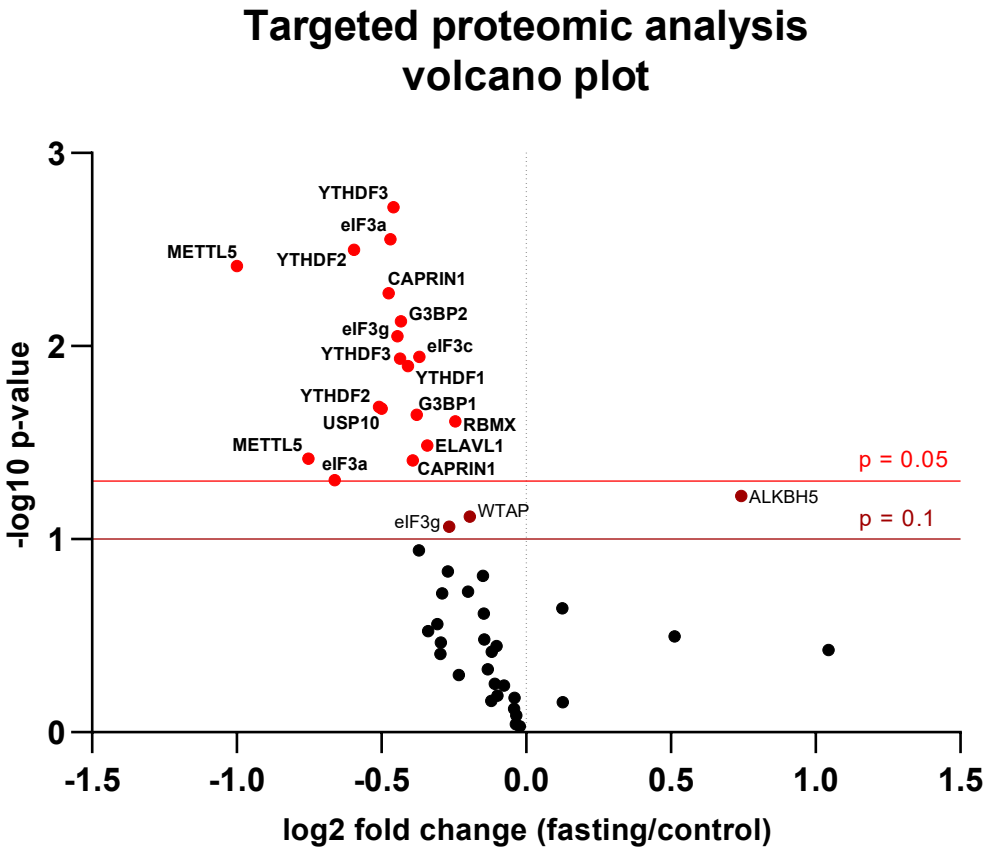

863

864 **Fig. 23**: Effect of fasting on peptide levels of m^{6}A and m^{6}Am regulators in the left ventricles
865 assessed by targeted proteomic analysis. ALKBH5 – alkB family member 5; CAPRIN1 – cell cycle
866 associated protein 1; eIF3a/c/g – eukaryotic initiation factor 3a/c/g; ELAVL1 – ELAV-like protein 1;
867 G3BP1/2 – G3BP stress granule assembly factor 1/2; RBMX – RNA-binding motif protein, X
868 chromosome; USP10 – ubiquitin specific peptidase 10; WTAP – Willms' tumor 1-associating protein;
869 YTHDC1 – YTH domain-containing protein 1; YTHDF1-3 – YTH domain-containing family protein 1-
870 3.

871 Concerning the main regulators (measured by RT-qPCR and WB), peptide levels of all YTHDF
872 readers exhibited a decrease: YTHDF1 by 25%, YTHDF2 by 34%, and YTHDF3 by 27%. While
873 demethylase ALKBH5, methyltransferase PCIF1, and reader YTHDC2 showed no significant change,
874 observable trends were evident (increasing in ALKBH5, PCIF1; decreasing in YTHDC2). Beyond the
875 main regulators, the proteomic analysis unveiled significant down-regulation in the peptide levels
876 of other crucial proteins within the m^{6}A machinery: methyltransferase METTL5 (by 50%); readers
877 eIF3a (by 37%), eIF3g (by 26%), eIF3c (by 23%), and RBMX (by 16%); and repelled proteins USP10
878 (by 29%), CAPRIN1 (by 28%), G3BP2 (by 26%), G3BP1 (by 23%), and ELAVL1 (by 21%). All peptide
879 changes with p-value < 0.1 are listed in Tab. 6.

Table 6. Targeted proteomic analysis in LVs from fasting rats – changes in peptide levels

Changes in peptide levels of epitranscriptomic regulators				
Protein	**Protein Accession**	**Peptide**	**Change**	**P-value**
		Writers		
METTL5	B0BNB3	LFDTVIMNPPFGTK	-50%	0.004
		YDLPALYNFHK	-41%	0.038
WTAP	D3ZPY0	TTSSEPVDQAEATSK	-13%	0.076 ×
		Erasers		
ALKBH5	D3ZKD3	YFFGEGYTYGAQLQK	67%	0.060 ×
		Readers		
eIF3a	Q1JU68	ALEVIKPAHILQEK	-37%	0.049
YTHDF2	E9PU11	LGSTEVASSVPK	-34%	0.003
		APGMNTIDQGMAALK	-30%	0.021
eIF3a	Q1JU68	LLDMDGIIVEK	-28%	0.003
YTHDF3	D3ZIY3	AITDGQAGFGNDTLSK	-27%	0.002
eIF3g	Q5RK09	GFAFISFHR	-26%	0.009
YTHDF3	D3ZIY3	HTTSIFDDFAHYEK	-26%	0.012
YTHDF1	Q4V8J6	HTTSIFDDFSHYEK	-25%	0.013
eIF3c	B5DFC8	LNEILQVR	-23%	0.011
RBMX	Q4V898	GGHMDDGGYSMNFTLSSSR	-16%	0.025
eIF3g	Q5RK09	LPGELEPVQAAQNK	-17%	0.086 ×
		m^6A-repelled proteins		
USP10	Q3KR59	QADFVQTPITGIFGGHIR	-29%	0.021
CAPRIN1	Q5M9G3	TVLELQYVLDK	-28%	0.005
G3BP2	Q6AY21	VDAKPEVQSQPPR	-26%	0.007
CAPRIN1	Q5M9G3	YQEVTNNLEFAK	-24%	0.039
G3BP1	D3ZYS7	DFFQSYGNVVELR	-23%	0.023
ELAVL1	B5DF91	VAGHSLGYGFVNYVTAK	-21%	0.033

The key regulators are in bold. Changes at the edge of significance are marked by '×'. ALKBH5 – alkB family member 5; CAPRIN1 – cell cycle associated protein 1; eIF3a/c/g – eukaryotic initiation factor 3a/c/g; ELAVL1 – ELAV-like protein 1; G3BP1/2 – G3BP stress granule assembly factor 1/2; RBMX – RNA-binding motif protein, X chromosome; USP10 – ubiquitin specific peptidase 10; WTAP – Willms' tumor 1-associating protein; YTHDC1 – YTH domain-containing protein 1; YTHDF1-3 – YTH domain-containing family protein 1-3. Taken from Benak et al. [183] (Attachment IV).

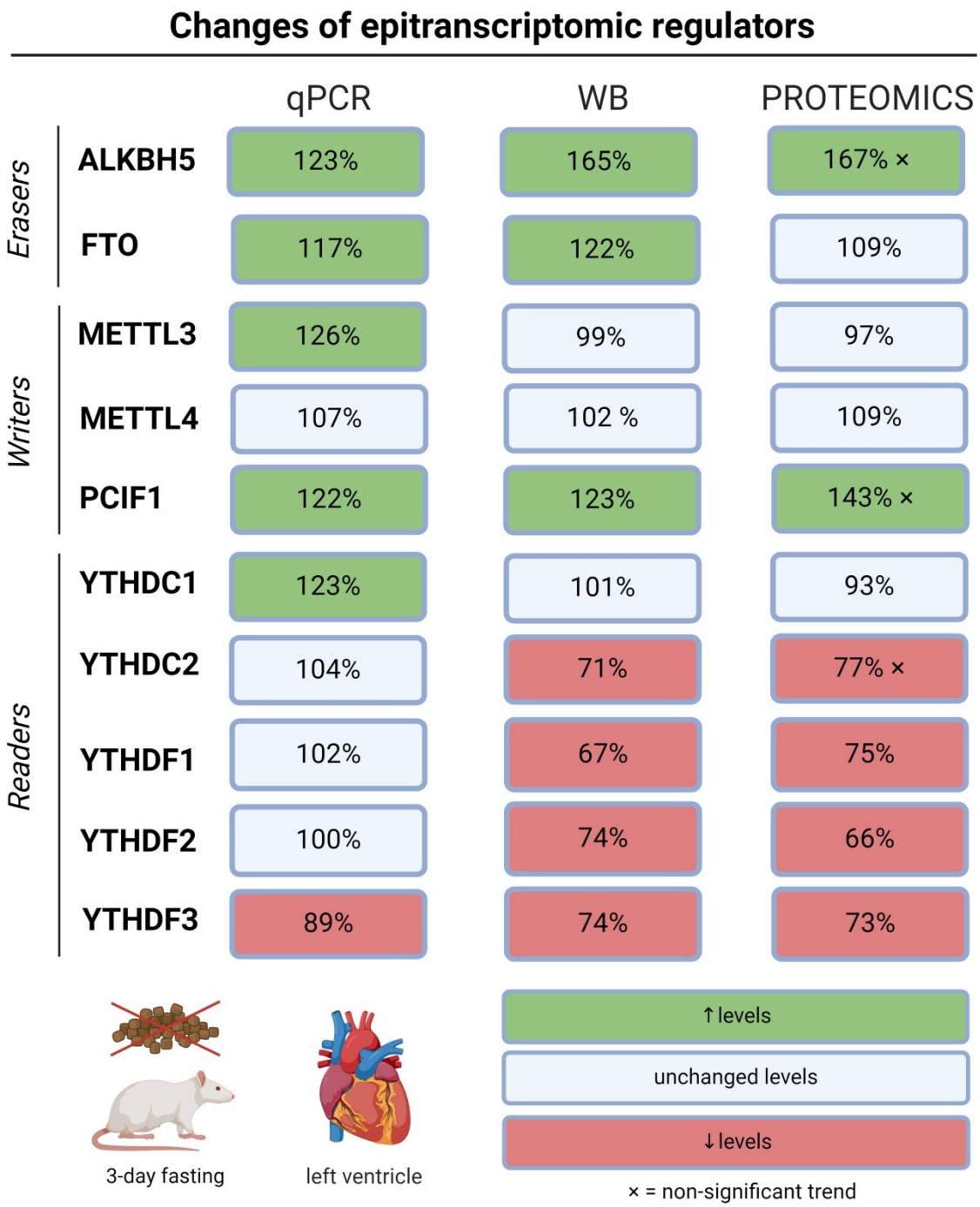

888

889 **Fig. 24**: Levels of m^{6}A and m^{6}Am regulators in the left ventricles of fasting rats assessed by
890 RT-qPCR (qPCR), Western blot (WB), and targeted proteomic analysis (proteomics). Out of the two
891 peptides measured for each protein in proteomic analysis, the peptide with more profound changes
892 was displayed. ALKBH5 – alkB family member 5; FTO – fat mass and obesity-associated protein;
893 METTL3/4 – methyltransferase-like 3/4; PCIF1 – phosphorylated CTD interacting factor 1; YTHDF1-
894 3 – YTH domain-containing family protein 1-3; YTHDC1/2 – YTH domain-containing protein 1/2.
895 Created with BioRender. Taken from Benak et al. [183] (Attachment IV).

896 Despite the slight variations in the data from three different methods, our data indicate

897 that the epitranscriptomic mechanisms in LVs of rats are influenced by fasting (Fig. 24). The

discrepancies observed between the levels of transcripts and proteins may be attributed to distinct regulatory mechanisms at the transcriptional and translational stages.

5.7. Effect of fasting on the global m^{6}A/m methylation levels in the left ventricles

The impact of adaptation to chronic hypoxia and fasting on m^{6}A/m methylation in total was assessed in LV samples obtained from both experimental and control rats. Fasting resulted in a significant decrease, reducing the methylation levels by 27% (Fig. 25).

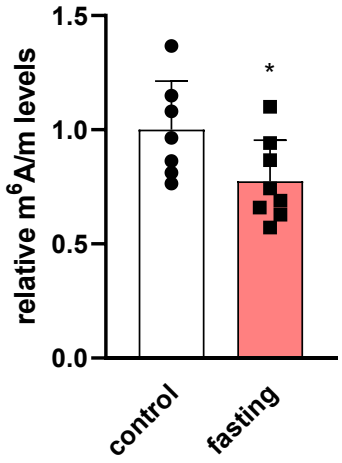

Fig. 25: Global m^{6}A/m levels in the left ventricles of fasting rats. Total RNA was used for this analysis. Values are means ± SD; n = 8; * $p < 0.05$. Taken from Benak et al. [183] (Attachment IV).

5.8. Methylation status of transcripts associated with cytoprotective effects of fasting

In fasting samples, a significant increase in methylation was observed in the case of *Nox4* (5.6-fold) and *Hdac1* (4.3-fold). Other transcripts (*Foxo3*, *Hif1a*, *Nfe2l2*, *Prkaa2*, *Rela*, *Sirt1*, *Sirt3*) did not change significantly, however, an increasing trend was evident (Fig. 26).

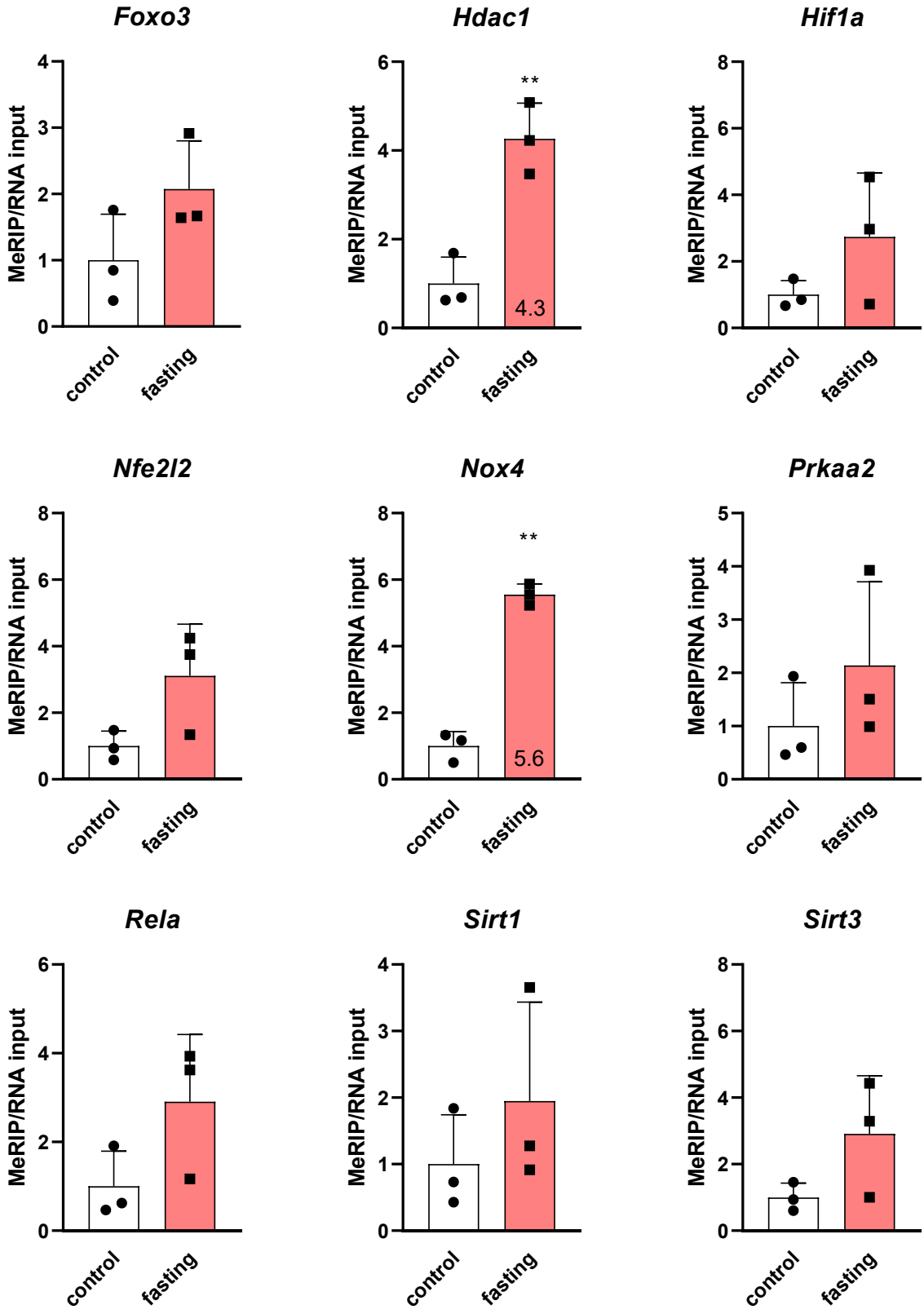

Fig. 26: The m^{6}A/m levels in specific mRNAs isolated from the left ventricles of control and fasting rats. The average of the control values is set to 1. Values are means ± SD; n = 3; ** $p < 0.01$ (t-test). *Foxo3* – forkhead box O3; *Hdac1* – histone deacetylase 1; *Hif1a* – hypoxia inducible factor 1 subunit alpha; *Nfe2l2* – NFE2 like BZIP transcription factor 2; *Nox4* – NADPH oxidase 4; *Prkaa2* –

protein kinase AMP-activated catalytic subunit alpha 2; *Rela* – RELA proto-oncogene, NF-KB Subunit; *Sirt1/3* – sirtuin 1/3. Taken from Benak et al. [183] (Attachment IV).

5.9. Inhibition of ALKBH5 or FTO impairs the hypoxic tolerance of AVCMs from fasting rats

To study the role of both demethylases (significantly increased in our cardioprotective models), we inspected the effect of ALKBH5i and FTOi on the viability of AVCMs from fasting and control rats using the SYTOX staining (Fig. 27).

The viability of AVCMs under normoxic conditions was not affected by the administration of inhibitors. Hypoxia significantly reduced the viability in untreated AVCMs isolated from both control (by 87%) and fasting (by 89%) animals. Under hypoxic conditions, inhibition of each demethylase further decreased the viability of the AVCMs isolated from fasting rats (ALKBH5i to 81% and FTOi to 78%), while the decrease in viability of AVCMs from control rats did not reach statistical significance.

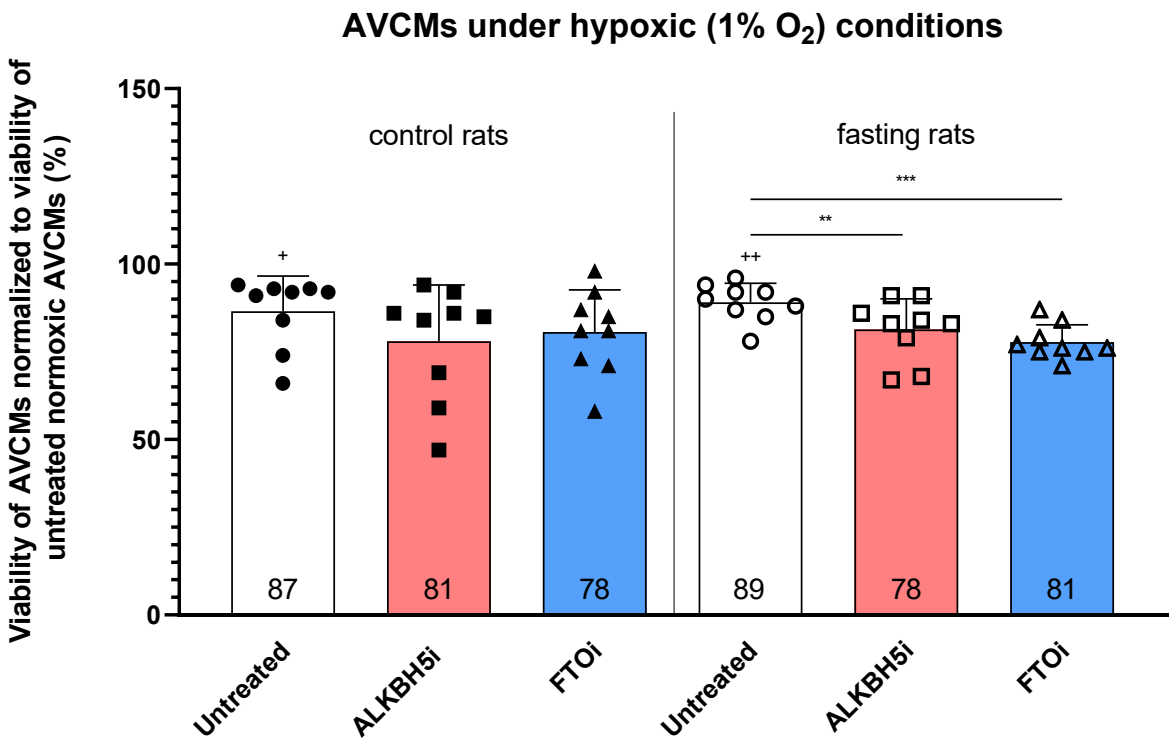

Fig. 27: Effect of ALKBH5 and FTO inhibition on hypoxic tolerance of AVCMs isolated from control and fasting rats. Values are means ± SD; n = 9; ** $p < 0.01$; *** $p < 0.001$ (one-way ANOVA); + $p < 0.05$ compared to normoxic untreated AVCMs; ++ $p < 0.01$ compared to normoxic untreated

AVCMs. ALKBH5i – ALKBH5 inhibitor; AVCMs – adult rat left ventricular cardiomyocytes; FTOi – FTO inhibitor. Taken from Benak et al. [183] (Attachment IV).

5.10. Summary of the fasting model results

We showed that 3-day fasting vastly affected the levels of epitranscriptomic regulators, including ALKBH5 and FTO. In line with this, global m^6A/m levels were decreased post-fasting, while methylation of specific transcripts – *Nox4* and *Hdac1* – was increased. We also showed that inhibition of demethylases ALKBH5 and FTO decreased the hypoxic tolerance of AVCMs isolated from fasting rats.

6. DISCUSSION

6.1. Cardioprotective interventions affect epitranscriptomic regulations

The heart experiences alterations in levels of epitranscriptomic modification m^6A and its principal regulators under various physiological and pathophysiological circumstances [189]. Nevertheless, there is insufficient documentation regarding the involvement of m^6A and m^6Am in cardioprotection and related models. Primarily, the demethylases FTO and ALKBH5 have been linked to cardioprotective effects [4-6]. However, the participation of epitranscriptomic regulations in protective models of chronic hypoxia and fasting was still hypothetical.

6.1.1. Epitranscriptomic regulations in rats adapted to chronic hypoxia

It has been described that m^6A was essential for the stabilization of specific mRNAs under hypoxic conditions [190]. A comprehensive transcriptome-wide analysis of m^6A has demonstrated significant reprogramming of m^6A epitranscriptome during cellular hypoxia [191]. HIF-1α, the key transcription factor responsible for cellular response to hypoxia, is among the m^6A-modified transcripts [192-194], and its translation is affected by m^6A readers [193, 195]. In turn, HIF-1α affects the expression of several m^6A/m^6Am regulators [196-199]. Moreover, individual epitranscriptomic regulators respond to oxygen levels, however, the results are often contradictory. Therefore, it is important to identify the factors (e.g., cell type, strength, or duration of exposure to hypoxia) involved in these regulations to better understand this problematics.

The Alkbh5 gene is a direct target of the well-known transcription factor HIF-1α and therefore it is not surprising that it is induced in hypoxia in a range of cell types [145, 191, 196, 200]. In line with this data, we observed up-regulation of ALKBH5 in hypoxic hearts on the protein level. Interestingly, the transcript levels were not affected by hypoxic adaptation.

FTO is an enzyme that oxidatively removes the methyl group from m^6A-containing RNAs and m^6Am-containing RNAs; thus, it is anticipated that the enzymatic activity of FTO would decrease during hypoxic conditions (irrespective of its expression level) [86]. Moreover, numerous studies

967 have demonstrated a decrease in FTO expression in hypoxic cardiomyocytes. However, since this
968 effect was not observed in other cell types (yet), it may be cell type-specific or dependent on the
969 severity of the hypoxic stimulus [4, 6, 7, 191]. Importantly, the up-regulation of FTO reversed the
970 decreased cell viability induced by H/R treatment [4-6]. We assessed FTO transcript and protein
971 levels in LVs of rats adapted to CNH *in vivo*. Surprisingly, we observed an elevation in FTO protein
972 levels while hypoxic adaptation did not affect mRNA levels.

973 Regarding the writers, also METTL3 is induced by hypoxia in a HIF-dependent manner. Its
974 increased expression under hypoxic conditions has been confirmed in various cell types, including
975 cardiomyocytes. Nevertheless, conflicting results exist in the literature, with some studies reporting
976 no impact or a decrease in METTL3 levels in hypoxic cells [115, 191, 198, 201, 202]. In our
977 experiments, the adaptation of rats to CNH did not result in any alterations in METTL3 levels in LVs.

978 The up-regulation of METTL4, an m^6Am methyltransferase, is induced by overexpression of
979 HIF-1α, and hypoxic treatment leads to an increase in mRNA and protein levels of METTL4, as
980 reported by Hao and others [172]. Contrasting with the above study, our observations revealed a
981 reduction in METTL4 protein levels in LVs of hypoxic rats, while mRNA levels remained unchanged.
982 PCIF1, a second m^6Am methyltransferase, is not reported to respond to hypoxia, and it did not
983 exhibit any reaction to hypoxic adaptation under our experimental conditions.

984 YTHDC1, an m^6A reader involved in splicing, was first identified in 1998 as a protein induced
985 by H/R in rat cultured astrocytes [203]. Subsequent research has shown its up-regulation under
986 hypoxic stress across various human cell lines [191]. Aligning with these observations, our findings
987 further confirm the elevation of YTHDC1 at the protein and transcript levels in the LVs of rats
988 adapted to CNH.

989 Reader YTHDC2 has been identified to promote the translation of HIF-1α [195]. Contrary to
990 the observations by Wang et al. [191], who reported decreased YTHDC2 levels in various cell lines
991 under hypoxic conditions, our experimental conditions revealed stable protein levels of YTHDC2 in
992 LVs of hypoxic animals.

YTHDF1-3, which function as readers of m^{6}A and mediate the decay of m^{6}A-mRNAs, were demonstrated to decrease in various human cell lines in response to hypoxic stress [191]. Additionally, YTHDF1 expression levels decreased in the liver and kidneys of highland cattle compared to lowland cattle, and the knockdown of YTHDF1 was shown to abolish hypoxia-induced cellular apoptosis [204]. Conversely, some studies have described the up-regulation of YTHDF1 levels under hypoxic conditions [205]. Our experiments revealed that all three YTHDF paralogs exhibited an increase in their protein levels in hypoxic LVs. However, RT-qPCR analysis revealed no significant changes in mRNA levels, except for a non-significant ($p = 0.06$) increase in the case of *Ythdf3*.

Also m^{6}A methylation levels itself were reported to react to oxygen deprivation. For instance, Wang et al. [206] reported that H/R elevated m^{6}A levels in total RNA isolated from H9c2 cells. Similarly, m^{6}A methylation was also elevated in RNA (it is not clear from the article whether it was mRNA or total RNA) from murine primary neonatal ventricular myocytes exposed to H/R [207]. Notably, in HEK293T cells, increased m^{6}A content was detected only in mRNA and not in total RNA after incubation in 1% hypoxia [190]. This suggests a cell-type and also an RNA-type dependent variation in the influence of hypoxia on m^{6}A methylation. In our observations, no significant change in m^{6}A levels was detected in the total RNA from the hearts of rats subjected to chronic hypoxia. However, this does not rule out the possibility of m^{6}A level changes in specific RNA types (such as mRNA) or specific cardiac cell types (such as cardiomyocytes). Further research is necessary to clarify these aspects and understand the intricate dynamics of m^{6}A methylation under various hypoxic conditions.

Several factors may account for the discrepancies between our findings and those of other studies. Firstly, diverse tissues and cell types exhibit distinct responses to hypoxic conditions. For example, in our experiments, we observed an elevation in FTO protein levels in the heart ventricles of hypoxic rats, while no changes were noted in the liver or cerebrum [208]. At the cellular level, Mathiyalagan et al. [7] reported a reduction in FTO levels in hypoxic cardiomyocytes, whereas Wang

et al. [191] observed no alterations in FTO levels in HeLa and SNNC7721 cells. The variation in results could also stem from differences between homogenous cardiomyocytes and the heterogeneous tissue composition of the heart, encompassing various cell types. Also, the variances might be attributed to a distinctive systemic response to chronic hypoxia *in vivo* compared to the *in vitro* response of isolated cells. Additionally, factors such as oxygen level, type of hypoxia (acute vs. chronic), duration of hypoxia, and the presence or absence of reoxygenation could significantly impact the outcomes. Our observations revealed a more pronounced increase in FTO protein levels in the left ventricle of rats adapted to stronger hypoxia (CNH 10% O_2) compared to milder hypoxia (CNH 12% O_2), suggesting an oxygen-dependent response [208]. In summary, the genes and proteins involved in the epitranscriptomic machinery may exhibit diverse reactions to oxygen deprivation under various conditions and in different cell types.

6.1.2. Epitranscriptomic regulations in rats subjected to fasting

Little information is available on how fasting affects epitranscriptomic regulation. A recent study by Xu et al. [209] found that IF safeguards mouse hearts through a process linked to reduced m^6A levels. Additionally, the reduction in m^6A methylation was accompanied by decreased METTL3 and increased FTO levels. In our model of 3-day fasting, we also observed decreased m^6A methylation and FTO expression in LVs from fasting rats, however, we did not observe altered METTL3 levels. This discrepancy might be explained by two factors: 1) different fasting models used (alternate-day fasting for 8 weeks vs. consecutive fasting for 3 days); 2) the difference between mouse and rat animal models. For the primary regulators not examined by Xu et al., we observed an increase in gene and protein expression of the second demethylase ALKBH5 and the methyltransferase PCIF1. The gene expression of reader *Ythdc1* was also up-regulated. On the contrary, other readers (YTHDC2 and YTHDF1-3) showed a decrease in their protein levels, with only *Ythdf3* down-regulated also on the gene level.

Besides the main epitranscriptomic machinery discussed above, we also focused on the less-known regulators in our targeted proteomic analysis. To date, there is no data on their possible

role in hearts of fasting rats, however, important functions in cardiac biology were proposed for these proteins. The most prominent reduction in protein levels was observed in the case of writer METTL5. This m^6A methyltransferase is known to regulate mRNA translation via 18S rRNA methylation [210]. Its cardiac-specific depletion has been linked to pressure overload-induced cardiomyocyte hypertrophy and adverse remodeling [211]. Other decreased proteins included eIF3 reader subunits (eIF3a/c/g) and reader RBMX. Notably, eIF3 is crucial in translation regulation, with eIF3a being its most prominent and studied subunit. A mutation in eIF3a has been discovered in patients suffering from left ventricular non-compaction cardiomyopathy, a genetic condition leading to thromboembolic events, arrhythmias, and heart failure. Further studies in H9c2 cells associate this mutation with reduced cell proliferation and increased apoptosis [212]. eIF3a's involvement in cardiac fibrosis has also been documented [213]. Another eIF3 subunit, eIF3c, is directly targeted by reader YTHDF1, which enhances eIF3c translation in an m^6A-dependent manner [214]. In the LVs of fasting animals, we observed a decrease in the YTHDF1-eIF3c axis as levels of both epitranscriptomic regulators were reduced. Additionally to the decreased levels of m^6A readers, LVs from fasting rats exhibited lower expression of most m^6A-repelled proteins (G3BP1/2, ELAVL1, USP10, CAPRIN1). G3BP1 is a key regulator in cardiac hypertrophy, atrial fibrillation, and coronary heart disease, while G3BP2 plays a role in cardiac hypertrophy and atherosclerosis development [215-218]. Moreover, G3BP2 overexpression can partly counteract apoptosis induced by hypoxia/reoxygenation in H9c2 cells [219]. However, our cardioprotective fasting model was associated with decreased and not increased G3BP2 levels. ELAVL1, another RNA-binding protein, has diverse cellular roles. For example, it associates with mRNAs of proteins responsive to hypoxia such as HIF-1α or VEGF, and enhances their expression under hypoxic conditions [220]. Up-regulation of ELAVL1 was detected in myocardial tissue after I/R injury, whereas its knockdown mitigated MI-induced cardiomyocyte apoptosis, infarct size, and fibrosis [221, 222]. Thus, our observation of ELAVL1 down-regulation in LVs of fasting rats could participate in the induction of cardioprotective phenotype associated with fasting. Protein USP10, another m^6A-repelled protein,

was associated with cardiac hypertrophy [223, 224]. Its levels were down-regulated in H9c2 cells after H/R injury and overexpression of USP10 increased the viability of H/R-induced cells [225]. However, we observed a down-regulation of this regulator in the hearts of fasting rats.

6.1.3. Comparison of epitranscriptomic regulations in two cardioprotective models – adaptation to chronic hypoxia and fasting

Comparison of both cardioprotective methods concerning epitranscriptomic regulation may deepen the knowledge of molecular cardioprotective pathways (Fig. 29). Given the pivotal role of proteins as primary regulatory units in cellular biology, this section is dedicated exclusively on proteins for a higher clarity of the text. Also, this part of the dissertation will concentrate solely on the findings from our study. Comparisons with existing literature have been thoroughly covered in the preceding sections.

Our experiments revealed that both cardioprotective interventions, namely adaptation to chronic hypoxia and fasting, exhibited a similar regulatory pattern in the protein levels of demethylases ALKBH5 and FTO. Also, the catalytic subunit of the MTC, METTL3, remained unaffected by either intervention. However, a differential regulation was observed in other proteins of the epitranscriptomic machinery.

Regarding m^6A/m writers, there was a notable down-regulation of METTL4 in rats adapted to chronic hypoxia, whereas PCIF1 levels remained unchanged. Conversely, during fasting, METTL4 levels did not exhibit significant changes, while PCIF1 was up-regulated. This differential regulation extended to the YTHDF readers as well; all three YTHDF readers were up-regulated in hypoxic conditions and down-regulated during fasting. Furthermore, YTHDC1 demonstrated an up-regulation post-hypoxia and remained unaffected post-fasting. In contrast, YTHDC2 did not show significant changes post-hypoxia but was down-regulated following fasting.

There was also a divergence in the m^6A/m methylation levels in response to hypoxia and fasting. Our *in vivo* experiments did not reveal any alterations in cardiac m^6A/m methylation in total RNA after hypoxic adaptation, whereas m^6A/m levels were significantly reduced after fasting.

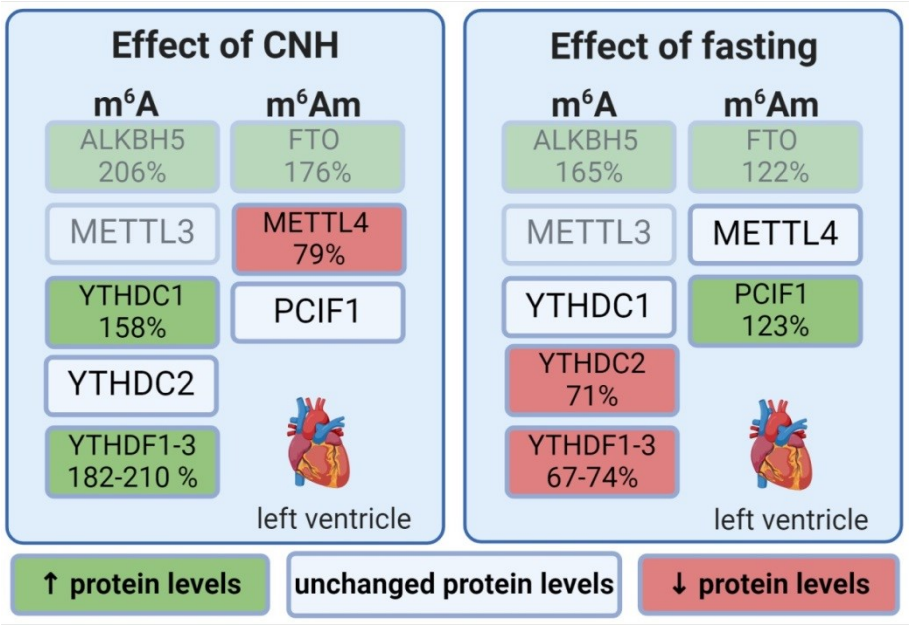

Fig. 29: Comparison of epitranscriptomic regulations in cardioprotective interventions. Changes in the same direction are made transparent to highlight the differences. ALKBH5 – alkB family member 5; CNH – continuous normobaric hypoxia; FTO – fat mass and obesity-associated protein; LV – left ventricle; m^6A – N^6-methyladenosine; m^6Am – N^6,2'-O-dimethyladenosine; m^6A/m – m^6A+m^6Am; METTL3/4 – methyltransferase like 3/4; PCIF1 – phosphorylated CTD interacting factor 1; YTHDF1-3 – YTH domain-containing family protein 1-3; YTHDC1/2 – YTH domain-containing protein 1/2.

This comparison underscores the intricate and diverse molecular responses induced by adaptation to chronic hypoxia and fasting in cardioprotective contexts. While certain regulatory proteins like ALKBH5 and FTO show uniform up-regulation in both conditions, others exhibit intervention-specific responses. This differential regulation, particularly in m^6Am writers and YTHDF readers, along with the variable m^6A/m methylation levels, highlights the complexity of RNA modifications in cardioprotection. Further investigation is needed to elucidate the precise mechanisms and implications of these distinct regulations in cardiac health and disease.

6.1.4. Up-methylation of *Nox4* and *Hdac1* transcripts in the hearts of fasting rats

Our MeRIP analysis did not reveal any differences in m^6A/m methylation in selected transcripts of genes associated with cardioprotection in chronically hypoxic hearts. However, analysis of hearts from fasting rats divulged some interesting findings. We focused on the connection between fasting, ketosis, and the protective functions of ketone bodies and discovered a significant m^6A/m up-methylation of *Nox4* and *Hdac1* transcripts, both of which are potentially related to the cytoprotective functions of ketone bodies.

The seeming discrepancy between decreased m^6A/m methylation levels in total RNA and increased m^6A/m methylation in the two specific transcripts may be explained by the complex epitranscriptomic regulations where different RNA types may be affected in opposite ways in hearts of fasting rats.

NOX4 is an enzyme known for producing reactive oxygen species (ROS), which are involved in various signaling pathways including cardiac adaptation to different types of physiological and pathophysiological stresses, and therefore plays both protective and detrimental roles in the heart [55]. Varga et al. [226] reported that extensive alternative splicing of NOX4 occurs in human hearts and that the full-length NOX4 was significantly increased in ischemic cardiomyopathy. Since regulation of splicing is one of the main functions of m^6A and m^6Am modifications [149, 173], changes in the level of methylation in the *Nox4* transcript may be critical for determining cardiac fate. The second cardiac transcript that was up-methylated after fasting was *Hdac1*. HDAC1 functions as an epigenetic regulator by removing acetyl groups from histones and it is inhibited by 3-hydroxybutyrate [61], the major ketone body elevated in our fasting model. Inhibition of HDAC1 has also been associated with protection of cardiomyocytes from hypoxia [227]. Hence, these results exposed altered epitranscriptomic regulation in cytoprotective pathways induced by ketone bodies in rat hearts during fasting.

6.1.5. Decreased hypoxic tolerance of AVCMs after FTO and ALKBH5 inhibition

The alterations observed in the LVs of fasting rats included an increased expression of both demethylases on both mRNA and protein levels. We did not find any significant effect of ALKBH5 or FTO inhibition on hypoxic tolerance (1% O_2, 24 h) in cells isolated from rats on a normal diet, even though the decreasing trend was apparent. Nevertheless, in the fasting animals, there was a significant reduction in AVCM viability following treatment with ALKBH5i and FTOi.

It is known that the expression level of FTO influences the survival of cardiomyocytes subjected to H/R insult. Deng et al. [4] reported that expression of FTO was low in human cardiomyocyte cell line AC16 exposed to H/R and found that up-regulation of FTO increased their viability after H/R treatment. Likewise, FTO overexpression inhibited apoptosis induced by acute H/R in mouse cardiomyocytes, while knockdown of this demethylase had the opposite effect [5]. Furthermore, decreased expression of FTO was detected in mouse hearts and isolated mouse cardiomyocytes subjected to I/R and acute H/R insults. FTO overexpression in these cells then attenuated the H/R-induced apoptosis [6]. ALKBH5 overexpression also inhibited apoptosis of cardiomyocytes after H/R insult [115, 207]. Consistent with these data, our observations confirm that the activity of RNA erasers ALKBH5 and FTO is crucial for cardiomyocyte tolerance to hypoxic insult.

7. CONCLUSION

This study focused on the epitranscriptomic modifications m^6A and m^6Am and their regulators in the unconventional cardioprotective methods – adaptation to chronic hypoxia and fasting. Given the profound impact of the epitranscriptomic machinery on numerous cellular processes, including gene expression, and its subsequent influence on cardiac physiology and pathophysiology, we hypothesized that epitranscriptomic modifications could be instrumental in fostering a cardioprotective phenotype in rats either adapted to chronic hypoxia or subjected to fasting.

Initially, our investigation aimed at the levels of epitranscriptomic regulators within the LVs of both experimental and control groups. Through various analytical methods (RT-qPCR, Western blot analysis, targeted proteomic analysis) we found compelling evidence that the epitranscriptomic machinery undergoes significant regulation in animals adapted to chronic hypoxia or subjected to fasting. Even though the two interventions differed in terms of epitranscriptomic regulation, they both included up-regulation of the two demethylases – ALKBH5 and FTO.

Building on these foundations, we observed a notable reduction in cardiac m^6A/m methylation levels in total RNA isolated from LVs of fasting animals. Additionally, specific transcripts (*Nox4* and *Hdac1*) potentially associated with the cell-protective functions of ketone bodies induced by fasting showed differential methylation in LVs of fasting rats. Such observations lend substantial support to the hypothesis that epitranscriptomic modifications play a crucial role in the heart's adaptation to stress conditions.

Since we observed altered methylation levels in fasting and not hypoxic rats, we continued our research with the fasting model only. Using inhibitors of demethylases ALKBH5 and FTO, we were able to demonstrate that inhibition of these enzymes decreases the hypoxic tolerance of cardiomyocytes isolated from fasting rats.

In conclusion, we shed light on the important role of epitranscriptomic regulation, particularly modifications m^6A and m^6Am, in establishing a cardioprotective phenotype in response to chronic hypoxia and fasting. Our results proved our hypothesis, that regulation of epitranscriptomic machinery plays a role in the cardioprotective phenotype induced by fasting. This study not only advances our understanding of the epitranscriptomic landscape in cardiac adaptation but also opens new avenues for therapeutic interventions targeting epitranscriptomic regulators to exploit their cardioprotective potential.

8. ABBREVIATIONS

-$(dP/dt)_{max}$ – peak rate of pressure decline

+$(dP/dt)_{max}$ – peak rate of pressure development

3‘UTR/5‘UTR – 3‘/5‘ untranslated region

6mA – N^6-methyldeoxyadenosine

AFD – alternate-day fasting

Akt1 – AKT serine/threonine kinase 1

ALKBH3/5 – alkB family member 5

ALKBH5i – ALKBH5 inhibitor

Am – 2‘-O-methyladenosine

AMPK – AMP-activated kinase

AVCMs – adult ventricular cardiomyocytes

AWTd – end-diastolic anterior wall thickness

AWTs – end-systolic anterior wall thickness

CABG – coronary artery bypass grafting

CAD – coronary artery disease

CAPRIN1 – cell cycle associated protein 1

CBLL1 – cbl proto-oncogene like 1

CI – cardiac index

circRNA – circular RNA

CNH – continuous normobaric hypoxia

CVDs – cardiovascular diseases

DIA – data-independent acquisition

DMSO – dimethyl sulfoxide

eIF3 – eukaryotic initiation factor 3

ELAVL1 – ELAV-like protein 1

EPO – erythropoietin

FMR1 – fragile X mental retardation protein

Foxo3 – forkhead box O3

FS – fractional shortening

FTO – fat mass and obesity-associated protein

FTOi – FTO inhibitor

G3BP1/2 – G3BP stress granule assembly factor 1/2

H/R – hypoxia-reoxygenation

Hdac1 – histone deacetylase 1

HIF-1 – hypoxia-inducible factor 1

Hif1a – hypoxia-inducible factor 1 subunit alpha

Hk2 – hexokinase 2

HNRNPs – heterogeneous nuclear ribonucleoproteins

HR – heart rate

i.p. – intraperitoneal

I/R – ischemia-reperfusion

IF – intermittent fasting

IGF2BPs – insulin-like growth factor 2 mRNA binding proteins

IHD – ischemic heart disease

IS – internal standard

LC-MS – liquid chromatography-mass spectrometry

LFQ – label-free quantification

lncRNA – long non-coding RNA

LRPPRC – leucine rich pentatricopeptide repeat containing

LTF – long-term fasting

LV – left ventricle

LVDd – end-diastolic LV cavity diameter

LVDs – end-systolic LV cavity diameter

m^1A – N^1-methyladenosine

m^5C – 5-methylcytosine

m^6A – N^6-methyladenosine

m^6Am – N^6,2‘-O-dimethyladenosine

1242 m^7G − 7-methylguanosine

1243 MeRIP – m^6A RNA immunoprecipitation

1244 METTL3/4/5/14/16 – methyltransferase-like 3/4/5/14/16

1245 MI – myocardial infarction

1246 miRNA – microRNA

1247 mRNA – messenger RNA

1248 MTC – multicomponent methyltransferase complex

1249 mtDNA – mitochondrial DNA

1250 Nfe2l2 – NFE2 like BZIP transcription factor 2

1251 *Nox4* – NADPH oxidase 4

1252 NRF2 – nuclear factor erythroid 2-related factor 2

1253 *Nupl2* – nucleoporin-like 2

1254 P0-90 – postnatal day 0-90

1255 PCI – primary percutaneous coronary intervention

1256 Pdev – developed pressure

1257 *Pdk4* – pyruvate dehydrogenase kinase 4

1258 Ped – end-diastolic pressure

1259 Pes – end-systolic pressure

1260 pO_2 – partial pressure of oxygen

1261 *Ppara* – peroxisome proliferator activated receptor alpha

Ppargc1a – PPARG coactivator 1 alpha

Prkaa2 – protein kinase AMP-activated catalytic subunit alpha 2

PRM – parallel reaction monitoring

PRRC2A – proline rich-coil 2A

PWTd – end-diastolic posterior wall thickness

PWTs – end-systolic posterior wall thickness

RBM15/42 – RNA binding motif protein 15/42

Rela – RELA proto-oncogene, NF-KB Subunit

rRNA – ribosomal RNA

RT-qPCR – reverse transcription-quantitative polymerase chain reaction

RV – right ventricle

RWT – relative wall thickness

Sirt1 – sirtuin 1

Sirt3 – sirtuin 3

snRNA – small nuclear RNA

STF - short-term fasting

T1DM – type 1 diabetes mellitus

T2DM – type 2 diabetes mellitus

Top1 – DNA topoisomerase I

TRE/F – time-restricted eating/feeding

TRMT112 – tRNA methyltransferase activator subunit 11-2

tRNA – transfer RNA

USP10 – ubiquitin specific peptidase 10

UTR – untranslated region

VEGFA – vascular endothelial growth factor A

VIRMA – vir-like m6A methyltransferase associated

WB – Western blot

WTAP – Willms' tumor 1-associating protein

YTHDCs – YTH domain-containing proteins

YTHDFs – YTH domain-containing family proteins

Ywhaz – tyrosin-3-monooxygenase/tryptophan 5 monooxygenase activation protein zeta

ZC3H13 – zinc finger CCCH-type containing 13

ZCCHC4 – zinc finger CCHC-type containing 4

Ψ – pseudouridine

9. LIST OF FIGURES AND TABLES

9.1. Figures

9.2. Tables

10. REFERENCES

1. WHO. *The top 10 causes of death.* 2020 November 24 2022]; Available from: https://www.who.int/news-room/fact-sheets/detail/the-top-10-causes-of-death.
2. Alanova, P., et al., *Myocardial ischemic tolerance in rats subjected to endurance exercise training during adaptation to chronic hypoxia.* J Appl Physiol (1985), 2017. **122**(6): p. 1452-1461.
3. Ma, Y., et al., *Alteration of N(6)-Methyladenosine mRNA Methylation in a Human Stem Cell-Derived Cardiomyocyte Model of Tyrosine Kinase Inhibitor-Induced Cardiotoxicity.* Front Cardiovasc Med, 2022. **9**: p. 849175.
4. Deng, W., Q. Jin, and L. Li, *Protective mechanism of demethylase fat mass and obesity-associated protein in energy metabolism disorder of hypoxia-reoxygenation-induced cardiomyocytes.* Exp Physiol, 2021. **106**(12): p. 2423-2433.
5. Shen, W., et al., *FTO overexpression inhibits apoptosis of hypoxia/reoxygenation-treated myocardial cells by regulating m6A modification of Mhrt.* Mol Cell Biochem, 2021. **476**(5): p. 2171-2179.
6. Ke, W.L., et al., *m(6)A demethylase FTO regulates the apoptosis and inflammation of cardiomyocytes via YAP1 in ischemia-reperfusion injury.* Bioengineered, 2022. **13**(3): p. 5443-5452.
7. Mathiyalagan, P., et al., *FTO-Dependent N(6)-Methyladenosine Regulates Cardiac Function During Remodeling and Repair.* Circulation, 2019. **139**(4): p. 518-532.
8. Zhang, X., et al., *Dexmedetomidine Postconditioning Alleviates Hypoxia/Reoxygenation Injury in Senescent Myocardial Cells by Regulating lncRNA H19 and m⁶A Modification.* Oxidative Medicine and Cellular Longevity, 2020. **2020**: p. 9250512.
9. Cui, Y., et al., *Cinnamic acid mitigates left ventricular hypertrophy and heart failure in part through modulating FTO-dependent N(6)-methyladenosine RNA modification in cardiomyocytes.* Biomed Pharmacother, 2023. **165**: p. 115168.
10. Yu, P., et al., *RNA m(6)A-Regulated circ-ZNF609 Suppression Ameliorates Doxorubicin-Induced Cardiotoxicity by Upregulating FTO.* JACC Basic Transl Sci, 2023. **8**(6): p. 677-698.
11. Gong, R., et al., *Loss of m(6)A methyltransferase METTL3 promotes heart regeneration and repair after myocardial injury.* Pharmacol Res, 2021. **174**: p. 105845.
12. Wu, C., et al., *The m(6)A methylation enzyme METTL14 regulates myocardial ischemia/reperfusion injury through the Akt/mTOR signaling pathway.* Mol Cell Biochem, 2023.
13. Khan, M.A., et al., *Global Epidemiology of Ischemic Heart Disease: Results from the Global Burden of Disease Study.* Cureus, 2020. **12**(7): p. e9349.
14. Kalra, S., H. Bhatt, and A.J. Kirtane, *Stenting in Primary Percutaneous Coronary Intervention for Acute ST-Segment Elevation Myocardial Infarction.* Methodist Debakey Cardiovasc J, 2018. **14**(1): p. 14-22.
15. Giacoppo, D., et al., *Percutaneous Coronary Intervention vs Coronary Artery Bypass Grafting in Patients With Left Main Coronary Artery Stenosis: A Systematic Review and Meta-analysis.* JAMA Cardiol, 2017. **2**(10): p. 1079-1088.
16. Grüntzig, A.R., A. Senning, and W.E. Siegenthaler, *Nonoperative dilatation of coronary-artery stenosis: percutaneous transluminal coronary angioplasty.* N Engl J Med, 1979. **301**(2): p. 61-8.
17. Sinnaeve, P. and F. Van de Werf, *Thrombolytic therapy. State of the art.* Thromb Res, 2001. **103 Suppl 1**: p. S71-9.
18. Davignon, J., *The cardioprotective effects of statins.* Curr Atheroscler Rep, 2004. **6**(1): p. 27-35.
19. Messerli, F.H., et al., *Cardioprotection with beta-blockers: myths, facts and Pascal's wager.* J Intern Med, 2009. **266**(3): p. 232-41.

20. Juggi, J.S., E. Koenig-Berard, and W.H. Van Gilst, *Cardioprotection by angiotensin-converting enzyme (ACE) inhibitors.* Can J Cardiol, 1993. **9**(4): p. 336-52.
21. Prasad, K., *Current Status of Primary, Secondary, and Tertiary Prevention of Coronary Artery Disease.* Int J Angiol, 2021. **30**(3): p. 177-186.
22. Murry, C.E., R.B. Jennings, and K.A. Reimer, *Preconditioning with ischemia: a delay of lethal cell injury in ischemic myocardium.* Circulation, 1986. **74**(5): p. 1124-36.
23. Zhao, Z.Q., et al., *Inhibition of myocardial injury by ischemic postconditioning during reperfusion: comparison with ischemic preconditioning.* Am J Physiol Heart Circ Physiol, 2003. **285**(2): p. H579-88.
24. Takaoka, A., et al., *Renal ischemia/reperfusion remotely improves myocardial energy metabolism during myocardial ischemia via adenosine receptors in rabbits: effects of "remote preconditioning".* J Am Coll Cardiol, 1999. **33**(2): p. 556-64.
25. Bøtker, H.E., et al., *Remote ischaemic conditioning before hospital admission, as a complement to angioplasty, and effect on myocardial salvage in patients with acute myocardial infarction: a randomised trial.* Lancet, 2010. **375**(9716): p. 727-34.
26. Crimi, G., et al., *Remote ischemic post-conditioning of the lower limb during primary percutaneous coronary intervention safely reduces enzymatic infarct size in anterior myocardial infarction: a randomized controlled trial.* JACC Cardiovasc Interv, 2013. **6**(10): p. 1055-63.
27. Prunier, F., et al., *The RIPOST-MI study, assessing remote ischemic perconditioning alone or in combination with local ischemic postconditioning in ST-segment elevation myocardial infarction.* Basic Res Cardiol, 2014. **109**(2): p. 400.
28. White, S.K., et al., *Remote ischemic conditioning reduces myocardial infarct size and edema in patients with ST-segment elevation myocardial infarction.* JACC Cardiovasc Interv, 2015. **8**(1 Pt B): p. 178-188.
29. Verouhis, D., et al., *Effect of remote ischemic conditioning on infarct size in patients with anterior ST-elevation myocardial infarction.* Am Heart J, 2016. **181**: p. 66-73.
30. Hausenloy, D.J., et al., *Effect of remote ischaemic conditioning on clinical outcomes in patients with acute myocardial infarction (CONDI-2/ERIC-PPCI): a single-blind randomised controlled trial.* Lancet, 2019. **394**(10207): p. 1415-1424.
31. Snorek, M., et al., *Short-term fasting reduces the extent of myocardial infarction and incidence of reperfusion arrhythmias in rats.* Physiol Res, 2012. **61**(6): p. 567-74.
32. Marvanova, A., et al., *Continuous short-term acclimation to moderate cold elicits cardioprotection in rats, and alters β-adrenergic signaling and immune status.* Sci Rep, 2023. **13**(1): p. 18287.
33. Yamashita, N., et al., *Whole-body hyperthermia provides biphasic cardioprotection against ischemia/reperfusion injury in the rat.* Circulation, 1998. **98**(14): p. 1414-21.
34. Shinlapawittayatorn, K., et al., *Low-amplitude, left vagus nerve stimulation significantly attenuates ventricular dysfunction and infarct size through prevention of mitochondrial dysfunction during acute ischemia-reperfusion injury.* Heart Rhythm, 2013. **10**(11): p. 1700-7.
35. Ostadal, B. and F. Kolar, *Cardiac adaptation to chronic high-altitude hypoxia: beneficial and adverse effects.* Respir Physiol Neurobiol, 2007. **158**(2-3): p. 224-36.
36. Papoušek, F., et al., *Left ventricular function and remodelling in rats exposed stepwise up to extreme chronic intermittent hypoxia.* Respir Physiol Neurobiol, 2020. **282**: p. 103526.
37. Benak, D., et al., *Selection of optimal reference genes for gene expression studies in chronically hypoxic rat heart.* Mol Cell Biochem, 2019. **461**(1-2): p. 15-22.
38. Nedvedova, I., et al., *Cardioprotective Regimen of Adaptation to Chronic Hypoxia Diversely Alters Myocardial Gene Expression in SHR and SHR-mt(BN) Conplastic Rat Strains.* Front Endocrinol (Lausanne), 2018. **9**: p. 809.

39. Míčová, P., et al., *Antioxidant tempol suppresses heart cytosolic phospholipase A(2)α stimulated by chronic intermittent hypoxia.* Can J Physiol Pharmacol, 2017. **95**(8): p. 920-927.
40. Hurtado, A., *Some clinical aspects of life at high altitudes.* Ann Intern Med, 1960. **53**: p. 247-58.
41. Kolář, F., *Cardioprotective Effects of Chronic Hypoxia: Relation to Preconditioning*, in *Myocardial Preconditioning*, C.L. Wainwright and J.R. Parratt, Editors. 1996, Springer Berlin Heidelberg: Berlin, Heidelberg. p. 261-275.
42. Neckár, J., et al., *Cardioprotective effects of chronic hypoxia and ischaemic preconditioning are not additive.* Basic Res Cardiol, 2002. **97**(2): p. 161-7.
43. Semenza, G.L. and G.L. Wang, *A nuclear factor induced by hypoxia via de novo protein synthesis binds to the human erythropoietin gene enhancer at a site required for transcriptional activation.* Mol Cell Biol, 1992. **12**(12): p. 5447-54.
44. Wang, G.L. and G.L. Semenza, *Purification and characterization of hypoxia-inducible factor 1.* J Biol Chem, 1995. **270**(3): p. 1230-7.
45. Forsythe, J.A., et al., *Activation of vascular endothelial growth factor gene transcription by hypoxia-inducible factor 1.* Mol Cell Biol, 1996. **16**(9): p. 4604-13.
46. Kohutova, J., et al., *Anti-arrhythmic Cardiac Phenotype Elicited by Chronic Intermittent Hypoxia Is Associated With Alterations in Connexin-43 Expression, Phosphorylation, and Distribution.* Front Endocrinol (Lausanne), 2018. **9**: p. 789.
47. Neckář, J., et al., *Selective replacement of mitochondrial DNA increases the cardioprotective effect of chronic continuous hypoxia in spontaneously hypertensive rats.* Clin Sci (Lond), 2017. **131**(9): p. 865-881.
48. Hlaváčková, M., et al., *Up-regulation and redistribution of protein kinase C-δ in chronically hypoxic heart.* Mol Cell Biochem, 2010. **345**(1-2): p. 271-82.
49. Seagroves, T.N., et al., *Transcription factor HIF-1 is a necessary mediator of the pasteur effect in mammalian cells.* Mol Cell Biol, 2001. **21**(10): p. 3436-44.
50. Holzerová, K., et al., *Involvement of PKCepsilon in cardioprotection induced by adaptation to chronic continuous hypoxia.* Physiol Res, 2015. **64**(2): p. 191-201.
51. Maslov, L.N., et al., *Role of endogenous opioid peptides in the infarct size-limiting effect of adaptation to chronic continuous hypoxia.* Life Sci, 2013. **93**(9-11): p. 373-9.
52. Antezana, A.M., et al., *Pulmonary hypertension in high-altitude chronic hypoxia: response to nifedipine.* Eur Respir J, 1998. **12**(5): p. 1181-5.
53. Wilhelmi de Toledo, F., et al., *Unravelling the health effects of fasting: a long road from obesity treatment to healthy life span increase and improved cognition.* Ann Med, 2020. **52**(5): p. 147-161.
54. Chaix, A., et al., *Time-Restricted Eating to Prevent and Manage Chronic Metabolic Diseases.* Annu Rev Nutr, 2019. **39**: p. 291-315.
55. Scholtens, E.L., et al., *Intermittent fasting 5:2 diet: What is the macronutrient and micronutrient intake and composition?* Clin Nutr, 2020. **39**(11): p. 3354-3360.
56. Trepanowski, J.F., et al., *Effect of Alternate-Day Fasting on Weight Loss, Weight Maintenance, and Cardioprotection Among Metabolically Healthy Obese Adults: A Randomized Clinical Trial.* JAMA Intern Med, 2017. **177**(7): p. 930-938.
57. Ahmet, I., et al., *Cardioprotection by intermittent fasting in rats.* Circulation, 2005. **112**(20): p. 3115-21.
58. Kale, V.P., et al., *Effect of fasting duration on clinical pathology results in Wistar rats.* Vet Clin Pathol, 2009. **38**(3): p. 361-6.
59. Wilhelmi de Toledo, F., et al., *Safety, health improvement and well-being during a 4 to 21-day fasting period in an observational study including 1422 subjects.* PLoS One, 2019. **14**(1): p. e0209353.
60. Agoston, D.V., *How to Translate Time? The Temporal Aspect of Human and Rodent Biology.* Front Neurol, 2017. **8**: p. 92.

61. Kolb, H., et al., *Ketone bodies: from enemy to friend and guardian angel.* BMC Med, 2021. **19**(1): p. 313.
62. Liepinsh, E., et al., *The heart is better protected against myocardial infarction in the fed state compared to the fasted state.* Metabolism, 2014. **63**(1): p. 127-36.
63. Ma, X., et al., *β-Hydroxybutyrate Exacerbates Hypoxic Injury by Inhibiting HIF-1α-Dependent Glycolysis in Cardiomyocytes-Adding Fuel to the Fire?* Cardiovasc Drugs Ther, 2022. **36**(3): p. 383-397.
64. Blanco, J.C., et al., *Starvation Ketoacidosis due to the Ketogenic Diet and Prolonged Fasting - A Possibly Dangerous Diet Trend.* Am J Case Rep, 2019. **20**: p. 1728-1731.
65. Crick, F.H., *On protein synthesis.* Symp Soc Exp Biol, 1958. **12**: p. 138-63.
66. Devaux, Y. and E.L. Robinson, *Preface*, in *Epigenetics in Cardiovascular Disease*, Y. Devaux and E.L. Robinson, Editors. 2021, Academic Press. p. XXI-XXVI.
67. Zhang, L., Q. Lu, and C. Chang, *Epigenetics in Health and Disease*, in *Epigenetics in Allergy and Autoimmunity*, C. Chang and Q. Lu, Editors. 2020, Springer Singapore: Singapore. p. 3-55.
68. Dieterich, C. and M. Völkers, *Chapter 6 - RNA modifications in cardiovascular disease—An experimental and computational perspective*, in *Epigenetics in Cardiovascular Disease*, Y. Devaux and E.L. Robinson, Editors. 2021, Academic Press. p. 113-125.
69. Benak, D., F. Kolar, and M. Hlavackova, *Epitranscriptomic regulations in the heart.* Physiol Res, 2024(online).
70. Boccaletto, P., et al., *MODOMICS: a database of RNA modification pathways. 2017 update.* Nucleic Acids Res, 2018. **46**(D1): p. D303-d307.
71. Roundtree, I.A., et al., *Dynamic RNA Modifications in Gene Expression Regulation.* Cell, 2017. **169**(7): p. 1187-1200.
72. Arguello, A.E., A.N. DeLiberto, and R.E. Kleiner, *RNA Chemical Proteomics Reveals the N(6)-Methyladenosine (m(6)A)-Regulated Protein-RNA Interactome.* J Am Chem Soc, 2017. **139**(48): p. 17249-17252.
73. Lee, Y., et al., *Molecular Mechanisms Driving mRNA Degradation by m(6)A Modification.* Trends Genet, 2020. **36**(3): p. 177-188.
74. Boo, S.H. and Y.K. Kim, *The emerging role of RNA modifications in the regulation of mRNA stability.* Exp Mol Med, 2020. **52**(3): p. 400-408.
75. Desrosiers, R., K. Friderici, and F. Rottman, *Identification of methylated nucleosides in messenger RNA from Novikoff hepatoma cells.* Proc Natl Acad Sci U S A, 1974. **71**(10): p. 3971-5.
76. Jia, G., et al., *N6-methyladenosine in nuclear RNA is a major substrate of the obesity-associated FTO.* Nat Chem Biol, 2011. **7**(12): p. 885-7.
77. Dominissini, D., et al., *Transcriptome-wide mapping of N(6)-methyladenosine by m(6)A-seq based on immunocapturing and massively parallel sequencing.* Nat Protoc, 2013. **8**(1): p. 176-89.
78. Huang, H., H. Weng, and J. Chen, *The Biogenesis and Precise Control of RNA m(6)A Methylation.* Trends Genet, 2020. **36**(1): p. 44-52.
79. Sweaad, W.K., et al., *Relevance of N6-methyladenosine regulators for transcriptome: Implications for development and the cardiovascular system.* J Mol Cell Cardiol, 2021. **160**: p. 56-70.
80. Perry, R.P., et al., *The methylated constituents of L cell messenger RNA: evidence for an unusual cluster at the 5' terminus.* Cell, 1975. **4**(4): p. 387-94.
81. Meyer, K.D., et al., *Comprehensive analysis of mRNA methylation reveals enrichment in 3' UTRs and near stop codons.* Cell, 2012. **149**(7): p. 1635-46.
82. Berulava, T., et al., *Changes in m6A RNA methylation contribute to heart failure progression by modulating translation.* Eur J Heart Fail, 2020. **22**(1): p. 54-66.
83. Huang, H., et al., *Histone H3 trimethylation at lysine 36 guides m(6)A RNA modification co-transcriptionally.* Nature, 2019. **567**(7748): p. 414-419.

84. Li, Y., et al., *N(6)-Methyladenosine co-transcriptionally directs the demethylation of histone H3K9me2.* Nat Genet, 2020. **52**(9): p. 870-877.
85. Niu, Y., et al., *N6-methyl-adenosine (m6A) in RNA: an old modification with a novel epigenetic function.* Genomics Proteomics Bioinformatics, 2013. **11**(1): p. 8-17.
86. Zhang, B., et al., *The critical roles of m6A modification in metabolic abnormality and cardiovascular diseases.* Genes Dis, 2021. **8**(6): p. 746-758.
87. Wang, P., K.A. Doxtader, and Y. Nam, *Structural Basis for Cooperative Function of Mettl3 and Mettl14 Methyltransferases.* Mol Cell, 2016. **63**(2): p. 306-317.
88. Wang, X., et al., *Structural basis of N(6)-adenosine methylation by the METTL3-METTL14 complex.* Nature, 2016. **534**(7608): p. 575-8.
89. Ping, X.L., et al., *Mammalian WTAP is a regulatory subunit of the RNA N6-methyladenosine methyltransferase.* Cell Res, 2014. **24**(2): p. 177-89.
90. Patil, D.P., et al., *m(6)A RNA methylation promotes XIST-mediated transcriptional repression.* Nature, 2016. **537**(7620): p. 369-373.
91. Yue, Y., et al., *VIRMA mediates preferential m(6)A mRNA methylation in 3'UTR and near stop codon and associates with alternative polyadenylation.* Cell Discov, 2018. **4**: p. 10.
92. Růžička, K., et al., *Identification of factors required for m(6) A mRNA methylation in Arabidopsis reveals a role for the conserved E3 ubiquitin ligase HAKAI.* New Phytol, 2017. **215**(1): p. 157-172.
93. Knuckles, P., et al., *Zc3h13/Flacc is required for adenosine methylation by bridging the mRNA-binding factor Rbm15/Spenito to the m(6)A machinery component Wtap/Fl(2)d.* Genes Dev, 2018. **32**(5-6): p. 415-429.
94. Pendleton, K.E., et al., *The U6 snRNA m(6)A Methyltransferase METTL16 Regulates SAM Synthetase Intron Retention.* Cell, 2017. **169**(5): p. 824-835.e14.
95. Warda, A.S., et al., *Human METTL16 is a N(6)-methyladenosine (m(6)A) methyltransferase that targets pre-mRNAs and various non-coding RNAs.* EMBO Rep, 2017. **18**(11): p. 2004-2014.
96. Oerum, S., et al., *A comprehensive review of m6A/m6Am RNA methyltransferase structures.* Nucleic Acids Res, 2021. **49**(13): p. 7239-7255.
97. van Tran, N., et al., *The human 18S rRNA m6A methyltransferase METTL5 is stabilized by TRMT112.* Nucleic Acids Res, 2019. **47**(15): p. 7719-7733.
98. Ma, H., et al., *N(6-)Methyladenosine methyltransferase ZCCHC4 mediates ribosomal RNA methylation.* Nat Chem Biol, 2019. **15**(1): p. 88-94.
99. Zheng, G., et al., *ALKBH5 is a mammalian RNA demethylase that impacts RNA metabolism and mouse fertility.* Mol Cell, 2013. **49**(1): p. 18-29.
100. Wang, Y., et al., *N(6)-methyladenosine in 7SK small nuclear RNA underlies RNA polymerase II transcription regulation.* Mol Cell, 2023. **83**(21): p. 3818-3834.e7.
101. Wei, J., et al., *Differential m(6)A, m(6)A(m), and m(1)A Demethylation Mediated by FTO in the Cell Nucleus and Cytoplasm.* Mol Cell, 2018. **71**(6): p. 973-985.e5.
102. Relier, S., et al., *FTO-mediated cytoplasmic m(6)A(m) demethylation adjusts stem-like properties in colorectal cancer cell.* Nat Commun, 2021. **12**(1): p. 1716.
103. Ueda, Y., et al., *AlkB homolog 3-mediated tRNA demethylation promotes protein synthesis in cancer cells.* Sci Rep, 2017. **7**: p. 42271.
104. Lei, K., S. Lin, and Q. Yuan, *N6-methyladenosine (m6A) modification of ribosomal RNAs (rRNAs): Critical roles in mRNA translation and diseases.* Genes Dis, 2023. **10**(1): p. 126-134.
105. Zaccara, S. and S.R. Jaffrey, *A Unified Model for the Function of YTHDF Proteins in Regulating m(6)A-Modified mRNA.* Cell, 2020. **181**(7): p. 1582-1595.e18.
106. Lasman, L., et al., *Context-dependent functional compensation between Ythdf m(6)A reader proteins.* Genes Dev, 2020. **34**(19-20): p. 1373-1391.
107. Wang, X., et al., *N6-methyladenosine-dependent regulation of messenger RNA stability.* Nature, 2014. **505**(7481): p. 117-20.

108. Wang, X., et al., *N(6)-methyladenosine Modulates Messenger RNA Translation Efficiency.* Cell, 2015. **161**(6): p. 1388-99.
109. Xiao, W., et al., *Nuclear m(6)A Reader YTHDC1 Regulates mRNA Splicing.* Mol Cell, 2016. **61**(4): p. 507-519.
110. Hsu, P.J., et al., *Ythdc2 is an N(6)-methyladenosine binding protein that regulates mammalian spermatogenesis.* Cell Res, 2017. **27**(9): p. 1115-1127.
111. Shi, H., et al., *YTHDF3 facilitates translation and decay of N(6)-methyladenosine-modified RNA.* Cell Res, 2017. **27**(3): p. 315-328.
112. Meyer, K.D., et al., *5' UTR m(6)A Promotes Cap-Independent Translation.* Cell, 2015. **163**(4): p. 999-1010.
113. Alarcón, C.R., et al., *HNRNPA2B1 Is a Mediator of m(6)A-Dependent Nuclear RNA Processing Events.* Cell, 2015. **162**(6): p. 1299-308.
114. Liu, N., et al., *N(6)-methyladenosine-dependent RNA structural switches regulate RNA-protein interactions.* Nature, 2015. **518**(7540): p. 560-4.
115. Song, H., et al., *METTL3 and ALKBH5 oppositely regulate m(6)A modification of TFEB mRNA, which dictates the fate of hypoxia/reoxygenation-treated cardiomyocytes.* Autophagy, 2019. **15**(8): p. 1419-1437.
116. Liu, N., et al., *N6-methyladenosine alters RNA structure to regulate binding of a low-complexity protein.* Nucleic Acids Res, 2017. **45**(10): p. 6051-6063.
117. Huang, H., et al., *Recognition of RNA N(6)-methyladenosine by IGF2BP proteins enhances mRNA stability and translation.* Nat Cell Biol, 2018. **20**(3): p. 285-295.
118. Zhang, F., et al., *Fragile X mental retardation protein modulates the stability of its m6A-marked messenger RNA targets.* Hum Mol Genet, 2018. **27**(22): p. 3936-3950.
119. Edupuganti, R.R., et al., *N(6)-methyladenosine (m(6)A) recruits and repels proteins to regulate mRNA homeostasis.* Nat Struct Mol Biol, 2017. **24**(10): p. 870-878.
120. Wu, R., et al., *A novel m(6)A reader Prrc2a controls oligodendroglial specification and myelination.* Cell Res, 2019. **29**(1): p. 23-41.
121. Wang, Y., et al., *N6-methyladenosine modification destabilizes developmental regulators in embryonic stem cells.* Nat Cell Biol, 2014. **16**(2): p. 191-8.
122. Liu, X.H., et al., *Co-effects of m6A and chromatin accessibility dynamics in the regulation of cardiomyocyte differentiation.* Epigenetics Chromatin, 2023. **16**(1): p. 32.
123. Han, Z., et al., *ALKBH5 regulates cardiomyocyte proliferation and heart regeneration by demethylating the mRNA of YTHDF1.* Theranostics, 2021. **11**(6): p. 3000-3016.
124. Yang, C., et al., *Comprehensive Analysis of the Transcriptome-Wide m6A Methylome of Heart via MeRIP After Birth: Day 0 vs. Day 7.* Front Cardiovasc Med, 2021. **8**: p. 633631.
125. Semenovykh, D., et al., *Myocardial m6A regulators in postnatal development: effect of sex.* Physiol Res, 2022. **71**(6): p. 877-882.
126. Boissel, S., et al., *Loss-of-function mutation in the dioxygenase-encoding FTO gene causes severe growth retardation and multiple malformations.* Am J Hum Genet, 2009. **85**(1): p. 106-11.
127. Liu, C., S. Mou, and C. Pan, *The FTO gene rs9939609 polymorphism predicts risk of cardiovascular disease: a systematic review and meta-analysis.* PLoS One, 2013. **8**(8): p. e71901.
128. Doney, A.S., et al., *The FTO gene is associated with an atherogenic lipid profile and myocardial infarction in patients with type 2 diabetes: a Genetics of Diabetes Audit and Research Study in Tayside Scotland (Go-DARTS) study.* Circ Cardiovasc Genet, 2009. **2**(3): p. 255-9.
129. Hubacek, J.A., et al., *Gene variants at FTO, 9p21, and 2q36.3 are age-independently associated with myocardial infarction in Czech men.* Clin Chim Acta, 2016. **454**: p. 119-23.
130. Hubacek, J.A., et al., *A FTO variant and risk of acute coronary syndrome.* Clin Chim Acta, 2010. **411**(15-16): p. 1069-72.

131. Hubacek, J.A., et al., *The fat mass and obesity related gene polymorphism influences the risk of rejection in heart transplant patients.* Clin Transplant, 2018. **32**(12): p. e13443.
132. Zhen, X., et al., *Genetic Variations Within METTL16 and Susceptibility to Sudden Cardiac Death in Chinese Populations With Coronary Artery Disease.* Am J Cardiol, 2023. **202**: p. 90-99.
133. Wakil, S.M., et al., *A genome-wide association study reveals susceptibility loci for myocardial infarction/coronary artery disease in Saudi Arabs.* Atherosclerosis, 2016. **245**: p. 62-70.
134. Zhang, R., et al., *METTL3 mediates Ang-II-induced cardiac hypertrophy through accelerating pri-miR-221/222 maturation in an m6A-dependent manner.* Cell Mol Biol Lett, 2022. **27**(1): p. 55.
135. Carnevali, L., et al., *Signs of cardiac autonomic imbalance and proarrhythmic remodeling in FTO deficient mice.* PLoS One, 2014. **9**(4): p. e95499.
136. Gan, X.T., et al., *Identification of fat mass and obesity associated (FTO) protein expression in cardiomyocytes: regulation by leptin and its contribution to leptin-induced hypertrophy.* PLoS One, 2013. **8**(9): p. e74235.
137. Dorn, L.E., et al., *The N(6)-Methyladenosine mRNA Methylase METTL3 Controls Cardiac Homeostasis and Hypertrophy.* Circulation, 2019. **139**(4): p. 533-545.
138. Zhu, S., et al., *Integrative Analysis of N6-methyladenosine RNA modifications related genes and their Influences on Immunoreaction or fibrosis in myocardial infarction.* Int J Med Sci, 2024. **21**(2): p. 219-233.
139. Li, T., et al., *Silencing of METTL3 attenuates cardiac fibrosis induced by myocardial infarction via inhibiting the activation of cardiac fibroblasts.* Faseb j, 2021. **35**(2): p. e21162.
140. Meng, Y., et al., *The inhibition of FTO attenuates the antifibrotic effect of leonurine in rat cardiac fibroblasts.* Biochem Biophys Res Commun, 2024. **693**: p. 149375.
141. Song, K., et al., *WTAP boosts lipid oxidation and induces diabetic cardiac fibrosis by enhancing AR methylation.* iScience, 2023. **26**(10): p. 107931.
142. Kmietczyk, V., et al., *m(6)A-mRNA methylation regulates cardiac gene expression and cellular growth.* Life Sci Alliance, 2019. **2**(2): p. e201800233.
143. Zhang, B., et al., *Alteration of m6A RNA Methylation in Heart Failure With Preserved Ejection Fraction.* Front Cardiovasc Med, 2021. **8**: p. 647806.
144. Zhang, B., et al., *m6A demethylase FTO attenuates cardiac dysfunction by regulating glucose uptake and glycolysis in mice with pressure overload-induced heart failure.* Signal Transduct Target Ther, 2021. **6**(1): p. 377.
145. Komal, S., et al., *ALKBH5 inhibitors as a potential treatment strategy in heart failure-inferences from gene expression profiling.* Front Cardiovasc Med, 2023. **10**: p. 1194311.
146. Shi, L., et al., *Downregulation of Wtap causes dilated cardiomyopathy and heart failure.* J Mol Cell Cardiol, 2024.
147. Ju, W., et al., *Changes in N6-Methyladenosine Modification Modulate Diabetic Cardiomyopathy by Reducing Myocardial Fibrosis and Myocyte Hypertrophy.* Front Cell Dev Biol, 2021. **9**: p. 702579.
148. Shao, Y., et al., *CircRNA CDR1as promotes cardiomyocyte apoptosis through activating hippo signaling pathway in diabetic cardiomyopathy.* Eur J Pharmacol, 2022. **922**: p. 174915.
149. Benak, D., et al., *The role of m6A and m6Am RNA modifications in the pathogenesis of diabetes mellitus.* Front Endocrinol (Lausanne), 2023. **14**: p. 1223583.
150. Longenecker, J.Z., et al., *Epitranscriptomics in the Heart: a Focus on m(6)A.* Curr Heart Fail Rep, 2020. **17**(5): p. 205-212.
151. Wu, S., et al., *m(6)A RNA Methylation in Cardiovascular Diseases.* Mol Ther, 2020. **28**(10): p. 2111-2119.
152. Qin, Y., et al., *Role of m6A RNA methylation in cardiovascular disease (Review).* Int J Mol Med, 2020. **46**(6): p. 1958-1972.

153. Paramasivam, A., J. Vijayashree Priyadharsini, and S. Raghunandhakumar, *N6-adenosine methylation (m6A): a promising new molecular target in hypertension and cardiovascular diseases.* Hypertens Res, 2020. **43**(2): p. 153-154.
154. Kumari, R., et al., *mRNA modifications in cardiovascular biology and disease: with a focus on m6A modification.* Cardiovasc Res, 2022. **118**(7): p. 1680-1692.
155. Leptidis, S., et al., *Epitranscriptomics of cardiovascular diseases (Review).* Int J Mol Med, 2022. **49**(1).
156. Chen, Y.S., et al., *N6-Adenosine Methylation (m(6)A) RNA Modification: an Emerging Role in Cardiovascular Diseases.* J Cardiovasc Transl Res, 2021. **14**(5): p. 857-872.
157. Zhou, W., et al., *RNA Methylations in Cardiovascular Diseases, Molecular Structure, Biological Functions and Regulatory Roles in Cardiovascular Diseases.* Front Pharmacol, 2021. **12**: p. 722728.
158. Xu, Z., et al., *Emerging Roles and Mechanism of m6A Methylation in Cardiometabolic Diseases.* Cells, 2022. **11**(7).
159. Li, Y., et al., *Analysis of urinary methylated nucleosides of patients with coronary artery disease by high-performance liquid chromatography/electrospray ionization tandem mass spectrometry.* Rapid Commun Mass Spectrom, 2014. **28**(19): p. 2054-8.
160. Wei, C., A. Gershowitz, and B. Moss, *N6, O2'-dimethyladenosine a novel methylated ribonucleoside next to the 5' terminal of animal cell and virus mRNAs.* Nature, 1975. **257**(5523): p. 251-3.
161. Bokar, J.A., *The biosynthesis and functional roles of methylated nucleosides in eukaryotic mRNA*, in *Fine-Tuning of RNA Functions by Modification and Editing*, H. Grosjean, Editor. 2005, Springer Berlin Heidelberg: Berlin, Heidelberg. p. 141-177.
162. Akichika, S., et al., *Cap-specific terminal N (6)-methylation of RNA by an RNA polymerase II-associated methyltransferase.* Science, 2019. **363**(6423).
163. Mauer, J., et al., *Reversible methylation of m(6)A(m) in the 5' cap controls mRNA stability.* Nature, 2017. **541**(7637): p. 371-375.
164. Mauer, J., et al., *FTO controls reversible m(6)Am RNA methylation during snRNA biogenesis.* Nat Chem Biol, 2019. **15**(4): p. 340-347.
165. Sun, H., et al., *Cap-specific, terminal N(6)-methylation by a mammalian m(6)Am methyltransferase.* Cell Res, 2019. **29**(1): p. 80-82.
166. Yu, D., et al., *Enzymatic characterization of mRNA cap adenosine-N6 methyltransferase PCIF1 activity on uncapped RNAs.* J Biol Chem, 2022. **298**(4): p. 101751.
167. Hirose, Y., et al., *Human phosphorylated CTD-interacting protein, PCIF1, negatively modulates gene expression by RNA polymerase II.* Biochem Biophys Res Commun, 2008. **369**(2): p. 449-55.
168. Sendinc, E., et al., *PCIF1 Catalyzes m6Am mRNA Methylation to Regulate Gene Expression.* Mol Cell, 2019. **75**(3): p. 620-630.e9.
169. Cowling, V.H., *CAPAM: The mRNA Cap Adenosine N6-Methyltransferase.* Trends Biochem Sci, 2019. **44**(3): p. 183-185.
170. Goh, Y.T., et al., *METTL4 catalyzes m6Am methylation in U2 snRNA to regulate pre-mRNA splicing.* Nucleic Acids Res, 2020. **48**(16): p. 9250-9261.
171. Chen, H., et al., *METTL4 is an snRNA m(6)Am methyltransferase that regulates RNA splicing.* Cell Res, 2020. **30**(6): p. 544-547.
172. Hao, Z., et al., *N(6)-Deoxyadenosine Methylation in Mammalian Mitochondrial DNA.* Mol Cell, 2020. **78**(3): p. 382-395.e8.
173. Benak, D., et al., *RNA modification m(6)Am: the role in cardiac biology.* Epigenetics, 2023. **18**(1): p. 2218771.
174. Mauer, J. and S.R. Jaffrey, *FTO, m(6) A(m) , and the hypothesis of reversible epitranscriptomic mRNA modifications.* FEBS Lett, 2018. **592**(12): p. 2012-2022.

175. Phan, A., P. Mathiyalangan, and S. Sahoo, *Abstract 13709: Cardioprotective Mechanisms of FTO-Regulated m⁶A in Heart Failure.* Circulation, 2022. **146**(Suppl_1): p. A13709-A13709.
176. Liu, J., et al., *Landscape and Regulation of m(6)A and m(6)Am Methylome across Human and Mouse Tissues.* Mol Cell, 2020. **77**(2): p. 426-440.e6.
177. Sistilli, G., et al., *Krill Oil Supplementation Reduces Exacerbated Hepatic Steatosis Induced by Thermoneutral Housing in Mice with Diet-Induced Obesity.* Nutrients, 2021. **13**(2).
178. Janovska, P., et al., *Dysregulation of epicardial adipose tissue in cachexia due to heart failure: the role of natriuretic peptides and cardiolipin.* J Cachexia Sarcopenia Muscle, 2020. **11**(6): p. 1614-1627.
179. Tsugawa, H., et al., *A lipidome atlas in MS-DIAL 4.* Nat Biotechnol, 2020. **38**(10): p. 1159-1163.
180. Johnston, H.E., et al., *Solvent Precipitation SP3 (SP4) Enhances Recovery for Proteomics Sample Preparation without Magnetic Beads.* Anal Chem, 2022. **94**(29): p. 10320-10328.
181. Hrdlička, J., et al., *Epoxyeicosatrienoic Acid-Based Therapy Attenuates the Progression of Postischemic Heart Failure in Normotensive Sprague-Dawley but Not in Hypertensive Ren-2 Transgenic Rats.* Front Pharmacol, 2019. **10**: p. 159.
182. Lee, T.M., M.S. Lin, and N.C. Chang, *Effect of ATP-sensitive potassium channel agonists on ventricular remodeling in healed rat infarcts.* J Am Coll Cardiol, 2008. **51**(13): p. 1309-18.
183. Benak, D., et al., *Epitranscriptomic regulation in fasting hearts: implications for cardiac health.* RNA Biology, 2024. **21**(1): p. 1-14.
184. Sander, H., et al., *Ponceau S waste: Ponceau S staining for total protein normalization.* Anal Biochem, 2019. **575**: p. 44-53.
185. Selberg, S., et al., *Rational Design of Novel Anticancer Small-Molecule RNA m6A Demethylase ALKBH5 Inhibitors.* ACS Omega, 2021. **6**(20): p. 13310-13320.
186. Zheng, G., et al., *Synthesis of a FTO inhibitor with anticonvulsant activity.* ACS Chem Neurosci, 2014. **5**(8): p. 658-65.
187. Pokorna, Z., et al., *In vitro and in vivo investigation of cardiotoxicity associated with anticancer proteasome inhibitors and their combination with anthracycline.* Clin Sci (Lond), 2019. **133**(16): p. 1827-1844.
188. Snytnikova, O., et al., *Quantitative Metabolomic Analysis of Changes in the Rat Blood Serum during Autophagy Modulation: A Focus on Accelerated Senescence.* Int J Mol Sci, 2022. **23**(21).
189. Peng, L., et al., *Emerging role of m(6) A modification in cardiovascular diseases.* Cell Biol Int, 2022. **46**(5): p. 711-722.
190. Fry, N.J., et al., *N(6)-methyladenosine is required for the hypoxic stabilization of specific mRNAs.* Rna, 2017. **23**(9): p. 1444-1455.
191. Wang, Y.J., et al., *Reprogramming of m(6)A epitranscriptome is crucial for shaping of transcriptome and proteome in response to hypoxia.* RNA.Biol., 2021. **18**(1): p. 131-143.
192. Yang, N., et al., *HBXIP drives metabolic reprogramming in hepatocellular carcinoma cells via METTL3-mediated m6A modification of HIF-1a.* J.Cell Physiol, 2021. **236**(5): p. 3863-3880.
193. Shmakova, A., et al., *PBRM1 Cooperates with YTHDF2 to Control HIF-1a Protein Translation.* Cells, 2021. **10**(6).
194. Wu, R., et al., *m6A methylation promotes white-to-beige fat transition by facilitating Hif1a translation.* EMBO Rep, 2021. **22**(11): p. e52348.
195. Tanabe, A., et al., *RNA helicase YTHDC2 promotes cancer metastasis via the enhancement of the efficiency by which HIF-1a mRNA is translated.* Cancer Lett., 2016. **376**(1): p. 34-42.
196. Thalhammer, A., et al., *Human AlkB homologue 5 is a nuclear 2-oxoglutarate dependent oxygenase and a direct target of hypoxia-inducible factor 1a (HIF-1a).* PLoS.One., 2011. **6**(1): p. e16210.
197. Hao, Z., et al., *N(6)-Deoxyadenosine Methylation in Mammalian Mitochondrial DNA.* Mol.Cell, 2020. **78**(3): p. 382-395.

198. Yao, M.D., et al., *Role of METTL3-Dependent N(6)-Methyladenosine mRNA Modification in the Promotion of Angiogenesis.* Mol.Ther., 2020. **28**(10): p. 2191-2202.
199. Li, Q., et al., *HIF-1a-induced expression of m6A reader YTHDF1 drives hypoxia-induced autophagy and malignancy of hepatocellular carcinoma by promoting ATG2A and ATG14 translation.* Signal.Transduct.Target Ther., 2021. **6**(1): p. 76.
200. Yang, K., et al., *ALKBH5 induces fibroblast-to-myofibroblast transformation during hypoxia to protect against cardiac rupture after myocardial infarction.* J Adv Res, 2023.
201. Su, Y., et al., *N6-methyladenosine methyltransferase plays a role in hypoxic preconditioning partially through the interaction with lncRNA H19.* Acta Biochim.Biophys.Sin.(Shanghai), 2020. **52**(12): p. 1306-1315.
202. Zhao, K., et al., *METTL3 improves cardiomyocyte proliferation upon myocardial infarction via upregulating miR-17-3p in a DGCR8-dependent manner.* Cell Death.Discov., 2021. **7**(1): p. 291.
203. Imai, Y., et al., *Cloning of a gene, YT521, for a novel RNA splicing-related protein induced by hypoxia/reoxygenation.* Brain Res Mol Brain Res, 1998. **53**(1-2): p. 33-40.
204. Shi, Y., et al., *YTHDF1 links hypoxia adaptation and non-small cell lung cancer progression.* Nat.Commun., 2019. **10**(1): p. 4892.
205. Hu, L., et al., *YTHDF1 Regulates Pulmonary Hypertension through Translational Control of MAGED1.* Am.J.Respir.Crit Care Med., 2021. **203**(9): p. 1158-1172.
206. Wang, H., et al., *m6A methyltransferase WTAP regulates myocardial ischemia reperfusion injury through YTHDF1/FOXO3a signaling.* Apoptosis, 2023. **28**(5-6): p. 830-839.
207. Liu, L. and Z. Liu, *m(6)A eraser ALKBH5 mitigates the apoptosis of cardiomyocytes in ischemia reperfusion injury through m(6)A/SIRT1 axis.* PeerJ, 2023. **11**: p. e15269.
208. Benak, D., *The role of demethylase FTO and adipokines in the heart: effect of chronic hypoxia*. 2017, Charles University in Prague: Prague. p. 59.
209. Xu, Z., et al., *Intermittent Fasting Improves High-Fat Diet-Induced Obesity Cardiomyopathy via Alleviating Lipid Deposition and Apoptosis and Decreasing m6A Methylation in the Heart.* Nutrients, 2022. **14**(2): p. 251.
210. Sepich-Poore, C., et al., *The METTL5-TRMT112 N(6)-methyladenosine methyltransferase complex regulates mRNA translation via 18S rRNA methylation.* J Biol Chem, 2022. **298**(3): p. 101590.
211. Han, Y., et al., *Loss of m(6)A Methyltransferase METTL5 Promotes Cardiac Hypertrophy Through Epitranscriptomic Control of SUZ12 Expression.* Front Cardiovasc Med, 2022. **9**: p. 852775.
212. Ge, M., et al., *An eIF3a gene mutation dysregulates myocardium growth with left ventricular noncompaction via the p-ERK1/2 pathway.* Genes Dis, 2021. **8**(4): p. 545-554.
213. Li, B., et al., *Knockdown of eIF3a ameliorates cardiac fibrosis by inhibiting the TGF-β1/Smad3 signaling pathway.* Cell Mol Biol (Noisy-le-grand), 2016. **62**(7): p. 97-101.
214. Liu, T., et al., *The m6A reader YTHDF1 promotes ovarian cancer progression via augmenting EIF3C translation.* Nucleic Acids Res, 2020. **48**(7): p. 3816-3831.
215. Ge, Y., et al., *The roles of G3BP1 in human diseases (review).* Gene, 2022. **821**: p. 146294.
216. Jin, G., et al., *G3BP2: Structure and function.* Pharmacol Res, 2022. **186**: p. 106548.
217. Hong, H.Q., et al., *G3BP2 is involved in isoproterenol-induced cardiac hypertrophy through activating the NF-κB signaling pathway.* Acta Pharmacol Sin, 2018. **39**(2): p. 184-194.
218. Li, T., et al., *Downregulation of G3BP2 reduces atherosclerotic lesions in ApoE(-/-) mice.* Atherosclerosis, 2020. **310**: p. 64-74.
219. Xiao, X., et al., *lncRNA XIST knockdown suppresses hypoxia/reoxygenation (H/R)-induced apoptosis of H9C2 cells by regulating miR-545-3p/G3BP2.* IUBMB Life, 2021. **73**(9): p. 1103-1114.
220. Masuda, K., K. Abdelmohsen, and M. Gorospe, *RNA-binding proteins implicated in the hypoxic response.* J Cell Mol Med, 2009. **13**(9a): p. 2759-69.

221. Chen, H.-Y., et al., *ELAVL1 is transcriptionally activated by FOXC1 and promotes ferroptosis in myocardial ischemia/reperfusion injury by regulating autophagy.* Molecular Medicine, 2021. **27**(1): p. 14.
222. Krishnamurthy, P., et al., *Myocardial knockdown of mRNA-stabilizing protein HuR attenuates post-MI inflammatory response and left ventricular dysfunction in IL-10-null mice.* Faseb j, 2010. **24**(7): p. 2484-94.
223. Zhang, D.H., et al., *Deubiquitinase Ubiquitin-Specific Protease 10 Deficiency Regulates Sirt6 signaling and Exacerbates Cardiac Hypertrophy.* J Am Heart Assoc, 2020. **9**(22): p. e017751.
224. Liu, L.B., et al., *Limonin stabilises sirtuin 6 (SIRT6) by activating ubiquitin specific peptidase 10 (USP10) in cardiac hypertrophy.* Br J Pharmacol, 2022. **179**(18): p. 4516-4533.
225. Huang, J., et al., *FoxO4 negatively modulates USP10 transcription to aggravate the apoptosis and oxidative stress of hypoxia/reoxygenation-induced cardiomyocytes by regulating the Hippo/YAP pathway.* J Bioenerg Biomembr, 2021. **53**(5): p. 541-551.
226. Varga, Z.V., et al., *Alternative Splicing of NOX4 in the Failing Human Heart.* Front Physiol, 2017. **8**: p. 935.
227. Li, Y., et al., *Histone Deacetylase 1 Inhibition Protects Against Hypoxia-Induced Swelling in H9c2 Cardiomyocytes Through Regulating Cell Stiffness.* Circ J, 2017. **82**(1): p. 192-202.

11. LIST OF ATTACHMENTS

I. Appendix to the doctoral thesis: ALKBH5 and FTO levels in postnatal development

II. **Benak D**, Sotakova-Kasparova D, Neckar J, Kolar F, Hlavackova M (2019). Selection of optimal reference genes for gene expression studies in chronically hypoxic rat heart. Mol Cell Biochem. 461(1-2):15-22.

III. Semenovykh D, **Benak D**, Holzerova K, Cerna B, Telensky P, Vavrikova T, Kolar F, Neckar J, Hlavackova M (2022). Myocardial m6A regulators in postnatal development: effect of sex. Physiol Res. 71(6):877-882.

IV. **Benak D**, Holzerova K, Hrdlicka J, Kolar F, Olsen M, Karelson M, Hlavackova M (2024). Epitranscriptomic regulation in fasting hearts: implications for cardiac health. RNA Biol. 21(1):1-14.

V. **Benak D**, Kolar F, Zhang L, Devaux Y, Hlavackova M (2023). RNA modification m^6Am: the role in cardiac biology. Epigenetics. 18(1):2218771.

VI. **Benak D**, Benakova S, Plecita-Hlavata L, Hlavackova M (2023). The role of m^6A and m^6Am RNA modifications in the pathogenesis of diabetes mellitus. Front Endocrinol (Lausanne). 14:1223583.

VII. **Benak D**, Kolar F, Hlavackova M (2024). Epitranscriptomic regulations in the heart. Physiol Res. (online)